



Universitetet
i Stavanger

FACULTY OF SCIENCE AND TECHNOLOGY

MASTER'S THESIS

Study programme/specialization: Master of Science in Petroleum Engineering/ Drilling Engineering	Spring semester, 2020. Open access
Author: Larisa Penkala	Digital Submission _____ (Author's signature)
Supervisor(s): Dr. Mahmoud Khalifeh Dr. Arild Saasen Dr. Knut Taugbøl	
Title of master's thesis: Development and Characterization of a Pressure Transmitting Sag Prevention Gel Pill	
Credits: 30 ECTS	
Keywords: Barite Sag Laponite Gel Pill Design Fluid Pills Water-Based Drilling Fluids	Number of pages: 123 + supplemental material/other: 21 Stavanger, 15th June 2020

**Development and Characterization of a Pressure Transmitting
Sag Prevention Gel Pill**

By

Larisa Penkala

Master's Thesis

Presented to the Faculty of Science and Technology

The University of Stavanger

THE UNIVERSITY OF STAVANGER

JUNE 2020

Acknowledgement

This thesis describes the work of a project in corporation with Equinor and the University of Stavanger. Considering this process, I would like to express my greatest gratitude to my research supervisor Dr. Mahmoud Khalifeh for creating the framework of this thesis and supervising me through the process. Without his dedicated involvement and guiding hand, the completion of this paper would not have been accomplished. Furthermore, a great thank you to Arild Saasen, who has supported me through discussions of literature and technical aspect of the project.

I wish to express a sincere thank you to Knut Taugbøl who has been my external supervisor representative from Equinor. Knut has been a guiding hand throughout the writing process, providing me with excellent ideas to improve this thesis work. I deeply appreciate the time Knut has invested in this thesis and his contributions. My appreciation continues with Bodil Aase from Equinor who has followed up on this project and showed great encourage and support.

My gratefulness is also shared with members of the Faculty of Energy and Petroleum for great support during the laboratory experiments. A warm thank you to Kim Andre Vorland for great assistance during tests, installation and for inspiring me toward improvements and academic discussions. I would like to express my gratitude to Johannes S. Jensen, Emil S. Kristiansen and Caroline Einvik who have contributed to all experiments, playing an active part in the development of the basis for this work. Thank you for your assistance, ideas for improvement and most importantly for providing me with tools to improve the quality of my work.

Getting through this process has both been interesting and challenging. It required more than academic support and I must thank my partner and family for great support, understanding and for at times having to tolerate me over the past months.

I also place on record, my sense of gratitude to one and all, who have directly or indirectly have lent their hand in this venture.

Abstract

Barite sag is a risky phenomenon to manage as particle settlement occurs in all types of drilling fluids containing weighting agents' materials to achieve density. This leads to the phenomenon of sag which is known to complicate operations associated with construction and completion of wells in addition to other well control issues. Inert particle settling is a mechanism where particles separate from the liquid phase in which these originally were suspended in. This mechanism can change the hydrostatic fluid column as particle settlement create bed formations at the point of accumulation influencing the desired bottom hole pressure significantly. Operational conditions such as static periods or low circulation rates in deviated sections accelerate the particle sag mechanism and do often require remedial action when drilling is proceeded.

This thesis work invented a sag prevention gel pill with barrier functionalities to controllably transmit hydrostatic pressure from the overlying fluid columns. Two gel pill designs based on bentonite and Laponite RD were characterized and tested in scaled up test setups to proof the concept and possible prevention of barite sag. The final target of investigation involved vertical, 20° and 40° inclined setups to simulate different sections of a well.

The designed gel pill forms sufficient gel structure to isolate fluids placed below and above the pill column, but not such gel strength to act as a barrier blocking pressure signals. Thus, formation of gel structure was adequate to maintain barrier functionalities while transmitting pressure signals from the heavier water-based drilling fluid spotted on top, in addition to provide a foundation for the settled barite.

Test results showed that the laponite-based pill provided even better performance during testing of both hindered and boycott driven particle settling. However, the bentonite-based pill provided better pressure transmitting communication throughout the test period.

Acronyms

°C	Degree Celsius
cm	Centi Meter
cP	Centipoise
ft	Foot
g	Gram
L	Liter
lbf	Pound-force
m	Meter
min	Minute
Pa	Pascal
Pa.s	Pascal second
psi	Pounds per square inch

Abbreviations

API	American Petroleum Institute
CEC	Cation Exchange Capacity
DP	Differential Pressure
ECD	Equivalent Circulation Density
FPTP	Fluid Pressure Transmission Pill
H-B	Herschel-Bulkley
HPHT	High-Pressure High-Temperature
ID	Inside/Inner Diameter
LSRYP	Low-Shear Rate Yield Point
MPD	Managed Pressure Drilling
MW	Fluid Density
OBCP	Off-Bottom Cement Plug Operation
OBM	Oil-Based Mud
pH	Potential Hydrogen
PV	Plastic Viscosity
rpm	Rotational Speed

SBM	Synthetic-Based Mud
sec	Second
SG	Specific Gravity
SUs	Structural Units
TVD	Total Vertical Depth
VG	Viscosity - Gel
VST	Viscometer Sag Test
WBDF	Water-Based Drilling Fluid
WBM	Water-Based Mud
YP	Yield Point
XG	Xanthan Gum
XP2i	Bottom Hole Pressure

List of Symbols

μ_a	Apparent viscosity
k	Consistency index
C°	Degree Celsius
ΔP	Differential Pressure
ρ	Density
η	Fluid's viscosity
τ_g	Gel strength
g	Gravitational constant
μ	Newtonian viscosity
D	Particle diameter
v_o	Particle settling velocity
L	Pill Length
μ_p	Plastic viscosity
R	Radius
n	Rheological index
S _R	Sag register
V _T	Settling velocity
γ	Shear rate

τ	Shear stress
τ_o	Yield stress
τ_y	Yield stress
θ	Rpm reading

Conversion Factors

cP	0.001 Pa.s
Pa	$0.51 * \text{lb}_f/100\text{ft}^2$
psi	0.068947575 bar

List of Contents

Acknowledgement.....	iii
Abstract	v
Acronyms	vi
Abbreviations	vi
List of Symbols	vii
Conversion Factors.....	ix
List of Contents	x
List of Figures	xiv
List of Tables.....	xviii
1 Research Question and Objectives	20
2. Introduction	22
2.1 Bentonite	22
2.1.1 Clay Mineralogy.....	22
2.1.2 Surface Potential of Bentonite.....	24
2.1.3 Swelling Mechanism	25
2.1.4 Clay Particle Interaction Mechanism	26
2.1.5 Gelation Mechanism	28
2.1.6 Laponite for Application in Laboratory Experiments	29
2.2 Drilling fluids	33
2.2.1 Water-Based Drilling Fluids	33
2.2.2 Drilling Fluid Additives	35
2.2.3 Fluid Pills	38
2.3 Rheological Fluid Properties	40
2.3.1 Viscosity.....	41
2.3.2 Rheology Models	42
2.3.3 Bingham Plastic Model	43

2.3.4 Herschel-Bulkley Model	43
2.3.5 Gel Strength.....	44
2.3.6 Thixotropic Fluids	45
2.3.7 Shear Thinning Fluid Property	45
2.3.8 Pseudoplastic Fluids	46
2.4 Barite Sag Mechanism	47
2.4.1 Hindering Effect.....	48
2.4.2 Boycott Effect	49
2.5 Operational Challenges Caused by Barite Sag.....	50
2.5.1 Occurrence of Barite Sag in Operations.....	51
2.5.2 Impact of Weighting Agent Rheology	52
2.5.3 Techniques Used to Detect and Measure Weighting Material Sag.....	53
2.5.4 Methods Used to Manage Barite Sag	56
2.6 Pills Used for Separating Fluids of Different Densities	58
2.6.1 A Fluid Pressure Transmission Pill Used during MPD.....	58
2.6.2 A Fluid Pill of Thixotropic Properties Serving as a Barrier Fluid	59
2.6.3 A New Water-Based Isolation Spacer for OBCP Operations	59
3 Methodology and Experimental Procedures	62
3.1 Experimental Procedure	62
3.1.2 Equipment	62
3.2 Design and Development of Fluids	66
3.2.1 Viscosified Brine.....	66
3.2.2 Gel Pill.....	67
3.2.3 Water-Based Drilling Fluid.....	68
3.3 Characterization of the Designed Fluids	69
3.3.1 Rheological Property Characterization	69
3.3.2 Criteria for Rheological Characterization	71

3.4 Large-Scale Testing.....	72
3.4.1 Large-Scale Setup	73
3.4.2 Pressure Sensors and Differential Pressure Gauge Sensors	74
3.4.3 Camera Recording and Stability Documentation.....	75
3.4.4 Large-Scale Test Procedure.....	75
3.4.5 Fluid Preparation for the Large-Scale Test	77
4 Results and Discussion.....	80
4.1 Bentonite-Based Sag Prevention Pill	80
4.1.1 Fluid Design and Rheological Characterization.....	80
4.1.2 Interface Stability and Isolation on the Large-Scale Test Setup	82
4.1.3 Pressure Transmission during Placement and Test Period.....	89
4.2 Laponite RD-Based Sag Prevention Pill	97
4.2.1 Fluid Design and Rheological Characterization.....	97
4.2.2 Interface Stability and Isolation on the Large-Scale Test Setup	100
4.2.3 Pressure Transmission during Placement and Test Period.....	105
4.3 Comparison of Test Results	112
4.3.1 Comparison of Rheological Parameters	112
4.3.2 Comparison of Pressure Data	113
4.5 Barite Sag Prevention.....	114
4.5.1 Effective Inclination Regarding Barite Settling and Sag Prevention	115
4.6 Challenges and Potential Reasons for Failure.....	116
5 Conclusion.....	119
6 References	120
Appendix A – Complimentary Information for Methodology.....	124
A.1 Modifications on the Water-Based Drilling Fluid.....	124
A.2 Rheology Measurement Procedure for the Gel Pills	125
A.3 Stability Tests Performed on Gel Pills	126

A.4 Improvement of Fluid Placement Procedure on Large-Scale.....	128
Appendix B - Additional Information	130
B.1 Viscosified Brine Design and Rheological Properties	130
B.2 Water-Based Drilling Fluid Design and Rheological Properties.....	132
B.3 Bentonite-Based Pill Design and Rheological Properties	134
B.4 Bentonite-Based Pill Stability Tests	137
B.5 Viscometer Data of the Laponite-Based Pill	141
B.6 Laponite-Based Pill Stability Tests	142
B.7 Water Used for Analysis of Pressure Instabilities	142
Appendix C - Suggestions on Improvement and Future Work	143
C.1 Potential Improvements	143
C.2 Way Forward	144

List of Figures

Fig. 2.1 Bonding between one octahedral sheet and two tetrahedral sheets through shared oxygen atoms (after Caenn et al. (2017)).....	24
Fig. 2.2 Schematic of charges of a montmorillonite crystal (modified from Skjeggstad (1989)).....	24
Fig. 2.3 Schematic of flocculation-deflocculation and aggregation-dispersion mechanisms (modified from Caenn et al. (2017)).....	27
Fig. 2.4 Laponite RD powder.....	29
Fig. 2.5 Laponite RD dispersed in a water-based system.....	29
Fig. 2.6 a) Empirical formula of Laponite. b) Idealised structural formula of Laponite (from Ruzicka & Zaccarelli (2011)).....	30
Fig. 2.7 a) Single Laponite platelet (modified from Ruzicka & Zaccarelli (2011)). b) Comparison of particle size between bentonite and laponite (modified from BYK Additives & Instruments (2014)).....	31
Fig. 2.8 Aggregated particle stacks dispersed into individual particle stacks (modified from BYK Additives & Instruments (2014)).....	31
Fig. 2.9 Hydration of sodium ions swelling inside the structure (modified from BYK Additives & Instruments (2014)).....	31
Fig. 2.10 House of Cards structure from gel formation (from BYK Additives & Instruments (2014)).....	32
Fig. 2.11 Schematic of increase in gel strength of various mud types with time (from Caenn et al. (2017)).....	44
Fig. 2.12 Shear stress loading curves (from Caenn et al. (2017)).....	45
Fig. 2.13 Structural interpretation of shear-thinning and plastic fluids (after Quemada (1998)).....	46
Fig. 2.14 Consistency curve of a pseudoplastic fluid (from Caenn et al. (2017)).....	47
Fig. 2.15 Hindered settling kinetics under static condition (from Zamora (2009)).....	48
Fig. 2.16 a) Boycott settling at 40°. b) Boycott settling illustration (modified from Zamora (2009)).....	50
Fig. 2.17 Mud weight monitoring (modified from M-I SWACO (1998)).....	56
Fig. 3.1 Heidolph Hei-Torque 100 value stirrer (left) and stirrer with obliquely blade construction (right).....	63
Fig. 3.2 Hobart N50-604 pt Planetary Mixer.....	63

Fig. 3.3 Ofite Model 900 Viscometer (left) and an illustration of the viscometer instrumental setup (right) (modified from Skjeggstad (1989)).....	64
Fig. 3.4 Ofite mud balance scale.....	65
Fig. 3.5 Mettler Toledo Benchtop pH meter.....	65
Fig. 3.6 Left: Illustration of the vertical test setup filled with fluids. Right: Vertical test setup with A: Transparent plastic pipe, B: Camera 1, C: Light panel, D: Camera 2, E: Differential pressure gauge DP1, F: Differential pressure gauge DP2, G: Supportive construction, H: Bottom hole pressure outlet, I: Valve for opening and closing the pipe.....	73
Fig. 3.7 a) Crystal XP2i pressure gauge sensor. b) pressure controller Marcol 82.....	74
Fig. 4.1 Rheology profile of recipe 2.BT on original mixing day and after 24 hours.....	81
Fig. 4.2 Interface right after placement (left) and interface at end of test (right) on vertical setup.....	82
Fig. 4.3 Interface right after placement (left) and interface at end of test (right) on the vertical setup.....	83
Fig. 4.4 Successful isolation by the bentonite-based pill on the vertical test setup.....	83
Fig. 4.5 Interface right after placement (left) and interface at end of test (right) on 20° inclined setup.....	84
Fig. 4.6 Interface right after placement (left) and interface at end of test (right) on the 20° inclined setup.....	85
Fig. 4.7 Air pocket inside the bentonite pill at the right corner established during placement.....	85
Fig. 4.8 Successful isolation by the bentonite-based pill on 20° inclination test setup...	86
Fig. 4.9 Interface right after placement (left) and interface at end of test (right) on 40° inclined setup.....	87
Fig. 4.10 Bentonite pill surface after placement with thin pill layer across the pipe wall.....	87
Fig. 4.11 Interface right after placement (left) and interface at end of test (right) on the 40° inclined setup.....	88
Fig. 4.12 Successful isolation by the bentonite-based pill on 40° test setup.....	88
Fig. 4.13 Bottom hole, DP1 and DP2 pressure reading during placement period, vertical setup.....	89
Fig. 4.14 Pressure monitoring during the test period of 24 hours, vertical setup.....	91

Fig. 4.15 Bottom hole, DP1 and DP2 pressure reading during placement period, 40° setup.....	92
Fig. 4.16 Pressure monitoring during the test period of 24 hours, 20° setup.....	93
Fig. 4.17 Bottom hole, DP1 and DP2 pressure reading during placement period, 40° setup.....	94
Fig. 4.18 Pressure monitoring during the test period of 24 hours, 40° setup.....	95
Fig. 4.19 Combined bottom hole pressure data from tests.....	97
Fig. 4.20 Rheological profile of all laponite-based pill recipes.....	98
Fig. 4.21 Rheological profile of recipe 3.LT.....	99
Fig. 4.22 Interface right after placement (left) and interface at end of test (right) on vertical setup.....	100
Fig. 4.23 Interface right after placement (left) and interface at end of test (right) on vertical setup.....	101
Fig. 4.24 Successful isolation by the laponite-based pill on the vertical test setup....	101
Fig. 4.25 Interface right after placement (left) and interface at test end (right) on the 20° inclined setup.....	102
Fig. 4.26 Interface right after placement (left) and interface at test end (right) on the 20° inclined setup.....	102
Fig. 4.27 Successful isolation by the laponite-based pill on 20° test setup.....	103
Fig. 4.28 Interface right after placement (left) and interface at test end (right) on the 40° inclined setup.....	103
Fig. 4.29 Interface right after placement (left) and interface at test end (right) on the 40° inclined setup.....	104
Fig. 4.30 Successful isolation by the laponite-based pill on 40° test setup.....	104
Fig. 4.31 Bottom hole, DP1 and DP2 pressure readings during placement period, vertical setup.....	105
Fig. 4.32 Pressure monitoring during the test period of 24 hours, vertical setup.....	107
Fig. 4.33 Bottom hole, DP1 and DP2 pressure readings during placement period, 20° setup.....	108
Fig. 4.34 Pressure monitoring during the test period of 24 hours, 20° setup.....	109
Fig. 4.35 Bottom hole, DP1 and DP2 pressure readings during placement period, 40° setup.....	109
Fig. 4.36 Pressure monitoring during the test period of 24 hours, 40° setup.....	110
Fig. 4.37 Combined bottom hole pressure data from tests, laponite-based pill.....	111

Fig. 4.38 Comparison of rheological profiles corresponding to recipe 2.BT and 3.LT.....	112
Fig. 4.39 Combined pressure data from tests performed using both pill types for comparison.....	114
Fig. 4.40 Boycott driven barite sag on the 40° inclined test setup.....	115
Fig. 4.41 Hindering effect on barite sag on the vertical test setup showing the sedimentation regimes in b) and c).....	115
Fig. 4.42 Source of channel (left) and channelling of WBDF along the pipe wall (right).....	117
Fig. 4.43 Pill Surface contaminated by fresh water from the sponge.....	118
Fig. A.1 Degree of barite sedimentation for recipe B1 (left) and recipe B2 (right).....	124
Fig. A.2 Bentonite pill recipe 2.B in sample cup tilted to horizontal.....	126
Fig. A.3 Recipe 1.B stability test.....	127
Fig. A.4 Recipe 5.L float test.....	127
Fig. A.5 Fluid break from the side (left) and from above (right).....	128
Fig. A.6 a) Fluid break placed up close to the pipe wall. b) WBDF flowing along the pipe wall.....	129
Fig. A.7 Foam removal using a hose.....	129
Fig. A.8 Pig used to clean the pipe wall and compress the pill from above.....	130
Fig. B.1 Rheological profile of brine, recipe AT.....	130
Fig. B.2 Rheological profile of WBDF, recipe BT.....	132
Fig. B.3 Rheological profile of recipe 1.B and 2.B combined.....	134
Fig. B.4 Isolation and stability test performed on recipe 1.B.....	138
Fig. B.5 Successful stability test using recipe 2.B.....	138
Fig. B.6 Test results after five days (left) and after twelve days (right).....	139
Fig. B.7 Source of WBDF channel created by pouring.....	140
Fig. B.8 a) First test – channel, b) First test – breakthrough and c) Second test – complete failure.....	140
Fig. B.9 Channelling of WBDF through recipe 2.L.....	142
Fig. B.10 Pressure profile corresponding to test pipe filled with water on the vertical setup.....	143

List of Tables

Table 2.1: Some common water-based fluid additives (modified from (Zamora & Stephens (n.d)).....	36
Table 2.2: Rheological Models (modified from Gabolde (2014)).....	42
Table 3.1: Original brine recipe A.....	66
Table 3.2: Bentonite-based pill recipes.....	67
Table 3.3: Laponite-based pill recipes.....	68
Table 3.4: Modified WBDF recipe B.....	69
Table 3.5: Gel strength values in lb/100ft ² displayed after mud program calculations.....	72
Table 3.6: Standard test procedure.....	76
Table 3.7: Mixing procedure and adjusted recipe 2.BT of the bentonite-based pill.....	78
Table 3.8: Mixing procedure and adjusted recipe 3.LT of the laponite-based pill.....	78
Table 3.9: Mixing procedure and adjusted recipe AT of the viscosified brine.....	78
Table 3.10: Mixing procedure and adjusted recipe BT of the water-based drilling fluid.....	79
Table 4.1: Rheological parameters of recipe 2.BT.....	81
Table 4.2: Viscometer data and rheological parameter of recipe 3.LT.....	99
Table A.1: Original base recipes used to develop and modify the WBDF recipe.....	124
Table A.2: Procedure for rheological measurements on original mixing day for the gel pill recipes.....	125
Table A.3: Procedure for rheological measurements after 24 hours for the gel pill recipes.....	126
Table B.1: Viscometer data and rheology parameters of the brine, recipe AT.....	131
Table B.2: Rheological parameters of the brine, recipe AT.....	132
Table B.3: Viscometer data of the WBDF, recipe BT.....	133
Table B.4: Rheological parameters of WBDF, recipe BT.....	133
Table B.5: Viscometer data of recipe 1.B.....	135
Table B.6: Viscometer data of recipe 2.B.....	135
Table B.7: Rheological parameters of recipe 1.B.....	136
Table B.8: Rheological parameters of recipe 2.B.....	136
Table B.9: Viscometer data of recipe 2.BT.....	137
Table B.10: Viscometer data of recipe 3.LT.....	141

1 Research Question and Objectives

Barite sag is known to cause problems during well construction and completion. As directional drilling and deviated wellbores become more common in production of challenging subterranean environments further problems regarding barite settling fall along with formation of particle bed on the low side of wellbore. Consequences as stuck pipe and in extreme cases hole abandonment can be experienced.

Barite sag occurs under certain well conditions both in static situations with absence of circulation and drill pipe rotation as well as dynamic situations involving low circulation rates. Followed by well geometries, temperature and pressures and is thereby hard to avoid. Due to the changes in the hydrostatic pressure profile caused by barite settling, well control issues and instabilities become a reality to deal with. Therefore, several studies have been conducted on developing methods and compositions for minimizing the sag of weighting materials in drilling fluids as well as controlling downhole pressure. Thus, these studies focus on cost efficiency with no further operational costs included to implement these methods and at the same time reduce rig down time.

Previous studies include methods for improving suspension of weighting agents without significantly increasing viscosity of the fluid (Temple, Paterson, & Leith, 2006), development of a fluid pressure transmission pill having high viscosity (Dobson, Tresco, & Geerdes, 2011) and a barrier functioning magnetorheological fluid spotted to isolate well zones (Kageler, 2014), among others.

This thesis contains a description of the development and characterization of a sag prevention gel pill minimizing the concerns associated with loss of bottom hole pressure profiles and additionally holding the settled barite in the experimental fluid system. The gel pill is utilized in a static fluid system where it is exposed to two interfaces: the lower one between a viscosified brine of 1.3 SG and the gel pill and that between a heavy water-based drilling fluid of 1.48 SG and the gel pill. The measured density of the gel pill was typically 1.03 SG.

The designed gel pills are clay-based, more specifically two individual pills being bentonite and laponite-based were designed. It is necessary to focus on the mineralogy and surface potentials of clays to get a deeper understanding of the essential properties. Such properties relate to as thixotropic behaviour, gel structure development and viscosity provided by clays when bentonite and laponite are dispersed in aqueous base fluids.

The sub-objective of the work described in this thesis intends to proof if the development and characterization of a sag prevention pill can prevent barite sag when applied in large-scale. Therefore, research questions are expressed as following:

1. What kind of rheological profile and properties shall the sag prevention pill have?
2. What is the maximum inclination at which the barite sag prevention pill is effective?
3. To what degree does the sag prevention pill transmit the hydrostatic pressure of the overlying fluid columns?
4. How effective is the sag prevention pill on tests performed on the large-scale test if the concept is approved?

To answer these research questions, experimental work was performed. Further, the work in this thesis can be divided into a main objective with supporting sub-objectives. The main objective of this thesis work intends to develop and characterize a sag prevention gel pill which transmits the hydrostatic pressure of overlying fluid columns placed above. Sub-objectives are listed as following:

- Characterizing rheological behaviour of the gel pill
- Testing the fluid designs fulfilling the criteria set on the large-scale test setup for proof of concept.
- Investigation of the developed fluid pills and further compare the functionalities of the bentonite-based pill with the laponite-based pill on large-scale.
- Studying possible penetration of barite particles into the gel pill.

2. Introduction

This chapter presents prior art review of supportive literature. The literature content starts with reviewing clay suspension behaviour and properties to gain a perspective of the importance regarding gel strength development. This part is a crucial criterion of the clay-based gel pill developed in this thesis work. Other supportive literature includes among others the concept and challenges regarding barite sag, methods used by the industry to deal with those and reviewing fluid pills implemented by the oil and gas industry.

2.1 Bentonite

Drilling fluids are connected to clay both via formations which are penetrated containing both clay and shale and via clay minerals, such as bentonite, added to the drilling fluid. Bentonite is an additive used in preparation of drilling fluids as a viscosifier and filter loss control agent. The most known and used bentonite is the Wyoming-bentonite from South Dakota, USA, which is the only natural source of pure sodium-based montmorillonite clay mineral. Bentonite produced in other regions often contains various amounts of calcium-montmorillonite which may result in different rheological properties. Therefore, such kind of bentonite is not accounted for the same quality and property as pure Wyoming-bentonite. In addition to the properties associated to the crystal structure of the montmorillonite and resultant surface properties, bentonite is further categorized as a dispersed colloidal system (Skjeggstad, 1989).

2.1.1 Clay Mineralogy

Colloidal Systems – Colloidal systems are characterized by the interaction behaviour between two phases of matter. They can consist of solids dispersed in liquids such as clay suspension and polymers, liquid droplets dispersed in liquids (emulsion), or solids dispersed in gases (smoke). Respectively to the thesis objective, this subsection will only consider solids (clays) dispersed in liquid such as water-based fluid systems.

Another characteristic for aqueous colloidal systems is that particles suspended in the liquid phase are so small that they are kept in suspension indefinitely by surrounded water molecules (i.e. gravity force does not act on them). The amount of colloids is often small in drilling fluids compared to the total solids content, but they play a significant role on mud

properties such as viscosity and carrying capacity which are controlled by surface properties. Their surface properties accounts for high activity in reactive forces due to the electrostatic imbalance of molecules in the surface layer. They have similar molecules on one side and dissimilar on the other side, whereas the interior phase has similar molecules on all sides, creating an electrostatic charge on the surface which depends on the coordination of atoms on both sides of the interface (Caenn, Darley, & Gray, 2017).

Hence, properties of colloidal systems depend on particle size, surface area and their specific properties, reactive forces between these particles (surface potential) as well as the surrounding medium (Skjeggstad, 1989). Therefore, colloids are further divided into two classes: clay minerals and organic colloids. Organic colloids account for macromolecules or long-chain polymers such as starches and other biopolymers, whose size provides the colloidal properties (Caenn et al., 2017).

Clay Minerals – Bentonite

Natural bentonite consists of several minerals, with the sodium-based montmorillonite being the dominant, followed by illite and kaolinite which can make up to 50% of the total composition of clay minerals in bentonite. In addition, 10 - 30% of non-clay minerals can also be present. The montmorillonite mineral, also known as smectite, constitutes for the hydration and thixotropic properties of bentonite (Skjeggstad, 1989).

Most clay structures consist of two fundamental crystal platelets, called octahedral and trioctahedral sheets (Loomis, Ford, & Fidiham, 1941). The octahedral sheet is coordinated with either oxygen (O) or hydroxide (OH) with aluminium atoms centred with equal distances to O or OH atoms. The aluminium atom can be exchanged by iron (Fe) or magnesium (Mg) atoms. If the metal atoms are magnesium, the structure is called brucite, $Mg_3(OH)_6$, and further termed trioctahedral with all three sites filled with magnesium atoms. In the montmorillonite structure, replacement of aluminium by magnesium atoms can vary (Skjeggstad, 1989; Caenn et al., 2017; Loomis et al., 1941).

Tetrahedral sheet – This sheet is structured with a silicon (Si) atom centred and coordinated with either oxygen or hydroxide in all four corners. Several silicon-tetrahedral sheets can tie up by sharing an O or OH atoms creating aggregates (Skjeggstad, 1989).

Smectite

As mentioned, montmorillonite accounts as a member of the smectite group and is the dominant clay mineral in bentonite. The montmorillonite mineral is constructed with two tetrahedral

sheets and the octahedral sheet sandwiched between them, sharing common oxygen atoms as shown in Fig. 2. 1 (Caenn et al., 2017).

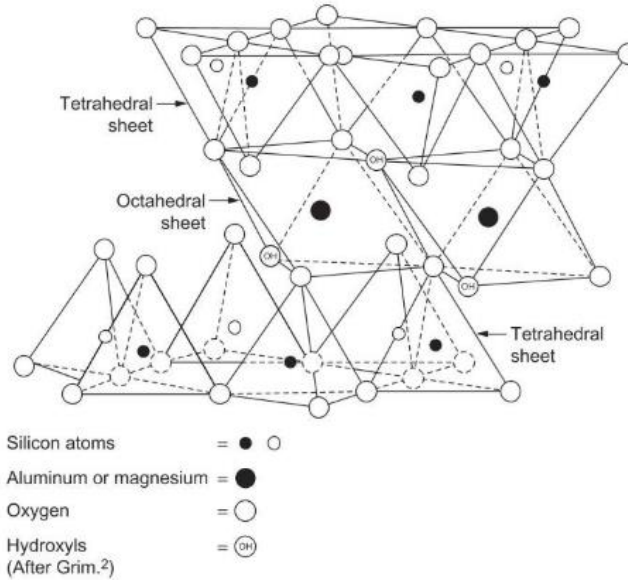


Fig. 2. 1 - Bonding between one octahedral sheet and two tetrahedral sheets through shared oxygen atoms (from Caenn et al. (2017))

2.1.2 Surface Potential of Bentonite

The montmorillonite crystal construction illustrated in Fig. 2. 2 , demonstrates an electrostatic neutral structure with silicon centred in all tetrahedral sheets and aluminium in the octahedral sheet. However, in nature crystal structure deficiency can occur resulting in more chemical and electrical active bentonite crystals. For instance and common for bentonite, if the aluminium atom (Al^{3+}) is replaced by a magnesium atom (Mg^{2+}), an immediate charge deficiency with a negative potential is created on the specific surface, as shown in Fig. 2. 2.

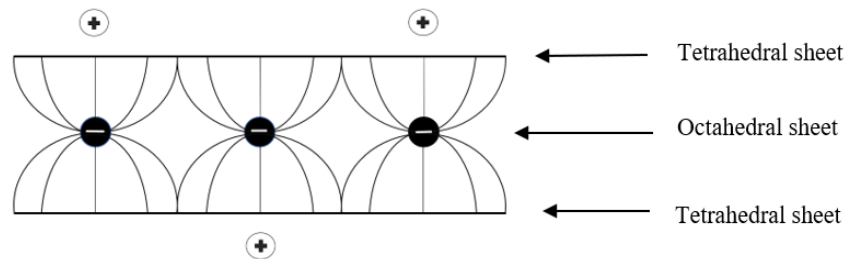


Fig. 2. 2 - Schematic of charges of a montmorillonite crystal (modified from Skjeggstad (1989))

This negative surface potential produces a negative charged electric field on the surface of the montmorillonite crystal. This negative potential is compensated by adsorption of cations reconstructing an electrostatic neutral crystal. In the presence of water, adsorption of cations can range from calcium (Ca^{2+}), sodium (Na^+), potassium (K^+) etc, and are known as exchangeable cations. The concentration of surrounding cations on the negatively surface potential will affect the cation exchange capacity (CEC). Meaning, that one type of cation bound to the surface can be exchanged by the same or another type of cation. For example, high concentrations of K^+ can in return exchange Ca^{2+} when the concentration of sodium is low (Skjeggstad, 1989; Caenn et al., 2017).

In addition to the charge originated in the octahedral sheet inside the montmorillonite structure creating the surface potential, fractures and breakage on the other hand provide a positive charge on the edge of the surface. Regardless, the crystal lattice is always negatively charged and dominate the effect of interaction between crystals, while the surface of fractures (edges) mostly are positive charged depending on the surrounding medium. If the surrounding fluid has a low pH (potential hydrogen), the charged edges are more likely to be positive charged compared to fluids having a high pH. The fact that low pH affects the electrical charge contributes to design drilling fluids of alkaline properties. Otherwise, the bentonite crystals tend to attract crystal lattices creating a flocculated mud which is not preferred (Skjeggstad, 1989).

2.1.3 Swelling Mechanism

The montmorillonite crystal accounts for the swelling mechanism of bentonite, where it can swell significantly by lattice expansion. More specifically, the sodium-based montmorillonite accounts for the greatest swelling capacity where sodium has been exchanged by calcium during electrical charge neutralization. The sodium ion (Na^+) does only tie up to one crystal surface, allowing larger volumes of water to further tie up on the crystal surfaces. The swelling pressure can become so strong that the sheets separate into smaller aggregates or individual layers, which further increases the swelling.

It is further anticipated that two different mechanisms control the clay swelling and thereby account for the large swelling capacity of the sodium-based montmorillonite crystal (Skjeggstad, 1989).

Crystalline Swelling

In crystalline swelling, water molecules bond to the tetrahedral sheet by adsorption. The water molecule (H_2O) acts as an electric dipole where the O-H bonds create angles of $103-106^\circ$ to each other forming a hexagonal structure which is similar to the tetrahedral sheet of angle 109° . There is currently no agreement on how the water molecules bond to the tetrahedral sheet, regardless, it is settled that such molecular and crystalline liquid films are created (Skjeggstad, 1989).

Osmotic Swelling

Osmotic swelling accounts for 80-90% of swelling associated with the sodium-based montmorillonite in the bentonite. This swelling mechanism occurs when multiple cations present in the liquid phase surround the crystal surface of the montmorillonite. The difference in cation concentration creates a chemical potential which is in imbalance. Hereby, water molecules are forced inside the clay crystals reducing the cation activity inside the crystal relative to the imbalance at the surface of the crystal. The bonding of cations in osmotic swelling is weaker compared to that of the crystalline mechanism (Skjeggstad, 1989).

2.1.4 Clay Particle Interaction Mechanism

Clay minerals accounting for colloidal suspensions in water-based fluids and their bonding forces play a major role in drilling fluid properties. The motive of adding bentonite to water-based systems is to obtain viscosity, yield point, thixotropic gel properties and filtration control. These properties give a signature to the desired rheological properties of the drilling fluid. However, these properties can easily be affected and manipulated by contamination from water-soluble formation clays which further react with the clay minerals in the drilling fluid. The interaction of bentonite minerals can be influenced by either attractive or repulsive forces which form different conditions of the bentonite-based drilling fluid. Additionally, mechanical shearing caused during stirring, composition of the solution in which bentonite crystals are suspended in followed by content of salt and pH value also can contribute to arrange different conditions (Skjeggstad, 1989).

Four mechanisms can generate these conditions of bentonite colloids suspended in water. These four conditions are illustrated in Fig. 2. 3 and are further described below.

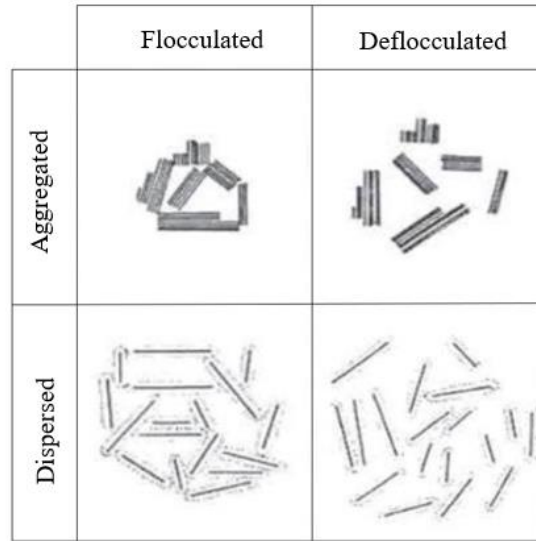


Fig. 2. 3 - Schematic of flocculation-deflocculation and aggregation-dispersion mechanisms (modified from Caenn et al. (2017))

Flocculation and Deflocculation

Flocculation of a solution containing suspended bentonite (montmorillonite) crystals occurs when the edges of fractured surfaces are positively charged. Crystals will create loose bonds to either edge to surface or edge to edge as demonstrated in the figure corresponding to flocculated and aggregated mechanisms (see Fig. 2. 3) (Skjeggstad, 1989). When referring to flocculate and aggregate conditions, it should be noted that the term flocculation is limited to the loose association of clay platelets that form flocs or gel structures (Caenn et al., 2017). Flocculation can be reversed or prevented by adding thinners which deflocculates the crystals by neutralizing the positive electrical charges at the edges of the crystals. The result is a mechanism of net negatively charged edges repulsing each other (Skjeggstad, 1989).

Aggregation and Dispersion

The term aggregation used in drilling fluids technology refers to the formation of aggregates of parallel platelets, where bentonite crystals are no longer separated into individual crystals. When aggregated, crystals are bonded and packet together deriving a suspension of fewer crystals and corresponding surfaces left for further bonding. Aggregated systems, stacks, can exist as both flocculated and deflocculated as represented in Fig. 2. 3 (Caenn et al., 2017).

During hydration or when exposed to strong mechanical shearing, these aggregated systems can be separated forming dispersion systems. Dispersion describes the mechanism of subdivision of particles aggregated in a suspension by electrochemical effects. Depending on

crystal surfaces being negative or positive charged, a dispersed system can be flocculated or deflocculated (Fig. 2. 3) (Skjeggstad, 1989).

2.1.5 Gelation Mechanism

For clays, such as bentonite, a mechanism of various linkages and plate orientations as described previously accounts for the gel structure development. These mechanisms refer to as:

- Crosslinked parallel plates forming so called “house of cards” structures by the negative and positive charged surface linkages.
- High repulsive potentials between the surface of clay minerals creating a parallel edge to edge platelet-oriented network.
- Parallel linkage of plates which are held together by water molecules between the plates.

The mechanism establishing a gel structure depends on the clay concentration in the given suspension as well as the strength and sign of charge potential on the platelet surfaces and edges. Gel structures in bentonite suspensions are not apparent unless salt is present to cause flocculation. If the concentration of clay in the suspension is high enough, in addition to the content of soluble salts, the mechanism of flocculation causes the formation of a continuous gel structure instead of individual flocs. Gel structures are developed slowly over time. Particles are oriented into positions of minimum free energy which is influenced by surrounding water molecules. A position of minimum free energy is obtained when for example a positive edge on one particle is attracted towards the negative surface of another particle. Thus, the time required for a bentonite suspension to attain maximum gel strength highly depends on the concentration of clay and salt and the involving flocculation value of the system. At very low concentrations of both, gelation can take days before it is observed. While high concentrations of salt can cause gelation almost instantaneously (Caenn et al., 2017).

2.1.6 Laponite for Application in Laboratory Experiments

Laponite RD (hereafter referred to Laponite) is a synthetic clay of layered silicate manufactured from naturally inorganic mineral sources. The synthetic laponite is produced in a process which involve the combination of sodium magnesium and lithium with sodium silicate producing an amorphous crystallised under controlled rates and high temperatures. The resulting laponite is eventually filtered, washed, dried, and milled to fine white powder (see Fig. 2. 4) (BYK Additives & Instruments, 2014).



Fig. 2. 4 - Laponite RD powder

Laponite is used as a rheology modifier and primarily added to water-based systems. Laponite is insoluble in water, but has properties leading to extreme hydration and swelling providing a clear and colourless colloidal dispersion as represented in Fig. 2. 5. The colourless and transparent dispersion property of laponite was the main reason for implementing this product in the experimental work to document possible penetration of barite particles through the designed gel pill.



Fig. 2. 5 - Laponite RD dispersed in a water-based system

Crystal Structure and Surface Potential

Laponite is a synthetic smectite clay with the corresponding empirical formula, see Fig. 2. 6 (a). The structure and composition of laponite is very similar to that of the natural clay mineral hectorite. The laponite crystal is constructed with an octahedral layer consisting of magnesium ions sandwiched between two parallel layers of tetrahedral with silicon atoms, as shown in Fig. 2. 6 (b). These platelets are electrically balanced by hydroxide groups and oxygen atoms with a natural positive charge provided by six divalent magnesium ions existing in the octahedral layer. This results in an anionic crystal.

In the case of magnesium atoms being substituted by lithium, a net negative charge is formed which is balanced by cations, primarily by sodium ions (Na^{2+}) (Ruzicka & Zaccarelli, 2011).

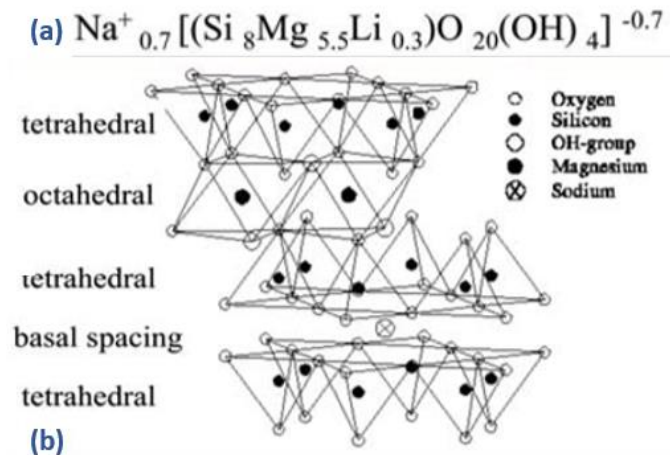


Fig. 2. 6 a) Empirical formula of Laponite. b) Idealised structural formula of Laponite (from Ruzicka & Zaccarelli (2011))

When laponite is dispersed in water, it forms a disc-shaped crystal due to its layer structure (see Fig. 2. 7 (a)) (Ruzicka & Zaccarelli, 2011). For comparison, bentonite has a similar disc-shaped crystal structure but is more than one order of magnitude larger in size, demonstrated in Fig. 2. 7 (b) (BYK Additives & Instruments, 2014).

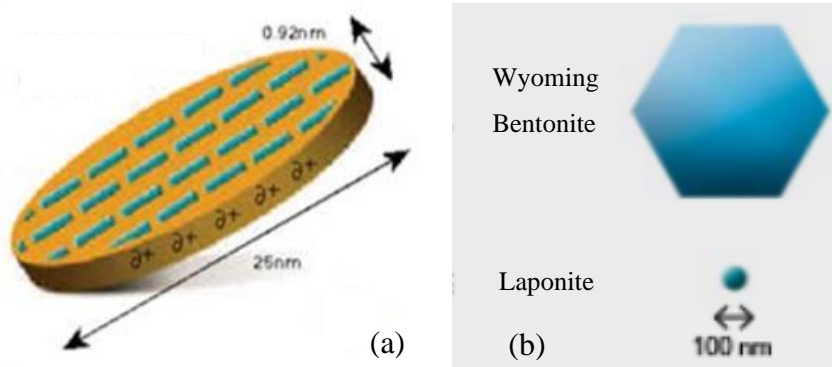


Fig. 2. 7 a) Single Laponite platelet (modified from Ruzicka & Zaccarelli (2011)). b) Comparison of particle size between bentonite and laponite (modified from BYK Additives & Instruments (2014))

Laponite forms highly thixotropic gels already at concentrations of 2% or greater when dispersed in water. Once added to water, laponite hydrates forming aggregated particle stacks. During the process of dispersion, these packs are further ruptured to individual particle stacks (see Fig. 2. 8).

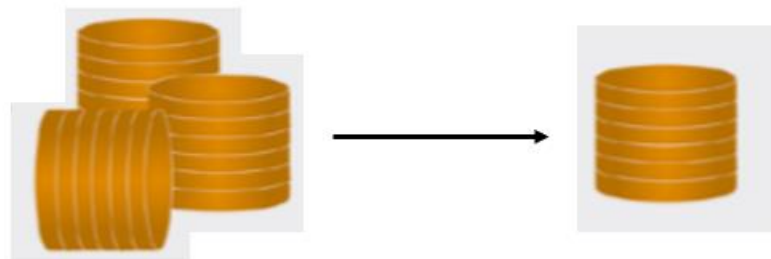


Fig. 2. 8 - Aggregated particle stacks dispersed into individual particle stacks (modified from BYK Additives & Instruments (2014))

As the surface area is reduced significantly, electrostatic attractions draw sodium ions being in solution (from salts) towards the crystal surface as shown in Fig. 2. 9. At this stage, with sodium ions between the electrical double layer, swelling proceeds and the osmotic pressure pulls the electrical double layer further apart exerted from the bulk of the water (see Fig. 2. 9).

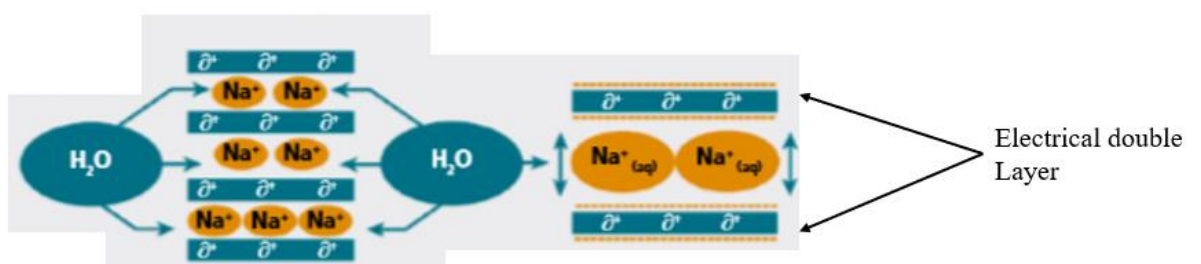


Fig. 2. 9 – Hydration of sodium ions swelling inside the structure (modified from BYK Additives & Instruments (2014))

However, the content of salt providing sodium ions controls the osmotic pressure distinct, allowing the electrical double layer to contract such that the positive charge on the edge of the crystals are able to interact with the negative surfaces of other surrounding crystals.

This process continues until a house of cards structure is developed creating a highly thixotropic gel. This particular gel structure consists of single flocculated particles held together by weak electrostatic charges as shown in Fig. 2. 10 (BYK Additives & Instruments, 2014).



Fig. 2. 10 - House of Cards structure from gel formation (from BYK Additives & Instruments (2014))

The gel structure is broken down by applied shear stress and the gel structure requires time to re-form after shear stress is removed as the particles must re-orient themselves into the house of card structure.

The addition of laponite in aqueous systems provides highly efficient fluid properties. It is mainly used as a rheology modifier due to its thixotropic shear sensitive viscosity. The viscosity of the laponite suspensions depends upon the solids and the electrolyte content of the liquid phase. Further, laponite-based suspensions are shear-thinning with a small degree of resistance to flow and low viscosity under high shear rates. As the structural bonds are ionic, temperature does not affect the viscosity. Thus, this significant property in addition to quick gel structure development for concentrations of 3% provide good suspension properties.

Important advantages regarding the use of laponite include superior flow control under high pressure and temperature. Laponite is not affected in a great sense of degradation when exposed to high shear processes or high temperatures. Like other colloidal materials, laponite is a natural film former. The unusual shape of the laponite crystal, combined with its anionic nature, enables the product to produce a film with properties such as barrier functionalities, conductive and anti-blocking (BYK Additives & Instruments, 2014).

2.2 Drilling fluids

Besides of acting as the primary barrier during drilling, functionality of drilling fluids in the well are various. Some of the most essential can be listed as: cuttings transport, suspend and release solids in the well, minimizing reservoir damage, ensuring adequate formation evaluation, control erosion as well as cooling and lubricate the drilling assembly and drilling bit. In addition to the functional tasks, drilling fluids are also used in operational sequences. These can be ranged as displacement of other fluids in the well, fracturing the formation during pressure tests for instance, cleaning the well, performance of acid treatment on formations and transmitting hydraulic horsepower to the drill bit, among others. Common types of drilling fluids used in operational drilling phases are water-based mud (WBM), oil-based mud (OBM), synthetic based mud (SBM) and so-called fluid pills of various properties and areas of utilization (American Society of Mechanical Engineers. Shale Shaker Committee, 2005).

2.2.1 Water-Based Drilling Fluids

For drilling fluids to perform the previous mentioned tasks and functionalities, different types of drilling fluids defined by required properties are used. Even though OBM, SBM and pneumatic drilling fluids are among the common mud systems available in the industry (Zamora & Stephens, n.d), only water-based drilling fluids will be covered as it the fluid system used in this thesis.

Water-based drilling fluids and water-based muds are often mention about each other by the industry and literature. The distinct difference is that water-based mud consists of clay minerals creating the base of the fluid's property. Water-based drilling fluids however are designed with other non-clay minerals and additives providing the necessary properties (M. Khalifeh, personal communication, May 2020). Thus, the abbreviation WBDF and water-based fluids will be used as a general term for water-based fluid systems in this thesis. Water-based mud will be referred to as WBM for clay-based systems only.

WBDFs are the most extensively drilling fluids used in the industry. They are in general easy to develop, inexpensive to maintain and can be designed to manage most drilling problems (Amoco Production Company, 1994). Water-based fluid systems are very sensitive to temperature, but relatively unaffected by pressure due to incompressibility. Thermal stability of water-based fluids is controlled by reduction of active solids concentration (especially bentonite) (Amoco Production Company, 1994; Zamora & Stephens, n.d). In addition,

polymeric additives are preferred for viscosity and suspension control. WBDF consists of an aqueous phase which can be treated with chemicals. The base fluid can be fresh water, seawater, saltwater, or saturated saltwater, depending on the necessary fluid properties. Additives are added to the fluid to gain desired properties. A known disadvantage regarding untreated WBDF is the chemical differences leading to interactions between the drilling fluid and reactive shales. These interactions can lead to shale swelling or softening which again causes problems such as sloughing and tight hole conditions (Zamora & Stephens, n.d). Salts are added to WBDF inhibiting the hydration and swelling of clays and reactive shales (Equinor, 2018).

As mentioned, the type of WBDF to use and its ability depend strongly on the well conditions followed by operational parameters. Water-based fluid systems have been used in deviated sections as well as extended-reach drilling. In such situations, WBDF has proven that lubrication can be preserved by additives used to lower the friction factor. Also, shale stabilities and required hole cleaning are achieved using water-based fluids (Caenn & Chillingar, 1996). As WBDF is characterized as nontoxic, inexpensive and provides an extensive area of use, future development concentrated on water-based systems performing like an OBM. As a range of application cannot be managed by other fluid types than OBM. Unique properties of the OBM account for resistance to contamination, highly lubricious, inhibitive regarding shale welling, non-corrosive and being stable at high temperature and pressure, to mention some (Zamora & Stephens, n.d).

Selection of a WBDF system is affected by several factors with efficiency being an important factor reflecting operational costs. Further selection of WBDF systems depends on well types and size, well conditions based on temperature and pressure and followed by drilling equipment available on the rig. The geology of the formation planned to drill through also plays a major role where knowledge about sand and shale type as well as formation types as salts, limestone and carbonate rocks also influence the choice of drilling fluid type (American Society of Mechanical Engineers. Shale Shaker Committee, 2005; Equinor, 2018). The fact that environmental, technical, and economic requirements are increasing in the industry, fluid selection criteria are constantly changing and the need of a fluid systems adapting to such requirements is essential.

Commonly used water-based fluid systems employed in Norway can be divided into three main groups:

1. Spud Mud

Spud mud consists of fresh water as base fluid and is typically viscosified using bentonite clay. These are simple fluids and often used as high viscous sweeps when drilling a top-hole section with seawater (Equinor, 2018). Spud mud weighted with barite is also used to displace the entire well once the total depth of a specific section is drilled prior to pull out of hole to run casings (K. Taugbøl, personal communication, April 2020).

2. Inhibitive Polymer Drilling Fluids

These are high performance-inhibitive systems consisting of KCl, polymers and glycol-based drilling fluids. These fluids are implemented in intermediate sections with the main focus on shale inhibition (Equinor, 2018). Further additives involve xanthan polymer for viscosity and rheology control, starch, and PAC polymers for fluid loss control. Barite is added for density and other chemicals can be added for pH control and lubricity. These systems are also used in exploration wells with temperature up to 120°C. As these fluids are characterized as environmentally friendly produced cuttings can be discharged to the sea (K. Taugbøl, personal communication, April 2020).

3. Brine-Based Reservoir Drilling Fluids

This fluid category is based on a heavy brine with low solids content where no weight materials are added. This system consists simply of polymers for viscosity and fluid loss control with calcium carbonate (CaCO_3) added for bridging. Such systems are used for drilling reservoir sections and are designed to minimize reservoir damage and maximize productivity (Equinor, 2018; K. Taugbøl, personal communication, April 2020).

2.2.2 Drilling Fluid Additives

Additives are materials added to drilling fluids to obtain desired fluid properties to prevent and correct fluid related problems. Application of additives further depend on fluid compositions, specific well conditions and requirements (Amoco Production Company, 1994). It is important that the supplemental additives accomplish their desired functions without disturbing the original rheological behaviour of the drilling fluid (Zamora & Stephens, n.d). Table 2. 1 represents common water-based fluid additives.

Table 2. 1: Some common water-based fluid additives (modified from (Zamora & Stephens (n.d)).

<i>Weight Materials:</i>	barite, hematite, calcium carbonate
<i>Viscosifiers:</i>	bentonite, biopolymers (xanthan and welan gum), guar gum
<i>Dispersants and Deflocculants:</i>	lignite, potassium, lignosulfonate
<i>Filtration- Control agents:</i>	starch, polyanionic cellulose (PAC), lignite
<i>Shale Stabilizers:</i>	potassium acetate, asphalt, KCl, glycol
<i>Lubricants:</i>	polyglycol, fatty acid blend, diesel oil, solid beads (plastic, glass)
<i>Lost-Circulation Materials:</i>	nut shells, mica, cane fiber, shredded paper
<i>Commercial Chemicals:</i>	sodium chloride (NaCl), calcium chloride (CaCl ₂), caustic soda (NaOH), soda ash (Na ₂ CO ₃)

When designing water-based fluid systems, the involvement of salts such as KCl combined with glycol is essential for shale stabilisation. Such potassium-based muds are referred to as inhibitive muds and used to prevent potential reactions with formation sections to be drilled (Skjeggstad, 1989). However, the type of additives used in the developing of drilling fluids in this thesis covers weight materials, viscosifier and commercial chemicals with the literature content focusing on these.

Weight materials are primarily used to increase the fluid density in order to control the hydrostatic pressure in the well with respect to formation pressure (pore pressure). An increase in mud weight is often required to manage wellbore instabilities caused by formation stresses in addition to improve the cuttings transport (M-I SWACO, 1998; Baroid Drilling Fluids, 1998).

Viscosifiers modify the fluid's rheology by increasing the viscosity and yield point to enhance transport abilities and suspensions of solids. Viscosifiers such as clays also provide gelatinous properties to employ low-shear viscosity fluids (M-I SWACO, 1998). While commercial chemicals cover mainly salts used for pH control and shale inhibition

Barite – BaSO₄

Barium Sulphate, called Barite is an inert solid with specific gravity of 4.2 (SG) providing a fluid density ranging roughly between 4194 to 4290 kg/m³. It is also known as a weight agent used in drilling fluids for density achievement. API grade barite has remained the standard weight material used by the fluid industry (Baroid Drilling Fluids, 1998). When employing barite, particle size plays a major role on the drilling fluid properties. When large particles are used, a thick drilling fluid for suspension is required and larger barite particles are removed by the shaker. Thus, more continues addition of barite is necessary to maintain a

desired mud weight. Too fine particles on the other hand are undesirable due to a large total surface area of solids in the suspension (American Society of Mechanical Engineers. Shale Shaker Committee, 2005).

Xanthan Gum

Xanthan Gum (XG) is a natural polymer (biopolymer), used as a viscosifiers to adjust rheological properties. XG has a high molecular weight and the entangled polymeric structure provides a non-Newtonian nature to the drilling fluid. Employment of XG provides good viscosity properties and reduces drag in turbulent flow at low solids content. The increase in viscosity obtained by the xanthan gum molecular structure provides shear thinning properties to the fluid. Other unique rheological properties include high, low-shear rate viscosity for suspension and carry capacity which is important for hole cleaning. XG is therefore used in applications as drilling, completion, coiled tubing and in fracturing fluids. Additionally, xanthan gum is very resistant to shear and temperature, but decomposition of xanthan gum by aerobic bacteria and degradation can occur at 120°C. (Caenn & Chillingar, 1996; Liu, Ren, Wen, & Dong, 2018; Caenn et al., 2017).

Calcium Chloride - CaCl_2

Calcium chloride is a type of salt widely used in drilling fluids and especially in completion fluids for consistency, increasing density and stabilizing formations such as shale (K. Taugbøl, personal communication, April 2020).

Sodium Carbonate – Na_2CO_3

Sodium Carbonate, also called Soda Ash is a weak alkaline equivalent to a pH of 11.0 for a 10% solution (Amoco Production Company, 1994). It was precisely used to control the pH of the fluid employed (M-I SWACO, 1998).

Sodium Hydroxide - NaOH

Sodium hydroxide, known as Caustic Soda, is a type of strong base material with a pH of 14.0 (Skjeggstad, 1989) and is often used to form a strong and stable alkaline pill and maintenance of higher pH values (Amoco Production Company, 1994).

2.2.3 Fluid Pills

Fluid pills define a relatively small volume with special properties to perform a specific task that regular drilling fluids cannot manage (American Society of Mechanical Engineers. Shale Shaker Committee, 2005). Examples on traditional pill systems used by the industry range from lost-circulation material pills, high-viscosity pills used for improved circulation and barrier functionalities, heavy displacement pills used during cementing and solids free pills employed in reservoir drill-in situations. Followed by saturated salt pill, also called kill pill, to isolate completions fluids from the production zone and freshwater pills implemented when drilling through salt sections (M-I SWACO, 1998). As a gelatinous pill was designed in this thesis, and the fact that gel pills often are confused with viscous pills, the usage and properties of a viscous and gel pill will be discussed supporting the application reflecting this thesis work.

Viscous pill

The employment of viscous pills was a methodology used in the Hassi-Massoud field at the beginning of the 1990s. The pill was design with respect to adequate pill density and required yield stress as well as gel strength with the aim of increasing the success rate regarding cement placement jobs (Fosso, Tina, Frigaard, & Crawshaw, 2000).

A designed viscous pill defines a highly viscous fluid pill with no real gel strength developed. Such pills are often constructed by polymers suspensions in water systems. When for instance biopolymers such as xanthan gum are used, the proper viscosity property is achieved by long chain mechanisms. The polymer molecules tend to associate with the long-chain backbones wrapping around each other. This mechanism develops massive dispersed packets for viscosity propose (Caenn et al., 2017). Generally, viscosity is obtained by polymers due to interactions between the polymer molecules and water, polymers themselves and by solids (Amoco Production Company, 1994).

The employment of viscous pills is mainly referred to off-bottom cement plug processes with the viscous pill acting as a spacer fluid achieving stability when it is placed between the cement plug and heavy drilling mud (Fosso et al., 2000). This method described is utilized to avoid Rayleigh-Taylor instabilities (Taylor, 1950).

Gel pill

Viscous and gelatinous based fluid pills are often mistaken and, in some cases, understood as being the same primary property in a designed fluid. This confusion may be originated by the

fact that development and characteristics of a gel structure in a suspension is widely controversial between scientists with different background. To obtain a consensus regarding the term gel is hard as different types of gels have widely different structures.

Over the past decades different authors have established some definitions of the term gel based on various fluid suspensions which have been pointed out to be partial to flaws. In the paper published by Almdal, Dyre, Hvidt, & Kramer (1993) existing definitions on the term gel given by P.H. Hermans are described. Herein, gels are defined as a) cohesive colloid dispersed systems consisting of at least two components, b) they involve characteristic mechanical properties of the solid state and c) that both the medium in which the components are dispersed in extend themselves continuously through the entire system.

However, the definitions proposed by Herman do not include fully reacted thermosets and produced cross-linked polymer suspensions. It is further argued that such systems consist of one large molecule and therefore are characterized as one-component systems. A classification of gels based on structural criteria was later introduced and named as the Flory-Stockmeyer theory and is mentioned by Almdal et al. (1993) as following: a) well-arranged lamellar structures which include gel mesophases, b) covalent polymeric networks which are completely disordered, c) polymer networks formed by physical aggregations and d) particulate and disorganized structures.

Also Flory's classifications was met with disagreement to a certain degree by the authors which further argued that Flory neglected the requirement of two components in addition to group d), describing a suspension of rods forming typical gel properties only at certain ranges of concentration.

More cautious phenomenological definitions of the term gel were established, stating that gel is a jellylike substance formed in the solid phase of colloidal solution and thereby is the opposite of a sol. Sol is defined as the solution of particles floating freely around in the solvent. For classical types of gels, it was stated that gel is a solid or semisolid material consisting of at least two components, of which one is the liquid phase and the other a soft and resilient material (Almdal et al., 1993).

The developed classifications and definitions on the term gel provided the basis to new phenomenological definitions which were proposed by Almdal et al. (1993). They stated that a gel is a homogenous, soft, solid or semisolid material with liquid present in considerable amounts.

The wide definition of gel and its degree of disagreement also yields for the physical details associated with the gel structure development. Regardless, it is universally accepted that

gel in clay-based systems is obtained by electrical attractive forces between clay minerals and suspended ions from the surrounding liquid. Followed by hydration of clay crystals forming highly thixotropic gel structures, as described previously. Common for gel pills is that shear forces exceeding the developed yield point of the fluid are required to initiate flow. As flow is induced and the developed gel structure is degraded, or broken, the viscosity will in return also be decreased (Caenn et al., 2017).

A bentonite-based gel pill represents a gel pill by its nature. However, polymer systems which are crosslinked could form a gel structure, and thus be characterized as a gel pill. Relative to clay-based systems, polymer suspensions develop a gel structure based on two individual mechanisms. Polymer gels are based on electrostatic forces between the molecules and surrounding medium and braiding of chain structures, while clay-based gel only depends on the electrostatic forces creating bonds to edge-edge or edge-surface area of the individual clay crystals. Dispersion of the individual clay crystals is also essential for gel formations. For instance, two large lumps of clays submerged in water will not form a gel structure. The electrostatic forces required to form gel become more attractive once crystals are dispersed freely such that the distance between individual platelets decreases forming a network. Disclosed and common for gel structures is the physical network formed by electrostatic forces and the fact that developed gel structures can both be irreversible and reversible where this network is regenerated after the gel structure has been ruptured (A. Saasen, personal communication, May 2020).

In recent studies, gel pills have mainly been developed to function as fluid barrier pills mainly to isolate different fluid sections as well as transmitting hydrostatic fluid pressure as described in chapter 2.6.

2.3 Rheological Fluid Properties

The drilling fluid industry relies on several parameters to describe rheological fluid properties. The science of fluid rheology is concerned with the deformation of all fluids reflecting the fluids behaviour at different flow regimes (laminar and turbulent flow), pressure and temperatures among other effects. Even though rheological models are essential to predict fluid characteristics for practical purpose, this chapter will mainly focus on the rheological properties rather than rheological models. Properties respectively to clay mineralogy and electrochemical

environment devotes the large deviation in consistency of drilling fluids. Further, consistency curves obtained from rotary viscometer differs from fluid to fluid depending on particle concentration, size, and shape. This is mostly experienced in low-solid fluids containing a high proportion of clay particles or long-chain polymers, and less for high-solid fluids containing barite for instance (Caenn et al., 2017).

2.3.1 Viscosity

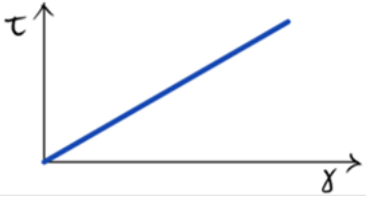
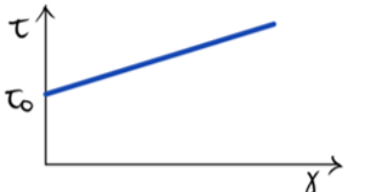
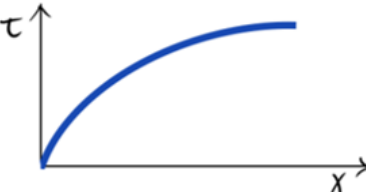
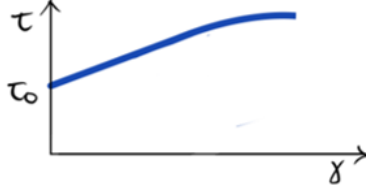
The term viscosity is used to describe a fluid's resistance to flow. The viscosity of a fluid further depends on parameters such as temperature, pressure, shear rate and the physical and chemical properties of a fluid. The resistance of a fluid to flow is caused by frictional forces between the particles in the suspension and attractive forces of the particles due to electrostatic charges. In more detail, the flow behaviour and its resistance to flow can be explained by a shear stress and shear rate relationship of the fluid. When a fluid is flowing, a force corresponding to shear stress oppose the flow. Shear stress can in this case be understood as a frictional force acting when one layer of fluids slides by another. The rate at which these layers are moving past other layers is called shear rate (American Society of Mechanical Engineers. Shale Shaker Committee, 2005).

For non-Newtonian fluids, the effective viscosity (μ) expressed in centipoise (cP) is obtained by dividing the fluid's shear stress (τ) over the corresponding shear rate (γ) at a certain point of shear stress/shear rate measurement as shown in Eq. 2-1 (M-I SWACO, 1998).

$$\text{Effective viscosity } (\mu) = \frac{\text{shear stress } (\tau)}{\text{shear rate } (\gamma)} \quad \text{Eq. 2-1}$$

2.3.2 Rheology Models

Table 2. 2: Rheological Models (modified from Gabolde (2014))

Rheological Models	Equation	Flow Curve	Rheological Formulae for concentric-cylinder viscometer	
Newtonian Model	$\tau = \mu_a \gamma$		$\mu_a = \frac{\theta_{600}}{2}$ Apparent viscosity (cP)	
Bingham Plastic Model	$\tau = \tau_o + \mu_p \gamma$		$\tau_o = 2\theta_{300} - \theta_{600}$ Yield value (lb/100ft ²) $\mu_p = \theta_{600} - \theta_{300}$ Plastic viscosity (cP)	
Power Law Model	$\tau = K \gamma^n$		Pipe Flow $n_p = 3.32 \log \frac{\theta_{600}}{\theta_{300}}$ $K_p = \frac{\theta_{300}}{511^{n_p}}$	Annular Flow $n_a = 0.657 \log \frac{\theta_{100}}{\theta_3}$ $K_a = \frac{\theta_{100}}{170.3^{n_a}}$
Herschel-Bulkley Model	$\tau = \tau_o + K \gamma^n$		$\tau_o = 2\theta_3 - \theta_6$ $n = 3.32 \log \frac{\theta_{600} - \tau_o}{\theta_{200} - \tau_o}$ $K = \frac{\theta_{300} - \tau_o}{511^n}$	
Where K_p , K_a , and K are the consistency indexes and n_p , n_a and n the rheological indexes.				

2.3.3 Bingham Plastic Model

The Bingham plastic model describes fluids with properties such as yield point and suspension of solid particles. This model also provides calculation of the important parameters as plastic viscosity and yield point of a fluid (see Table 2. 2), provided by the mud program on the viscometer used (M-I SWACO, 1998).

Plastic viscosity (PV) - Describes the quantity of stress (mechanical friction) creating a resistance to flow and is further used as an indicator for size, distribution, and portion of solids in the fluid. PV also provides a measured value for the viscosity of the liquid phase under dynamic flow conditions (American Society of Mechanical Engineers. Shale Shaker Committee, 2005)

Yield Point (YP) - The yield point of a fluid (often expressed in lb/100ft²) defines the force required to initiate laminar flow. YP is a measurement indicating the electrical attractive forces in the fluid under flowing conditions and is dependent on surface properties of the solids suspended in the fluid, concentration of solids and the electrical environment created by the liquid phase (Baroid Drilling Fluids, 1998;K. Taugbøl, personal communication, May 2020).

2.3.4 Herschel-Bulkley Model

The Herschel-Bulkley Model (H-B), also called Yield Power Law Model is the most accurate model used to predict the rheological behaviour of most drilling fluids (Baroid Drilling Fluids, 1998). This model displays a combination of pseudoplastic and thixotropic fluid characteristics. The H-B model does also consider that most drilling fluids exhibits yield stress and describes the behaviour of a fluid by Eq. 2-2:

$$\tau = \tau_o + K * \gamma^n \quad \text{Eq. 2-2}$$

with the associated parameters provided in Table 2. 2. In the H-B model the parameter τ_o equivalent to τ_y used in calculations can be considered as the gel strength of the fluid at zero time. When the fluid's flow index, n, or also called rheological index is equal to one, the H-B model is reduced to the Bingham. Moreover, the model is reduced to the power law model when τ_o is equal to zero (Amoco Production Company, 1994).

2.3.5 Gel Strength

Gel strength is a time-dependent measurement of a fluid's shear stress, hence measuring the attractive forces under static conditions related to time. The gel strength value of a particular fluid is obtained by measuring the shear stress after the fluid has been static for a certain time period when circulation is regained at low shear rates. Common recordings are the initial gel strength obtained after 10-seconds, and 10-minutes value obtained after 10-minutes at static before the gel structure is broken by higher shear rates.

The development of gel strength in relationship to time varies widely from mud to mud type depending on composition and its degree of flocculation as demonstrated in Fig. 2. 11.

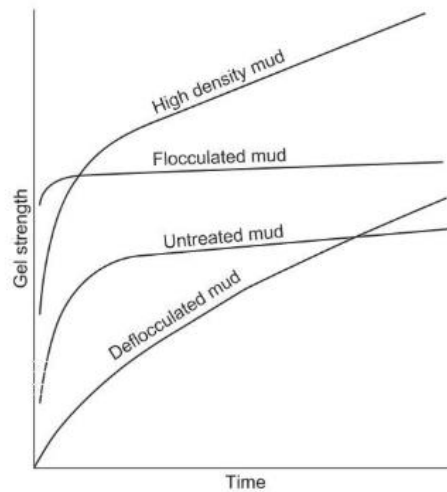


Fig. 2. 11 - Schematic of increase in gel strength of various mud types with time (from Caenn et al. (2017))

Gel strength can additionally give an indication on the fluid's capacity to suspend solid particles in the fluid when circulation is stopped or ceased to prevent particle sag related problems. Requirements for gel strength involve sufficient solids suspension, but simultaneously not negatively affect the equivalent circulation density (ECD) management. Followed by high pump pressure in regard with fracturing the formation causing extensive fluid loss when breaking the gel strength by regaining circulation (Caenn et al., 2017).

As mentioned, the development of the gel structure is time dependent. Fig. 2. 12 demonstrates the deviation in gel strength of a fluid immediately after breakdown (Curve A) and after a longer static period (Curve B). Moreover, Caenn et al. (2017) relates to studies that have discovered that the 10-minute gel strength value might not be a reliable indication of the ultimate gel strength. Reasoned by the fact that two individual fluids can have approximately

same 10-min gel strength values but show large diversity in the ultimate gel strength value reached.

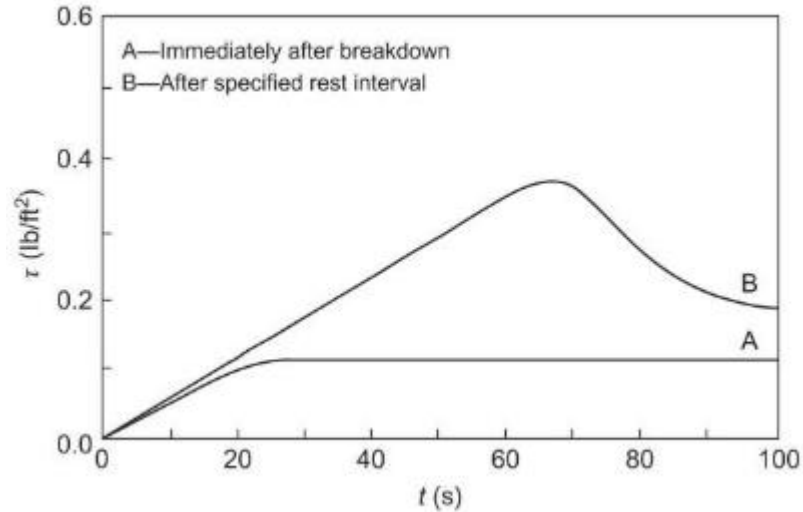


Fig. 2. 12 - Shear stress loading curves (from Caenn et al. (2017))

2.3.6 Thixotropic Fluids

Water-based drilling fluid systems exhibits thixotropic properties which is caused by the presence of electrically charged particles or polymers by linkage forming a rigid matrix (M-I SWACO,1998). For clay-based systems, the colloidal solutions form a gel, which is caused by clay platelets slowly arranging in position of minimum free energy to satisfy the current electrostatic surface charges. At constant rate of shear, the clay platelets adjust themselves gradually to the applied shear conditions. In respond, the viscosity of a thixotropic fluid depends on the shear rate and time of shearing respectively due to the changes of the structural components over time. The thixotropic effect is observed from rheological parameters as the change in torque when sheared at constant rate over time. However, thixotropy should not be confused with plastic fluid properties, as the effective viscosity depends on the applied shear rate and the fluid's resistance to shear (Caenn et al., 2017).

2.3.7 Shear Thinning Fluid Property

Plastic fluids require a finite stress to initiate and maintain flow due to their yield point. Quemada (1998) expressed complex drilling fluids which are multi-component systems as

concentrated dispersions. Followed by that fluid properties large diversity is based on their existence of internal structures (microstructure) as well as shear-induced changes of these microstructures. Quemada (1998) further introduced the term shear-dependent structures which is based on the behaviour of Structural Units (SUs). SUs are defined as the structure of any concentrated dispersion which cannot be characterized by its microstructure alone. In fact, complex SUs are either individual particles or primary flocs which can form larger groups such as clusters, aggregates and flocs creating a sample spanning structure. Common for these structural units is that they are dependent on applied shear stresses. Fig. 2. 13 demonstrates the shear thinning behaviour on the structure (Quemada, 1998).

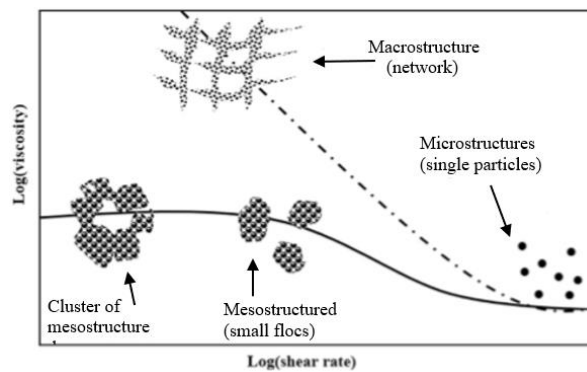


Fig. 2. 13 - Structural interpretation of shear-thinning and plastic fluids (after Quemada (1998))

Groups of clusters are present at low shear rates. As the shear rate increases, particles align and orient with respect to the direction of flow which decreases the effect of attractive forces between particles. Large cluster networks are ruptured due to hydrodynamic stresses forming smaller clusters which eventually create a single particle system. This behaviour is associated with a fluid having shear-thinning properties. Thus, the term shear-thinning applies for fluids consisting of microstructures where the effective viscosity decreases with respect to increased shear rate (Quemada, 1998).

2.3.8 Pseudoplastic Fluids

These fluids are characterized as shown in Fig. 2. 14 with the fluid's effective viscosity decreasing as shear rates increase. Their consistency curve is further characterized by no yield point. Long chain polymer suspensions create this typical pseudoplastic fluid behaviour. When at rest, the chains are randomly distributed and do not set into structures due to repulsive

electrostatic forces. Shear rate initiating the fluid in motion is required to align chains parallel of themselves in the direction of flow. This behaviour increases with respect to increased shear rate causing the effective viscosity to decrease (Caenn et al., 2017).

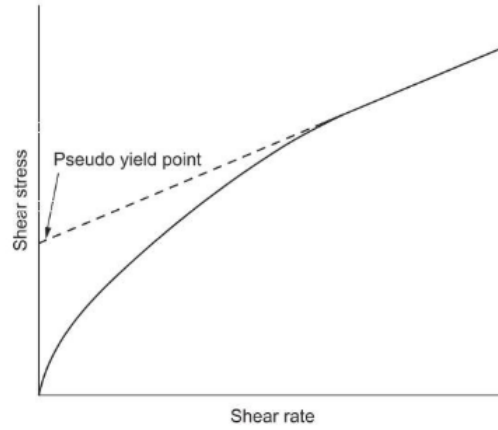


Fig. 2. 14 - Consistency curve of a pseudoplastic fluid (from Caenn et al. (2017))

2.4 Barite Sag Mechanism

Barite sag accounts for the same category as weight material sag (calcium carbonate, hematite, etc), and hence sag occurs in all drilling fluid types where weight materials are used to achieve density. The sag mechanism of inert particles is therefore important to understand.

Barite sag is the mechanism when particles separate from the liquid phase in which particles originally were suspended in. These inert solid particles settle and at appropriate shear rate conditions, formation of an ultra-high density slurry or often called barite bed is created at either the low side of the hole for deviated situations or at a point where particle accumulation is possible (M-I SWACO, 1998). Shear rate conditions at which particles start to sink downwards, further depends on the particle size, diameter, and density. This is linked to suspension properties of the drilling fluid regarding density and viscosity. It is fundamental to understand the motion of particles at such critical shear rates which is described by Stoke's law below (Omland, Saasen, & Amundsen, 2007).

$$V_T = \frac{2Rg(\rho - \rho_o)}{9\eta} \quad \text{Eq. 2-3}$$

Eq. 2-3 expresses the settling velocity of a single particle (V_T), where R is the particle radius, g the gravitational constant of 9.81 m/s and η is the fluid's viscosity. Particle density is given by ρ and ρ_0 corresponds to the density of the fluid in which the particle is suspended in. However, Stoke's law neglects the particle-particle interaction and does not account for temperature effects nor a polydisperse particle distribution (Omland et al., 2007).

2.4.1 Hinderling Effect

In vertical wells, the hindered settling is noticeable slower than the free settling rate of a single particle (Stoke's Law) due to particle-particle interaction hindering each other and thereby lowering their settling velocity. A single particle or floc settling in a static fluid system has a specific settling velocity with respect to its shape, size and density in addition to the fluid's viscosity. With increased concentration of particles, they start to interfere and hinder each other, known as the hindered settling effect. As the particle concentration increases, particles are in constant contact with each other building a particle framework. Up to this point, the water supporting system is changed to a sediment supporting system (Dankers & Winterwerp, 2007).

Fig. 2. 15 demonstrates the settling mechanism of particles affected by the hinderling effect in a vertical tube. Particles denser than the suspending fluid settle vertically downwards due to gravitational effects at a rate of v_0 . During hindered settling, three regimes of particle sedimentation occur with the particle concentration predominately increasing from top towards bottom over time until equilibrium is reached (Zamora, 2009).

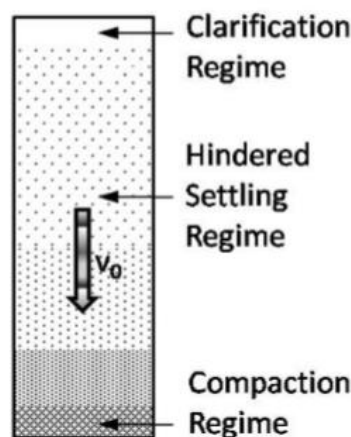


Fig. 2. 15 - Hindered settling kinetics under static condition (from Zamora (2009))

In more detail, these sedimentation regimes are defined as:

Clarification Regime - The few remaining particles left in the fluid phase settle individually, also referred to as free settling, where minimal interference from the tube walls and nearby particles. In this regime, the particle settlement applies Stoke's Law (Zamora, 2009).

Hindered Settling Regime - In this region, the particle concentration is so high that surrounding particle accumulation interfere with the settling of individual particles. This mechanism contributes to reduction of the settling rate below to that of free settling. In case of fluid properties causing particles to aggregate and form clusters or flocs, the settling rate however can be increased due to increased floc sizes (Zamora, 2009).

Compaction Regime - The compaction regime accounts for the sediment supported system at the bottom of the tube. The transition from water to sediment supporting system is called gelling, where at this point the gelling concentration reflects the concentration of the suspension. In this regime, early consolidation begins with particles supporting each other mechanically. Effective stresses exerted by the particles expel fluids upwards as the bed compacts further (Dankers & Winterwerp, 2007; Zamora, 2009).

2.4.2 Boycott Effect

In deviated wells, the complex settling mechanisms called Boycott effect contributes to a significant increase in settling rate of particles. This phenomenon was reported by A.E Boycott in 1920, who discovered that blood corpuscles settled faster (3 to 5 times) in inclined tubes compared to vertical placed tubes (M-I SWACO, 1998). Fig. 2. 16 (a) presents the effect of gravity driven boycott effect on a 40° inclined tube containing heavy drilling fluid at static, while Fig. 2. 16 (b) illustrates the boycott settling mechanism.

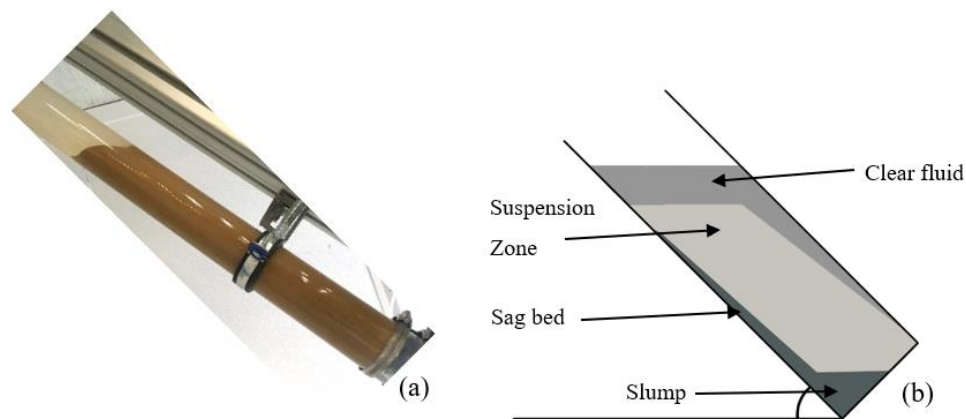


Fig. 2.16 a) Boycott settling at 40°. b) Boycott settling illustration (modified from Zamora (2009))

In deviated systems at static condition, particles settle vertically downwards with the travel distance significantly reduces. In boycott driven settling, the clarified fluid layer (low-density fluids) is formed quickly flowing upwards and hence covering the entire high side of the tube due to buoyancy. This fluid motion accelerates the displacement and settling rate. In effect, the solid particles slide on the low side of the tube, forming a sediment bed slumping downwards and accumulate at the bottom of the tube (Zamora, 2009). This motion of particles is induced immediately when settling occurs, creating a pressure imbalance between the low and high side over the cross-sectional area of the tube. Thus, forcing the low-density clear fluid layer upwards and the high-density fluid downwards (Omland et al., 2007).

Barite bed formation takes place in wellbores of 30° inclination (M-I SWACO, 1998), while the maximum clarified layer development and settling rate occurs at inclinations of around 45°. At higher angles, the buoyancy effect on the clear fluid layer is reduced and thereby lower the settling rate of particles proportionally (Zamora, 2009).

2.5 Operational Challenges Caused by Barite Sag

In drilling fluids, the phenomenon of weighting material settlement can cause several problems during drilling and completion operations. These can range from insufficient drilling fluid density and down hole pressure irregularities to fracturing the formation when regaining circulation after static conditions in the well caused by the material bed. Additionally, problems regarding running casings and hindered displacement efficiency during cementing operations can be results from barite sag and particle bed formations (Omland et al., 2007).

2.5.1 Occurrence of Barite Sag in Operations

Common for all wells experiencing sag incidents are high inclination or longer tangent sections. Followed by operational issues as twisting of the bottom hole assembly, cementing operations prior to side-tracking and tripping involving running liners or casings. These operational sequences lead to significantly reduced velocities in the annulus and were further limited by ECD. In more severe cases, barite sag has led to lost circulation and gas in flux due to instabilities in the hydrostatic fluid column as circulation bottoms-up was proceeded (Bybee, 2004).

Barite sag and its consequences can only be minimized when all related factors are under adequate control. Knowledge of proper fluid rheology and hydraulics must be combined with appropriate sag-reducing drilling practice and monitoring to prevent sag (M-I SWACO, 1998).

Deviation and borehole Conditions

The frequency of barite sag in deviated wells is more often, starting at 30° and more intensively at high-angle wells (inclination greater than 50°). Additionally to the sediment mechanism of particles in complex drilling fluid systems, the gravity-driven boycott effect contributes to a more intense sag in deviated wells at 75° (Omland et al., 2007; M-I SWACO, 1998). Annular clearance, drill pipe diameter and circulation velocities are major key factors for sag problems when it comes to the hole diameter. From field experience, sag tendency is considerable for hole sizes larger than 152 mm (6 in) in which higher flow velocities are required for sufficient cuttings transport and barite bed disturbance (M-I SWACO, 1998). Prevention of barite sag is harder to manage for dynamic sag taking place at low flow velocities compared to static sag conditions. In directional wells where dynamic condition is limited by laminar flow regimes, the boycott settling is complicated by several factors. Fluid dynamics is often dominated by low flow rates resulting in particle settlement where the low-density fluids are forces upwards. This fluid behaviour creates a pressure imbalance which further accelerates the fluids motion and separation process resulting in a more rapid barite bed formation (Omland et al., 2007). This settling behaviour known as the accelerated or dynamically enhanced Boycott settling can be prevented by increased annular velocity and pipe rotation (M-I SWACO, 1998).

The same effect is presence during static conditions with longer non-circulating periods. Particle accumulation during static conditions can form extreme barite beds and challenge the process when circulating bottom-up to proceed circulation and drilling. In worst case, stuck

pipe or formation fracturing can be a result of significant pump increase to preserve circulation (M-I SWACO, 1998).

Properties of Drilling Mud

Barite sag is more potentially to occur when the drilling fluid weight containing weighting agents exceeds about 1440 kg/m³ (roughly 12 lb/gal) (M-I SWACO, 1998). In general, barite sag takes place in low viscosity and low gel strength fluids providing insufficient suspension (Caenn et al., 2017). Sag is also more likely to occur in freshly prepared fluids as the content of drilling solids play a part in gel strength development of the drilling fluid. New drilling fluids are often diluted with minimal content of drilling solids accumulated in the fluid phase when exposed to low shear rates (K. Taugbøl, personal communication, April 2020). This is due to the reduced hindering effect as the overall particle concentration and potential for interfering by particle interaction is reduced affecting the settling velocity (Dankers & Winterwerp, 2007).

Further, when extended reach wells are drilled under high pressure and high temperature (HPHT), sag tendency can increase critically. High temperatures increase particle settlement due to reduction in viscosity and hence thinning the drilling fluid (M-I SWACO, 1998).

2.5.2 Impact of Weighting Agent Rheology

Early studies performed on parameters such as viscosity on Stoke's law as well as relations between plastic viscosity, yield point, 10- second and 10-min gel strength, proved to be inadequate sag indicators (Omland et al., 2007). Investigation performed by Saasen, Liu, & Marken (1995), showed on the other hand better correlation to sag when studying the effect of fluid's viscoelastic properties on material sag. This gave rise to questions regarding gel structure development in fluids (Saasen et al., 1995).

The gel structure of a fluid must overcome the gravitational force exerted by the particle minus the buoyancy force. Further, the required gel structure strength (τ_g) to preserve suspension of particles is expressed by Eq. 2-4:

$$\tau_g \geq \frac{g D \Delta\rho}{6} \quad \text{Eq. 2-4}$$

where g is the gravitational constant, D the particle diameter and $\Delta\rho$ the difference in density between the fluid and the particle. The required gel strength will further depend on particle

types and base fluid used. Most importantly is how the gel structure is created with respect to additives used in the water-based fluid. The gel structure created in polymer-based fluids is based on a stronger network suspending particles and is therefore very robust. For clay minerals used, however, the gel structure is weaker resulting in a mud being more prone to sag (Omland et al., 2007).

There is still no universal agreement on the key rheological parameter having the greatest impact on sag, considering the wide range of drilling fluid systems. However, the terms yield stress and low-shear-rate viscosity are more recent and acknowledged parameters related to dynamic particle settling (Zamora & Power, 2002). Followed by the low-shear rate yield point (LSRYP) which has proven to be a key term in the process of correcting and being a more reliable indicator for sag-related rheological properties. The LSRYP can simply be determined using the 3 and 6 rpm shear stress readings and is then calculated by Eq. 2-5 (Skalle, Backe, Lyomov, & Sveen, 1997).

$$LSRYP = (2 * \theta_3 \text{ rpm} - \theta_6 \text{ rpm}) \quad \text{Eq. 2-5}$$

Settling of particles is significantly reduced if the drilling fluid develop gel structures and contains suspension additives to further improve the total suspension ability (Skalle et al., 1997). Generally, required ECD restricting for low shear rheology, costs and lack of knowledge can lead to inappropriate LSYP values for sag incident prevention (Bybee, 2004). It should also be noted that larger hole sizes require higher LSYP values (M-I SWACO, 1998).

2.5.3 Techniques Used to Detect and Measure Weighting Material Sag

Despite the wide range of literature presenting techniques used to detect and measure barite sag, discussions with competent specialists with long experience in drilling operations revealed the industry's lack of sufficient tools and techniques used to detect barite sag in operational sequences. During ongoing offshore operations, detection of barite sag is mainly done by analysing drilling fluid samples taken from the flow line after a longer static period. Greater variations of fluid densities obtained reveal whether barite sag has occurred or not, which often is the case of a delayed detection. Thus, the industry describes a current need of sufficient and reliable sag detection methods implemented in the field (K. Taugbøl, private communication, May 2020).

Moreover, future plans involving implementation of fully automatized systems for flow and rheology control of the well stream might hopefully form a basis for continuous measurements and herein provide data of important fluid properties of the employed fluid system in the well. The transition from manual drilling fluid measurements performed by field personnel to automated systems could provide a better picture of the fluid properties regarding barite sag occurrence and thereby contribute to develop new and enhanced solutions for sag detection (K. Taugbøl, private communication, May 2020).

However, some testing methods such as standard viscometers available in the field to more advanced techniques like sag flow loop for sag performance are developed and their functionalities and limitations are described by Omland et al. (2007).

Static Sag Testing

The static sag testing accounts for the most common method used in laboratories but is also used offshore on critical wells. A smaller volume of drilling fluid is filled into steel cells and then placed into a heating cabinet at set temperatures for a specific period. Eventually, the densities of the top and bottom layers of the fluid is measured to detect the sag tendency. The sag tendency is further expressed as the sag factor relative to the fluid and defined by Eq. 2-6 (Omland et al., 2007).

$$SF = \frac{MW_{bottom}}{MW_{bottom} + MW_{top}} \quad \text{Eq. 2-6}$$

MW_{bottom} and MW_{top} are the corresponding densities of the fluid at the top and bottom of the test cell. A sag factor of 0.5 expresses non-sagging fluids, while a sag factor above 0.52 can indicate a fluid with potential to cause operational problems.

This method is useful when large number of tests need to be run, but it does not consider the operational conditions arising at low-shear rates, which are most potentially for sag. Also, the free liquid level being displaced to the surface by the settling particles is not taken into account by this method (Omland et al., 2007).

Viscometer Sag Testing

The Viscometer Sag Test (VST) is a simple test using shear developed by an OFITE 900 viscometer at 100 rpm to simulate dynamic settling conditions both in laboratories and offshore on crucial projects.

Mud weight changes are measured over time from a sample fluid placed in a thermal cup and shared for 30 minutes. Further, the fluid density of the portion at the bottom of the cup is measured and compared to the initial fluid density. The difference in fluid density measured is then used as a sag indicator. This simple technique was improved by implementing a “sag shoe” to correct for sensitivity of the standard VST. With the sag shoe placed at the bottom of the viscometer cup, sag is provoked by accelerate settling and concentrating the mass of weight material into a collection well at the bottom of the cup. By comparison of obtained data from the standard VST, modified VST in addition to sag flow test data, the sag tendency can be expressed by Eq. 2-7 (Omland et al., 2007).

$$S_R = -k \frac{\Delta MW}{MW} \quad \text{Eq. 2-7}$$

Eq. 2-7 states the sag register (S_R), where ΔMW stands for the density difference between the initial fluid density, MW , and the one obtained after two runs. The constant, k , fits the correlation for the modifies VST with $k = 10.9$ and data from flow-loop tests with $k = 50.0$. The calculated value of S_R equal to 1.0 indicates no sag (Omland et al., 2007). Further, experience from field data advise to encounter for minimal sag problems by the range of $1.0 < S_R < 2.5$, where S_R values above 5.0 signal severe sag. As an example, when circulation is regained bottoms-up after a static period and barite sag was detected by samples from the flowline, a typical sag register value could be 2.55 (M-I SWACO, 1998).

Sag Flow Loop

This more sophisticated technique is only used for laboratory experiments analysing drilling fluid systems having adequate sag preventive properties. The initial tests performed by the sag flow loop in the 1990’s, confirmed the fact that barite sag is a problem dominated by dynamic settling rather than for static conditions. In addition, flow loops were built with possibility of inclining the casing highlighting the impact of the boycott effect. Results from flow loop tests performed on new sag fluid systems are also used to create baselines for sag detection (Omland et al., 2007). Sag flow loops are associated with advanced instrumentations and require relatively large fluid volumes to provide data regarding basic sag mechanisms. However, these flow loop systems are capable of simulate actual bore hole angles, annular velocity, drill pipe rotation in addition to temperature effects and hole geometries. Continues monitoring of weight

material additions to the circulating mud weight in the system can provide direct measurements of weight material deposited in the bed (M-I SWACO, 1998).

2.5.4 Methods Used to Manage Barite Sag

It is by now understood that barite sag can be minimized by adjusting the rheological properties, composition and formulation of drilling fluids used in the industry. However, barite sag is also accepted to be more than just limited to a fluid property problem. Practical sag guidelines have been developed based on oil field experience and laboratory measurements (M-I SWACO, 1998). Also case histories from field experiences have contributed to characterize best practice creating a guideline for barite-sag management (Bybee, 2004).

Barite sag measurement in the field – “Trip Report”

An example on how sag is detected and managed in the field is provided by Halliburton. Halliburton uses actual measurement of mud weight from shakers under flow to monitor changes in mud weight during ongoing drilling performance. The monitoring of actual mud weight compared to the baseline is shown in Fig. 2. 17.

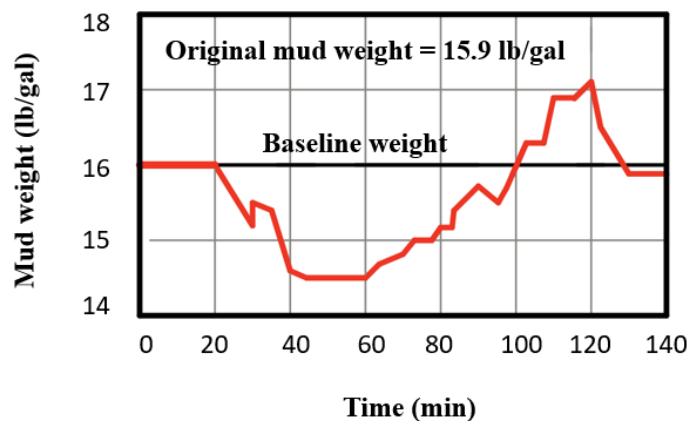


Fig. 2. 17 - Mud weight monitoring (modified from M-I SWACO (1998))

In the field lab, all relevant fluid properties are monitored in real-time to implement remediate action when necessary. During normal drilling operation involving circulation and drill pipe rotation, all fluid properties are reported to be within required specifications. This is indicated by the red line (see Fig. 2. 17) toning the baseline weight between the time interval of 0 – 20 minutes. The baseline weight represents the adequate mud weight corresponding to

the mud weight entering the wellbore being equal to the mud weight coming out of the well measured by field engineers at the shaker.

In situations where it is necessary to trip out of the hole, the bore hole is further circulated cleaning the hole prior to switch off pumps. When circulation and pumps are turned off and the drill pipe retrieved, the well is under static condition creating potential barite sag issues. As the drill pipe is placed back to bottom and circulation off-bottom proceeds, significant density variations are noticed and displayed on the monitor as demonstrated after 20 minutes in the figure above. Thus, the actual mud weight in the circulation system deviates from the required baseline weight. As the deviation in mud weight continues during drilling, a remediate action is required to re-establish baseline mud weight in the well. At this point, further drilling is stopped while circulation is continued. Simultaneously, the field personnel performing mud tests to detect the cause of barite sag and thereby adjusting the mud system with additional chemicals. The adjusted fluid system is implemented and circulated until chemical treatment is completed and consistent mud weight reported at the shaker. During the time interval of 120 to 140 minutes, significant and stable mud weight is regained, and normal drilling operation is proceeded (Halliburton, 2012).

Sag Management Guidelines

Several companies have formulated barite sag guidelines based on best practice to avoid barite sag. These include categories as (1) well planning, (2) drilling fluid properties and testing, (3) operational practice and (4) well site monitoring.

According to (1) well planning, wells of higher inclination than 30° drilled with a drilling fluid density above 1440 kg/m³ (12 lb/gal) are categorized as sag problem candidates. One should be aware of the narrow margin between pore pressure and fracture gradient in these wells limiting for required flow rates. Well environment affected by HPHT can change fluid properties. Repeated rheology measurements are important. Casing designs shall be constructed with respect to situations where low annular velocity is expected. Awareness regarding increased sag tendency in larger hole diameters (> 152mm) and annular clearance shall be managed with flow velocities respectively (M-I SWACO, 1998).

For (2) drilling fluid properties and testing, performance of sag tests should be done in the laboratory during well planning and in the lab/field simultaneously while drilling. It is also considered that when drilling through reactive formation with WBM, sag may be harder to notice. Drilling fluid systems shall be modified addressing required rheology such as low-shear rheology and gel structure in addition to operational conditions. Experience from case studies

reported that sag problems were related to inadequate fluid systems not suited for the well condition resulting in too low LSRYP values. Changes in LSRYP often indicating sag problems. To prevent sag, LSRYP values should be maintained ranging from 3 to 7 Pa (7 to 15 lb/100ft²) to provide an adequate barite suspension (M-I SWACO, 1998). In case studies presented by Bybee (2004), WBM and SBM were treated with a combination of organophilic clay and surfactants, resulting in a more stable fluid of higher low-shear rheology. In one case, attempts on treatment were done by applying biopolymer and bentonite to the WBM, with limited success. Besides, treatment with fluid-loss additives can cause viscosity reductions and thereby increase the possibility of sag occurrence (M-I SWACO, 1998).

When it comes to (3) operational practice and low circulation rates, sag beds should be removed using high flow rates and rotary speeds within the operational limits prior to tripping out. When proceeding circulation bottom-up, sign of sag is indicated by larger variations in mud weight measured at the flowline. In particular situations, it is recommended to stop circulation and trip out and stag back in order to prevent lost circulation when initiating higher pump pressure to circulate the heavy mud accumulation. When extended time periods between trips are planned, barite bed formation should be disturbed frequently. The same procedure is also recommended after drilling practice involving sliding. Overtreatment by diluting the drilling fluid should be avoided prior to cementing and casing (M-I SWACO, 1998).

Typically for (4) well site monitoring, elements such as fluctuating standpipe pressure, high torque and overpull, stuck pipe, unexpected fluid loss and changes in mud weight are used as symptoms for barite sag (Bybee, 2004).

2.6 Pills Used for Separating Fluids of Different Densities

2.6.1 A Fluid Pressure Transmission Pill Used during MPD

The work published by Ronaes et al. (2008) states the successful use of a fluid pressure transmission pill (FPTP) for logging and completion operations during managed pressure drilling (MPD) in HTHP environments. A solids free crosslinked polymer pill was developed with the intention to transmit pressure to the bottom of the well and with sufficient integrity to isolate the high-density fluid on top from the lighter fluid in the deeper section. Pressure data and monitoring obtained from operations performed on the Kvitebjørn field, certified that it was possible to run wireline logs and test liners through the pill without any indication of

instabilities and further interfacing of the different fluids. Simultaneously the FPTP maintained a pre-determined hydrostatic pressure and thereby controlled the well pressure with no need of additional applied pressure. After a test period of two weeks, the FPTP was successfully displaced by circulation without any treatment at the surface needed. Hence, the performance of such a FPTP is determined to reduce costs and logistic challenges regarding displacement of the entire circulation system to balance the reservoir pressure for future operations (Ronaes et al., 2008).

2.6.2 A Fluid Pill of Thixotropic Properties Serving as a Barrier Fluid

Common for more recent studies working on fluid pills is the association of MPD and tripping operations when employing drilling fluids of special designed properties. The work published by Riker, Turner, Lovorn, & Kale (2012) describes the use of a fluid pill with robust thixotropic properties to serve as a barrier fluid spotted between a heavier mud cap and drilling fluid below the barrier fluid. A high density “mud cap” is commonly used as a tripping pill to provide sufficient hydrostatic pressure at a desired depth for well control during MPD.

However, practice where a high-density tripping fluid is placed on top of a lower density drilling fluid is an attempt to oppose gravity. The result is often of large volumes comingling and contaminating both fluids creating wellbore instabilities. The work performed by Riker et al. (2012) showed that the barrier fluid provided successful separation between the drilling mud with nominal density of 1740 kg/m^3 (roughly 14.5 lb/gal) and mud cap of 1930 kg/m^3 (roughly 16.1 lb/gal). The barrier fluid’s density was mixed to be slightly lower than the drilling fluid. The barrier pill was weighted up with barite without affecting its gelation properties. After spotting, the barrier pill was left at rest to rapidly develop a gel structure. During the experiment on a test well of 13.876 feet (TVD), flow and pressure monitoring confirmed that the barrier pill kept the other wellbore fluids in place. After completing the trip, drilling mud returns showed constant fluid densities, reconfirming that no incompatibility issues had occurred (Riker et al., 2012).

2.6.3 A New Water-Based Isolation Spacer for OBCP Operations

In general, off-bottom cement plug operations (OBCP) have been associated with problematic operations in the oilfield for decades. The application of high viscosity support spacers

traditionally prepared with polymers or bentonitic clays have been a widely used method to support the cement. These spacer systems have shown inadequate cement plug support due to deficient viscosity and poor placement operations resulting in cement slumping through the spacer fluid with the entire operation failing (Webber & Turner, 2019).

A new spacer technology was adapted and tested by Webber & Turner (2019) achieving successful OBCP operations on field trials in the North Sea. The spacer technology used synthetic inorganic viscosifiers to obtain a water-based thixotropic fluid. Once the spacer was placed in the wellbore, it was left undisturbed to gain full gel strength before the cement was spotted above the spacer. Based on achieved results, application of the spacer confirmed that the OBCP remained at its desired place rather than slumping through the spacer. This is often the case due to the density differences between the cement plug and the spacer fluid. The spacer fluid developed, successfully isolated, and supported the cement above the bridge plug. No challenges regarding the pumping operation for spotting and further circulation through perforations were documented.

The authors acknowledge the fact that achievement of elevated Bingham yield point should not be used as a key indicator of a fluid's support potential. They understood that a viscous isolation spacer also required thixotropic fluid properties, despite being pumpable and yet forming a strong gel structure when spotted (Webber & Turner, 2019).

3 Methodology and Experimental Procedures

This chapter explains the methodological approach to develop the desired mix designs, experimental methods and equipment used to characterize the rheological profile. And further qualify the integrity of the gel pill at different stages. It is worth to mention that both the viscosified brine and water-based drilling fluid had to be designed and characterized.

3.1 Experimental Procedure

This experimental work can be divided into three parts involving different experimental apparatus and various methods. The first part covered the development of the fluid mix designs corresponding to the modified brine, water-based drilling fluid, bentonite and laponite-based gel pills, respectively. This part further included rheological measurements to characterize fluid properties. As the attempt was to design a gel pill rather than a viscous pill, the formation of the gel structure was an important parameter to investigate and was further used to determine a gel pill design employed on large-scale.

The second part of the project consisted of scaled-up versions of stability tests. The intention was to qualify the pill's ability to function as a barrier when placed between the modified brine and water-based drilling fluid, in small scale.

The third part was performed on the large-scale test setup which is described more detailed in chapter 3.4. This part provided the opportunity to test the system and its integrity on a larger scale when exposing the gel pills to greater stresses and overlying fluid columns. Moreover, the pill's capability to controllably transmit pressure from the overlying fluids and maintain a desired hydrostatic bottom hole pressure was tested.

3.1.2 Equipment

As for all sort of work in the laboratory, standard tools and equipment such as metal sample cups, pipettes, spoon, storage containers and balance scales have been used in this project. Such standard tools will not be described further, as this chapter focuses on the materials and apparatus specifically used to develop the sag prevention gel pill.

Mixing Devices

Two different types of mixers were used in this project. A Heidolph stirrer was used for standard stirring tasks on smaller fluid volumes covering approximately 350 mL. Fig. 3. 1 shows the Heidolph Hei-Torque value 100 instrument and the stirring rod used on all fluids. The stirring rod has a special construction with obliquely blades and was used with the intention to preserve clay mineral structures during stirring.



Fig. 3. 1 - Heidolph Hei - Torque 100 value stirrer (left) and stirrer with obliquely blade construction (right)

For the third part, larger fluid volumes between 2-3 litres had to be prepared for the large-scale tests. These fluid volumes had to be mixed using a Hobart N50-60 mixer bench model as the steel bowl holds up to approximately 3.5 L, (see Fig. 3. 2).



Fig. 3. 2 – Hobart N50 - 604 pt Planetary Mixer

Viscometer

Rheological measurements were performed in the laboratory on all fluid recipes using an Ofite Model 900 VG-meter (Viscosity-Gel meter), (see Fig. 3. 3). The viscometer is a coaxial rotational viscometer employing a transducer to measure the induced angle of rotation of the bob by a fluid sample. The viscous drag exerted by the fluid creates a torque on the bob, where the angular displacement is measured by the transducer providing calculated output data based on the applied shear rate (Ofite, 2015).

The viscometer has a mud programme available which was used on all fluid recipes. By pressing the button “mud” also shown in Fig. 3. 3, tests were automatically performed obtaining data. Data such as plastic viscosity in centipoise (cP) and yield point in the shear stress unit specified to be lb/100ft², were recorded automatically based on Bingham plastic analysis models. The same yields for the 10-sec and 10-min gel strength values.

After test completion, the 10-sec and 10-min gel strength values were displayed in lb/100ft². The mud programme operated the rotor at 600 rpm for 15 seconds and 300 rpm for 10 seconds to shear the fluid properly before the 10-sec gel time interval was started. The rotor was stopped completely during the gel time intervals. The 10-sec gel strength was recorded after shearing the sample at 3 rpm to break the gel strength. Afterwards, the mixture was premixed at 300 rpm for 10 seconds before the 10-min gel time interval started. The 10-min gel strength was eventually recorded after breaking the gel structure at 300 rpm for 10 seconds.

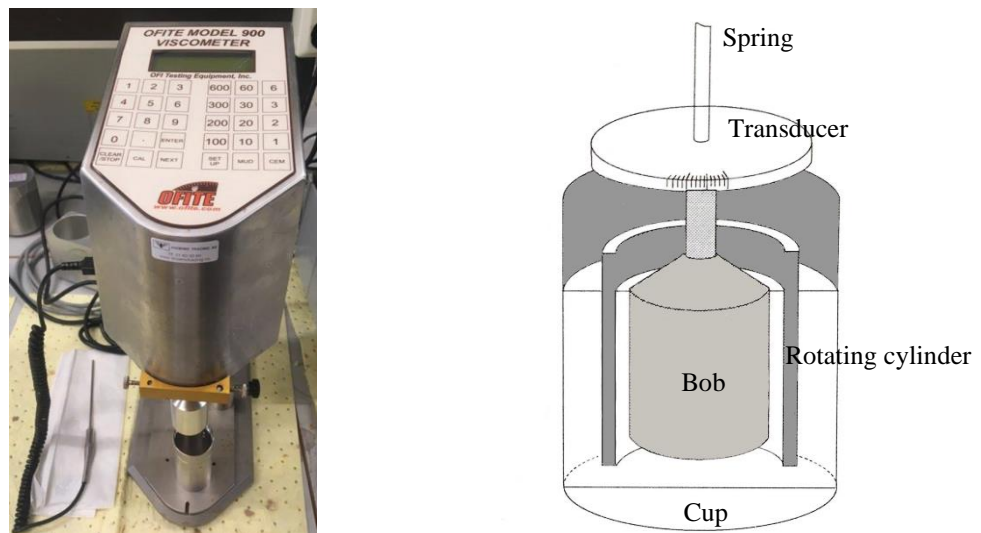


Fig. 3. 3 – Ofite Model 900 Viscometer (left) and an illustration of the viscometer instrumental setup (right) (modified from Skjeggstad (1989))

Moreover, small deviations on calculations provided by this particular viscometer were observed regarding the 20 rpm readings. Measurements performed at 20 rpm had margin errors resulting in generally lower rheology values. This can also be seen by small tangential deviations on rheology profiles represented in chapter 4.

Density and pH measurement

Density and potential hydrogen (pH) values of the fluids were measured at a later stage during the third part of the experimental work. At this stage, it was of interest to track the densities of the fluids. This was done to document the gel pill's integrity when placed between a denser brine and even denser water-based drilling fluid as gravity was defied in such a static fluid system. Density was measured using a simple Ofite mud balance scale as shown in Fig. 3. 4.



Fig. 3. 4 – Ofite mud balance scale

pH measurements gave an indication of how alkaline the pill was regarding hydration properties of the clay minerals. The pH values were obtained using a Mettler Toledo Benchtop pH meter (see Fig. 3. 5).



Fig. 3. 5 – Mettler Toledo Benchtop pH meter

3.2 Design and Development of Fluids

All chemicals and additives used in the various fluid recipes have been presented in chapter 2. The modified brine and water-based drilling fluid were designed and tested for the direct development of the sag prevention pill. All recipes prepared will be provided in separate tables including the mixing procedure. Description on the fluid design in this section is constructed in the same order as fluids placed during all tests performed, starting with the modified brine placed in the lower section of the pipe. For all recipes, chemical substances were added slowly during ongoing mixing to prevent formation of “fish eyes”.

3.2.1 Viscosified Brine

The design of the viscosified brine (hereafter referred to brine) was chosen to demonstrate a typical completion fluid spotted in the bottom section of the wellbore, whereas the sag prevention pill would be placed above it.

The recipe for the brine used in this study is shown in Table 3. 1.

Table 3. 1: Original brine recipe A.

Chemicals	Recipe A
Water	248.96 [g]
Xanthan Gum	0.181 [g]
Mix for 15 minutes	
CaCl ₂ * 2H ₂ O	113.16 [g]
Mix for 30 minutes	

When designing the brine, calcium chloride dihydrate was used, providing the same properties as calcium chloride. The designed recipe accounted for the difference in calcium chloride concentration between pure calcium chloride and calcium chloride dihydrate. The intention of using calcium chloride in the brine was to develop a typical solids free completion fluid of high density. Xanthan gum was added to adjust the viscosity of the fluid to a minor degree.

It was also of interest to create a scenario where the gel pill of lower density was to be spotted on top of the heavier brine. With the density difference between these fluids, it was

crucial to gather results confirming that the gel pill was able to be spotted and stay intact on top of the brine with low viscosity and yield point. The large density differences require significant stability and yield strength of the pill to prevent swab effects in case of comingling.

3.2.2 Gel Pill

The sag prevention pill's aqueous base fluid consisted of water, NaCO₃ and NaOH, with additional bentonite and laponite RD respectively for the bentonite and laponite-based gel pill. Caustic Soda (NaOH) and Sodium Carbonate (NaCO₃) were used for their functionalities as controlling the pH and support the hydration and yielding of the clay minerals.

Further, the aqueous base fluid remained constant while the concentration of bentonite and laponite was changed during the recipe design. During the experimental work, two different recipes for the bentonite-based pill have been mixed and analysed for testing. While four different recipes were tested associated to the laponite-based pill. The recipes for the bentonite and laponite pills are presented in Table 3. 2 and Table 3. 3. Mixing procedures in addition to the chemicals used are also included.

Table 3. 2: Bentonite-based pill recipes.

Chemicals	Recipe 1.B	Recipe 2.B
Water	343.0 [g]	343.0 [g]
NaCO ₃	0.02 [g]	0.02 [g]
Mix for 7 minutes		
NaOH	1.0 [g]	1.0 [g]
Mix for 3 minutes		
Bentonite	10.0 [g]	20.0 [g]
Mix for 5 minutes		
Left at rest for 30 minutes		
Mix for 45 - 60 minutes		

Table 3. 3: Laponite-based pill recipes.

Chemicals	Recipe 1.L	Recipe 2.L	Recipe 3.L	Recipe 4.L	Recipe 5.L
Water	343.0 [g]	343.0 [g]	343.0 [g]	343.0 [g]	343.0 [g]
NaCO ₃	0.02 [g]	0.02 [g]	0.02 [g]	0.02 [g]	0.02 [g]
Mix for 7 minutes					
NaOH	1.0 [g]	1.0 [g]	1.0 [g]	1.0 [g]	1.0 [g]
Mix for 3 minutes					
Laponite RD	8.5 [g]	10.0 [g]	12.0 [g]	15.0 [g]	20.0 [g]
Mix for 5 minutes					
Left at rest for 30 minutes					
Mix for 45 – 60 minutes					

After either bentonite or laponite was introduced to the aqueous base fluid and mixed for a few minutes, the mixture was left static for 30 minutes to enable the clay minerals to hydrate further which also reduced the mixing time considerably.

The term gel pill is in this thesis used for both bentonite and laponite-based gel pill. When addressing the bentonite or laponite-based pill specifically, terms such as bentonite-based, laponite-based pill or bentonite pill and laponite pill will be used.

3.2.3 Water-Based Drilling Fluid

The drilling fluid in this project consists of a simple water-based drilling fluid (hereafter referred to WBDF) containing water, xanthan gum and barite. The barite employed was a micronized barite used by petroleum industry (API specifications 13 A). Several WBDF recipes were tested with change in xanthan gum and barite concentration, while the amount of water was kept constant.

The goal was to obtain a WBDF of rapid barite sag when static to collect data and document the sag prevention by the pill within the 24 hours test period on large-scale. The final recipe shown in Table 3. 4 was designed such that particle settling was occurring already after 15 minutes when left undisturbed. The corresponding procedure of design modification is provided in chapter A.1.

Table 3. 4: Modified WBDF recipe B.

Chemicals	Recipe B
Water	248.87 [g]
Xanthan Gum	0.3 [g]
Mix for 20 minutes	
Barite	184.91 [g]
Mix for 30 minutes	

3.3 Characterization of the Designed Fluids

After mixing, rheological measurements were performed on all designed recipes. Rheological measurements on recipes for brine and WBDF were mainly conducted to detect deviations from the anticipated rheological profile. Further intention was to control reproducibility of fluid profiles and properties to exclude contamination. Selection of the WBDF recipe was not completely based on the rheological profile, but rather on rapid barite settling which was determined by simple static barite sedimentation tests (see chapter A.1). As mentioned, criteria for rheological parameters were established to simplify provision of the different fluid recipes.

3.3.1 Rheological Property Characterization

All rheology measurements were performed at room temperature and no sensitivity analysis on temperature was performed. Instrumental readings such as shear stress (lb/100ft²), viscosity (cP) and temperature (C^o) were taken at rotational speed (rpm) ranging from 600 towards 1 rpm available on the viscometer. One should note that the accuracy of low rotational speeds (1 and 2 rpm) might be source of uncertainty.

The rheological measurement procedure for brine and WBDF differed from the gel pill. For brine and WBDF, standard drilling fluid measuring procedure was used. For the gel pill, a separate procedure described in chapter A.2 was implemented due to rapid gel structure development forming at low shear rates equivalent to 20 rpm. Further, rheological measurements were conducted on the original mixing date right after preparation (initial condition) and re-taken after 24 hours.

In addition to obtained viscometer data, other rheology related calculations were implemented. Calculations were performed using Herschel-Bulkley equations reflecting the rheology profiles of certain recipes. Followed by estimating the quantity of differential pressure the gel strength of the bentonite and laponite pill were able to resist when placed in the static fluid system on the large-scale test setup.

At first, shear stress and gel strength values displayed in lb/100ft² were converted to pascal (Pa) using Eq. 3-1.

$$\text{Shear Stress [Pa]} = \text{Shear Stress} \left[\frac{\text{lb}}{100\text{ft}^2} \right] * 0.51 \quad \text{Eq. 3-1}$$

The yield stress (τ_y) corresponding to the H-B model was calculated by Eq. 3-2 with the shear stress values in Pa associated to θ_3 and θ_6 readings.

$$\tau_y = (2 * \theta_3 - \theta_6) \quad \text{Eq. 3-2}$$

The rheological index (n) and consistency index (k) were determined by Eq. 3-3 and Eq. 3-4 shown below.

$$n = \frac{\log \frac{\tau_1 - \tau_y}{\tau_2 - \tau_y}}{\log \frac{\gamma_1}{\gamma_2}} \quad \text{Eq. 3-3}$$

$$K = \frac{\tau_1 - \tau_y}{170.23^n} \quad \text{Eq. 3-4}$$

For all calculations, τ_1 and τ_2 are the shear stress values corresponding to 60 and 100 rpm, respectively. Further employed with γ_1 equal to the shear rate of 102.14 1/s (60 rpm) and γ_2 to the one of 170.23 1/s (100 rpm).

Eq. 3-5 represents the quantity of differential pressure in Pa across the pill column resisted by its gel strength.

$$\Delta P = \frac{4 * \tau_g * L}{ID} \quad \text{Eq. 3-5}$$

The parameter τ_g corresponds to the obtained 10-min gel strength values, L to the gel pill length of approximately 0.6 m and ID the inner diameter of the test pipe measured to be 0.0497 m.

3.3.2 Criteria for Rheological Characterization

Criteria for characterization of the fluids were established before and after rheological measurements were performed on all recipes. The reason for applying criteria when analysing the different recipes was to simplify the determination and characterization of the fluids to be further tested on the large-scale. The focus on established criteria applied primarily the bentonite and laponite-based pill recipes as these were the most critical designs for this project involving several criterions. For brine and WBDF recipes, the criteria mainly reflected repetition and similar trends of the rheological profile at both initial condition and repeated tests after 24 hours. Additional criterion for the WBDF included a typical shear thinning rheology model.

During preparation and rheology analysis conducted on the pills, it was early discovered that the bentonite and laponite gel pill differ in rheological values such as shear stress, viscosity, and gel strength values (10-sec and 10-min). Regardless, the same criteria were used for both pill types. Beyond the criterion for repetitive rheological profiles, further criteria to simplify the determination and characterization of the gel pills can be listed as:

- **Hydraulically displaceable**

The gel pill should not be too viscous when exposed to low shear rates to ensure pumpability and hydraulic displacement. This criterion was established to position the pill inside the pipe on large-scale by a hand-driven piston pump and additionally meet potential well bore requirements. The criterion established for viscosity readings was to not exceed a viscosity of 20 000 cP measured at a shear rate of 1.7 (1/s) (1 rpm). This criterion enabled to exclude laponite-based recipes such as 4 and 5.L.

- **Gel strength values**

This criterion was established at a later stage when tests on the large-scale setup started with the intention to ensure success. The gel strength value calculated after 10-minutes by the mud program was a key factor. It was of interest to proceed further testing on a pill recipe meeting

criterion for quick gel structure development given by the 10-second gel strength value and for maintaining stable gel structures provided by the 10-minute gel strength value. A minimum value of 50 lb/100ft² displayed on the viscometer for the 10-min gel strength was set as a criterion. For the lower gel strength range, a minimum value for the 10-sec gel strength was chosen to be approximately 20 lb/100ft². These criteria contributed to exclude recipes as 5.L (20 g laponite), 1.L (8.5 g laponite) and 2.L (10.0 g laponite).

For demonstrational purpose, Table 3. 5 presents typical gel strength values after 10 seconds and 10 minutes obtained at initial condition for bentonite and laponite pill recipes.

Table 3. 5: Gel strength values in lb/100ft² displayed after mud program calculations.

[lb/100ft ²]	1.B	2.B	1.L	2.L	3.L	4.L	5.L
10 seconds	19.8	58.6	11.4	18.1	32.1	78.1	168.0
10 minutes	24.6	81.6	76.9	107.1	141.0	191.5	319.4

It should be noted that these gel strength values for the individual recipes did differ among the series of rheology measurements conducted, though remained in a range creating a pattern for gel structure development.

Even though recipe 1.B corresponding to the 10g bentonite-based pill did not fulfil the criteria, it was chosen to include this recipe on stability tests conducted at the early stage of the experimental work.

3.4 Large-Scale Testing

The third part focused on the pill's ability to prevent barite sag by isolating the lower and upper fluid columns relative to the pill. Followed by documenting the pill's capability to controllably transmits hydrostatic pressure from the overlying fluid columns and maintenances of constant bottom hole pressure during the test period. To assess the mentioned targets above, series of observational laboratory tests were conducted using both vertically and oriented test setups to simulate a wellbore. Monitoring throughout the 24 hours test period was provided by pressure gauge sensors measuring pressure along the wall and bottom of the pipe. In addition, two sets of cameras were equipped for visual documentation at the two interfaces associated to the pill.

3.4.1 Large-Scale Setup

The large-scale setup consists of a 3.85 m long transparent plastic pipe with a 4.97 cm inner diameter. The pipe was installed and fasten in such a way that it could be oriented from vertical to deviations of 20° and 40° from vertical, which were established throughout the test series.

For presentational purpose, Fig. 3. 6 illustrates the concept regarding the test pipe (left) and further presents the installed pipe with additional equipment (right). The illustrated concept shows the test pipe filled with fluids where blue exemplifies brine, yellow the pill and brown the WBDF.

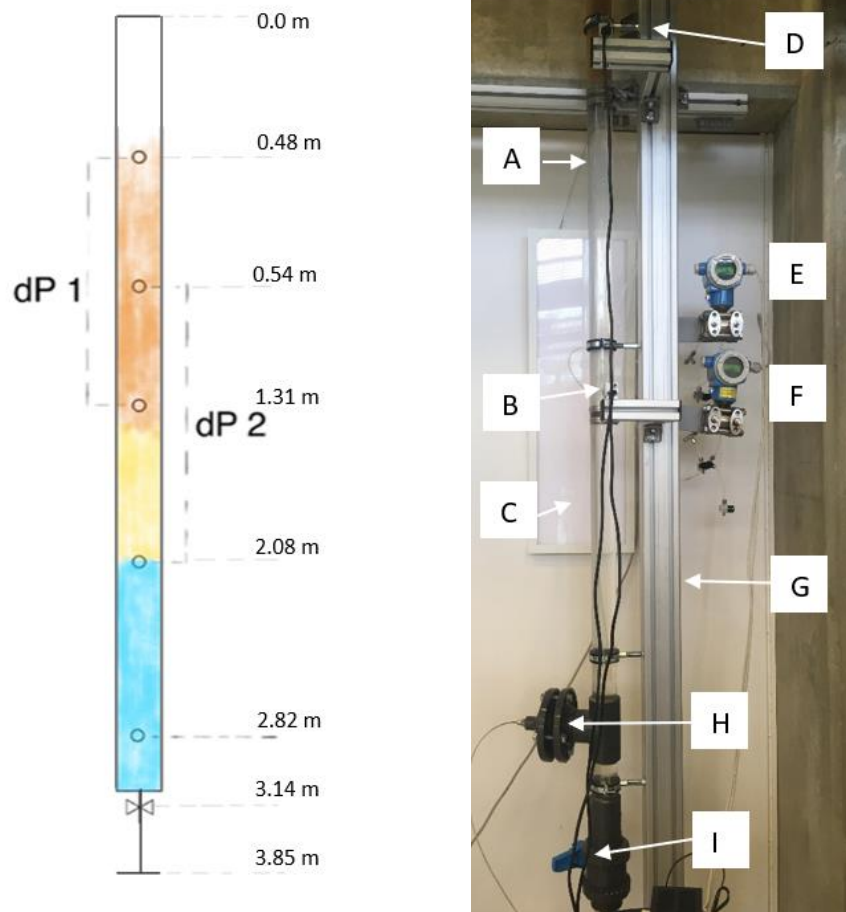


Fig. 3. 6 – Left) Illustration of the vertical test setup filled with fluids. Right) Vertical test setup with A: Transparent plastic pipe, B: Camera 1, C: Light panel, D: Camera 2, E: Differential pressure gauge DP1, F: Differential pressure gauge DP2, G: Supportive construction, H: Bottom hole pressure outlet, I: Valve for opening and closing the pipe

3.4.2 Pressure Sensors and Differential Pressure Gauge Sensors

The pipe was equipped with a total of five outlet lines along the pipe wall connected to pressure gauge sensors. Connected to the five outlet lines were a bottom hole pressure gauge sensor and two differential pressure transducers installed separately. Moreover, all pressure sensors are connected to a pump controller of type Marcol 82 which provides monitoring and data collection on a computer programme. As demonstrated in Fig. 3. 6 (left), fluids are placed in a specific order with the intention to cover the different outlet lines to obtain pressure data. The blue colour depicts the brine covering outlet line of the bottom hole pressure sensor (XP2i) and lower outlet line of the differential pressure sensor DP2. Yellow representing the pill covered the lower outlet line of differential pressure sensor DP1. The WBDF is illustrated by the brown colour corresponding to the upper outlet line of differential pressure DP2. The upper outlet line of DP1 was installed at the very upper section of the pipe which during tests was covered by water added to the WBDF column.

The lowest pressure outlet line was linked to the bottom hole pressure sensor of type Crystal XP2i which is connected to a pressure transducer being an integrated part of the Marcol 82 pump controller. The Crystal XP2i pressure gauge sensor is a digital sensor providing pressure data in bar with 0,1 bar resolution. Crystal XP2i pressure gauge sensor and pressure controller (Marcol 82) are shown in Fig. 3. 7.

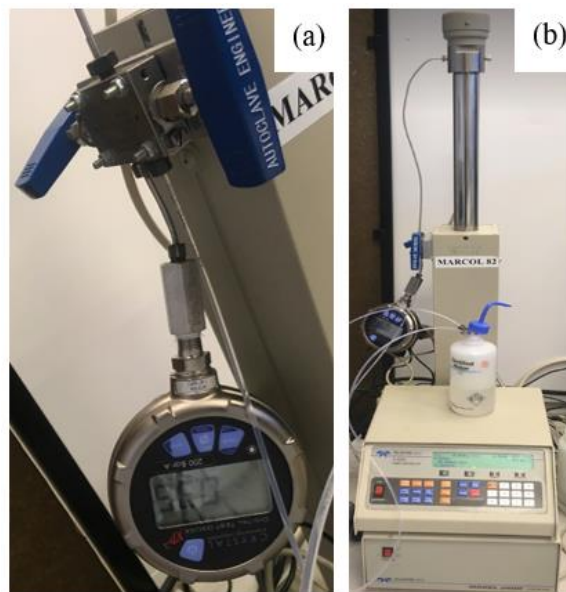


Fig. 3. 7 a) Crystal XP2i pressure gauge sensor. b) pressure controller Marcol 82

The partial differential pressure sensors marked B (DP1) and C (DP2) in Fig. 3. 6 (right), are both of type Deltabar PMD75. These were originally factory calibrated from 0.0 to 2.0 bar. For test purpose, adjustments were done such that these pressure sensors only measure a span of -0.2 bar to + 0.2 bar, for more accuracy corresponding to low hydrostatic pressure values.

3.4.3 Camera Recording and Stability Documentation

For proper visual documentation of the fluid interfaces and long-term recording, two cameras were installed. Camera 1 (marked F in Fig. 3. 6) was installed at the lower part of the pipe documenting the interface between brine and gel pill during and after placement. After brine was placed and the pill was about to be positioned, camera 1 was started recording one frame picture per every other second to document the placement of the pill. Camera 2 (marked D in Fig. 3. 6) was installed at the upper part documenting the interface between the gel pill and WBDF. Before WBDF was added to the fluid column in the pipe, camera 2 was started recording one frame picture per every other second. The purpose of rapid frames during placement of fluids was to document changes at interfaces and possible failures such as intermixing, channelling and or breakthrough of fluids. Shortly after all fluids were spotted and no instabilities observed, frame speed was decreased to one frame per every second minute to record the interfaces for 24 hours on both cameras. Location of camera 1 and 2 installed remained the same throughout the entire test period of 24 hours for all series of tests executed.

3.4.4 Large-Scale Test Procedure

Several tests have been conducted on vertical, 20° and 40° inclined setup to identify the behaviour of the pill spotted when exposed to the fluids inside the pipe. It was of further interest to determine the maximum inclination at which the sag prevention pill was most effective. This investigation was based on the barite settling mechanism occurring differently going from vertical to inclined systems. As for inclined pipe setup, the contribution of gravity driven boycott effect on barite settling was noticed while the hindering effect was observed in the vertical pipe.

To ensure success of the sag prevention gel pill, further tests were required with a minimum of two successful test runs executed per setup before inclination of the pipe was

changed for additional series of tests. A test was defined successful when the sag prevention pill showed sufficient integrity on isolation with no channels or intermixing observed. Other criteria included transmission of pressure signals through the pill (originated by added fluid columns) and the total bottom hole pressure kept approximately constant for 24 hours.

Moreover, placement of fluids proved to be comprehensive and is elaborated in more detail in chapter 4.6 and A.4. Preparation, equipment installed and procedure during tests remained primarily identical for all series of tests conducted. In some cases, challenges and operational situations lead to slight deviation in the standard procedure and will be highlighted when reviewing these individual tests. The standard test procedure was performed as described in Table 3. 6.

Table 3. 6: Standard test procedure.

1. Transparent plastic pipe was filled with water.
2. All tubes associated to the pressure sensors were cleaned by pumping water from the pipe through the tubes to ensure that no particles from previous fluids are affecting the pressure readings.
3. All pressure sensors started monitoring set off by the computer programme.
4. Brine was placed inside the pipe covering the lower section going from bottom of the pipe to the lower outlet of DP2.
5. Foam formed during placement accumulated on the surface of the brine and was removed by a hose to improve visibility.
6. Camera 1 recording was started taking one frame per every second.
7. Sag prevention pill was placed on top of the brine by a pump and pull method, reaching up to the outlet of DP1 and thereby establishing a pill column with a length of roughly 60 cm.
8. After the pill was successfully spotted, it was left at rest for 30 – 45 minutes.
9. Camera 2 was started to record taking one frame per every second.
10. WBDF was poured and placed on top of the pill by a pump and pull method reaching up to the DP2 outlet.
11. Water was additionally filled on top of WBDF completely covering the upper outlet of DP1.

12. When no channelling of WBDF nor intermixing of the fluids were observed after fluid placement, camera 1 and camera 2 recordings were changed to one frame per every two minutes to record the remaining test period.
13. After 24 hours from original test start, pressure monitoring and camera recording was ended, and data collected to verify the test results
14. The light panel (marked H in Fig. 3. 6) was kept on throughout the entire test period to ensure picture documentation overnight.

3.4.5 Fluid Preparation for the Large-Scale Test

Rheological profile characterization and stability tests performed in the second part in addition to establish criteria, created the foundation for determining which gel pill recipes to implement on large-scale. The pill designs of recipe 2.B for the bentonite-based gel pill and recipe 3.L for the laponite-based pill were chosen and respectively adjusted. Recipe A corresponding to the brine and recipe B for WBDF already modified for rapid barite sag were also involved. These recipes had to be adjusted to larger volumes to fill the transparent plastic pipe on the large-scale setup holding approximately 8 litres.

All presented fluids were mixed using the Hobart bench mixer at the lowest mixing speed available on the machine. To avoid early barite settling, the WBDF was prepared on the test days and mixed continuously until to be placed. Meaning that the WBDF was mixed throughout the entire time of ongoing test performance involving placement of brine, gel pill and rest time for pill before spotting the WBDF on top of the pill. Brine and gel pills were on the other hand prepared the day before the test days due to limited time during the actual test days. The following tables present the adjusted recipes including individual mixing procedures.

Table 3. 7: *Mixing procedure and adjusted recipe 2.BT of the bentonite-based pill.*

Chemicals	Recipe 2. BT
Water	3100.0 [g]
NaCO ₃	0.1808 [g]
Mix for 15 minutes	
NaOH	9.037 [g]
Mix for 5 minutes	
Bentonite	180.74 [g]
Mix for 2 – 5 minutes	
Left at rest for 30 minutes	
Mix for approximately 60 minutes until completely homogeneous	
Density: 1.03 SG	

Table 3. 8: *Mixing procedure and adjusted recipe 3.LT of the laponite-based pill.*

Chemicals	Recipe 3. LT
Water	3100.0 [g]
NaCO ₃	0.1808 [g]
Mix for 15 minutes	
NaOH	9.037 [g]
Mix for 5 minutes	
Laponite RD	108.45 [g]
Mix for 2 – 5 minutes	
Left at rest for 30 minutes	
Mix for approximately 60 minutes until completely homogeneous	
Density: 1.01 SG	

Table 3. 9: *Mixing procedure and adjusted recipe AT of the viscosified brine.*

Chemicals	Recipe AT
Water	3100.0 [g]
Xanthan Gum	1.128 [g]
Mix for 20 minutes	
CaCl(2H ₂ O)	1409.85 [g]
Mix for 45 – 60 minutes until mixture became transparent	
Density: 1.3 SG	

Table 3. 10: Mixing procedure and adjusted recipe BT of the water-based drilling fluid.

Chemicals	Recipe BT
Water	2100.0 [g]
Xanthan Gum	2.532 [g]
Mix for 20 minutes	
Barite	1560.61 [g]
Mix for entire time of ongoing test performance	
Density: 1.48 SG	

4 Results and Discussion

As mentioned in chapter 3, all fluids were designed based on desired properties. The selected recipes were further analysed and tested regarding characterization of their properties prior to large-scale tests performed to qualify the pill's stability. This foundation contributed to further qualify the sag prevention pill as a method to prevent barite sag by isolating fluid sections above and below the pill in addition to test the pill's ability to transmit and control hydrostatic pressure. In this chapter, characteristic properties, results obtained from specific fluid recipes and test data from the large-scale tests will be presented and argued in detail.

Test results regarding the design and rheological properties of brine and WBDF are presented in the Appendix B.1 and B.2. Additional results available in the Appendix are associated to tables providing rheological data of the bentonite and laponite-based gel pills. Also included are results from stability tests performed on the pills regarding the second part of the experimental work.

4.1 Bentonite-Based Sag Prevention Pill

4.1.1 Fluid Design and Rheological Characterization

The rheological profiles of recipe 2.BT (shown in Fig. 4. 1) are based on shear stress versus shear rate data provided in Table B. 9 (see Appendix B.3). No significant deviations between the profile corresponding to the data obtained on the original day right after preparation, marked by initial in black, and after 24 hours are observed. This observation was common for all rheological profiles obtained from the bentonite pill. However, common for all data after 24 hours were the decrease in shear stress values at lower shear rate readings as it can be seen in the figure below. When comparing the bentonite-based pill profiles, the best accordance is found with the Herschel-Bulkley model.

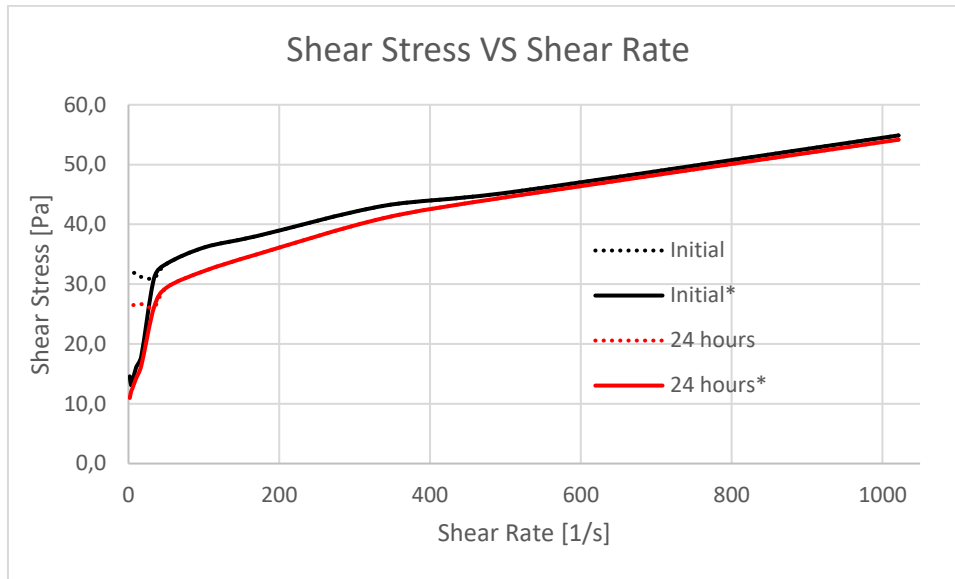


Fig. 4. 1 - Rheology profile of recipe 2.BT on original mixing day and after 24 hours

Table 4. 1 provides rheological parameters showing the same trend as observed in the rheological profile. PV, YP, gel strength values as well as Herschel-Bulkley parameters decrease after 24 hours compared to parameters at initial condition. This might be explained by the difference in temperature of the sample fluids at the individual measurement conditions.

Table 4. 1: Rheological parameters of recipe 2.BT.

	Initial Condition	After 24 hours
Temperature [°C]	20.0	24.7
pH	NA	11.86
Density [SG]	NA	1.03
Plastic Viscosity [cP]	22.1	19.3
Yield Point [lb/100ft ²]	63.3	82.9
Gel 10 sec	43.6	47.1
Gel 10 min	66.9	59.2
T _y [Pa]	11.22	10.81
n	0.14	0.23
k	13.15	7.34
ΔP [Pa]	1650.83	1460.82

As the viscometer programme calculated PV, YP and gel strength values based on the Bingham plastic analysis model, additional calculations were performed using the Herschel-Bulkley equations presented in chapter 3.3.1. All shear stress and shear rate values used and

referred to during H-B calculations are taken from Table B. 9 in Appendix B.3. Shear stress values initially displayed in lb/100ft² were converted to pascal (Pa) to simplify the mentioned calculations.

4.1.2 Interface Stability and Isolation on the Large-Scale Test Setup

When all fluids are placed in the static fluids system, the gel pill placed on top of the brine is further covered by a heavier WBDF. Densities of the fluids were typically measured to be 1.03 SG for the pill, 1.48 SG for WBDF and 1.3 SG for the brine. Hence, there is a natural tendency for the heavier WBDF to fall through the lighter pill beneath it as gravity is defied. Further, the spotted gel pill has two interfaces: the lower between the brine and pill and that between the gel pill and WBDF. It was of interest to both document the pill's ability to prevent instabilities at the interfaces as well as maintaining its integrity associated with complete isolation of the fluids regarding the density differences. This yields all tests performed on test setups from vertical with inclinations up to 40°. The same was investigated and documented for the laponite gel pill, which is presented in section 4.2.2.

Vertical test setup

Starting with tests performed on the vertical test setup, Fig. 4. 2 represents the interface of brine and the bentonite gel pill right after placement (left) and at the end of the test (right).



Fig. 4. 2 – Interface right after placement (left) and interface at end of test (right) on vertical setup

It was observed that the interface level of brine and pill sunken during the test period of 24 hours. This could at first sight be explained by either the total overlying fluid weight displacing the pill phase, or by ongoing swelling of the gel pill. Further hydration of the pill alone would result in compression of the brine column and increase of downhole pressure. As this was not the case, it was more reasonable to account for the scenario where the small air

bubbles trapped in the brine phase are compressed when the gel pill swells. In return, the brine penetrated the front of the gel pill entering the gel structure, just in the vicinity of the interface. Both explanations can account for the change in brine and bentonite pill interface level.

The statement of the bentonite pill phase being pushed down by the overlying fluid column becomes controversial when analysing the bentonite-based pill and WBDF interface. Fig. 4. 3 shows no indication of interface level displacement during the entire test period. This observation was supported by the fact that the camera location during recording remained the same throughout the test period.



Fig. 4. 3 – Interface right after placement (left) and interface at end of test (right) on the vertical setup

Fig. 4. 4 represents complete isolation achieved by the bentonite-based pill throughout the entire test period of 24 hours. Additionally, no sign indicating displacement of the pill phase was observed at test end.



Fig. 4. 4 - Successful isolation by the bentonite-based pill on the vertical test setup

20° inclined test setup

The brine and bentonite pill interface showed sign of a minimal displacement indicated by the arrows of identical size in Fig. 4. 5. The reduced subsidence compared to the vertical setup can be explained by a reduced overlying fluid weight on the 20° inclination compared to a greater hydrostatic weight exerting on the pill when the setup is vertical. Based on this explanation, the reduced weight exerted on the pill compresses the trapped air bubbles in the brine phase to a smaller extent. Thus, the interface displacement was created by smaller volumes of brine penetrating the front of the gel pill.

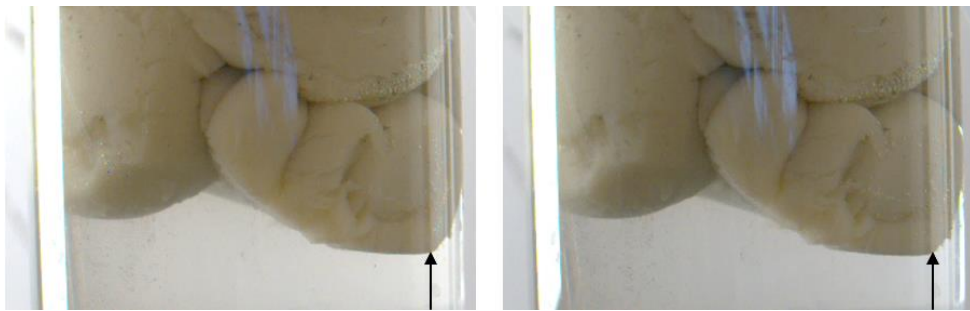


Fig. 4. 5 – Interface right after placement (left) and interface at end of test (right) on 20° inclined setup

The corresponding bentonite pill and WBDF interface represented in Fig. 4. 6 reveal a greater degree of displacement. The subsidence of the interface is related to the barite sag and more compact accumulation of barite particles resting on the pills surface compared to the situation on the vertical setup. This can also be seen by the change in WBDF phase. Right after WBDF placement, the fluid phase had a more uneven particle and floc distribution. After static barite settling the WBDF phase demonstrates a more compact phase, as shown below. As no signs confirmed that the entire pill phase had been displaced downwards, it is more feasible that the bentonite pill column was compressed by the WBDF.

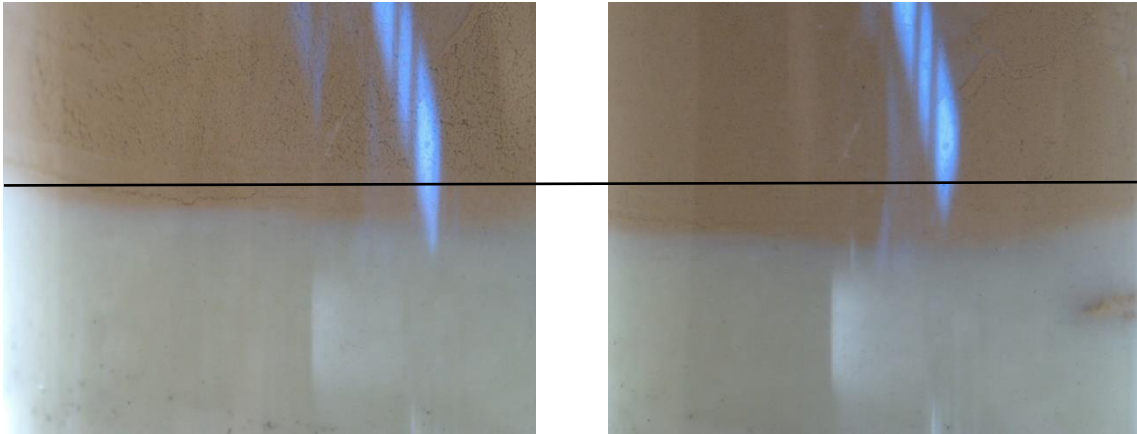


Fig. 4. 6 – Interface right after placement (left) and interface at end of test (right) on the 20° inclined setup

The small WBDF pocket accumulated in the bentonite pill phase (right side in Fig. 4. 6) was not originated by channelling. The WBDF simply filled an air pocket (see Fig. 4. 7) created during placement of the pill which was not possible to remove when compressing the pill during the pig operation.



Fig. 4. 7 - Air pocket inside the bentonite pill at the right corner established during placement

Fig. 4. 8 demonstrates the 20° inclined setup with all fluids spotted inside the tube. The bentonite-based pill successfully isolated the different fluids while maintaining its integrity throughout the test period.

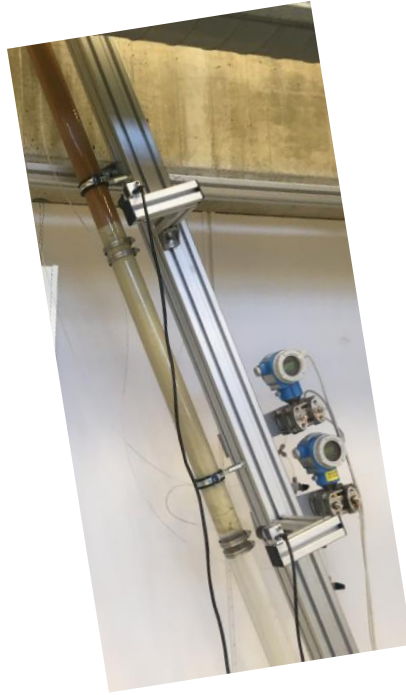


Fig. 4. 8 - Successful isolation by the bentonite-based pill on 20° inclination test setup

40° inclined setup

The final target was associated with results obtained from the 40° inclination from vertical closing this part chapter. No changes in vertical displacement of the interface section were observed. However, changes of the bentonite pill column in the horizontal direction are observed as indicated by the arrows in Fig. 4. 9. The lowest point of the bentonite pill was moved to the left apart from the pipe wall during the test period. This behaviour of lateral displacement might be based on a scenario involving several factors. The overlying fluid weight is significantly affected by inclination. Moreover, clay hydration was occurring parallel to compression of air bubbles resulting in brine penetrating the pill phase at the interface. Thus, results from the 40° inclined setup provide data to reflect that these factors combined create the change in the interface section throughout the test period.

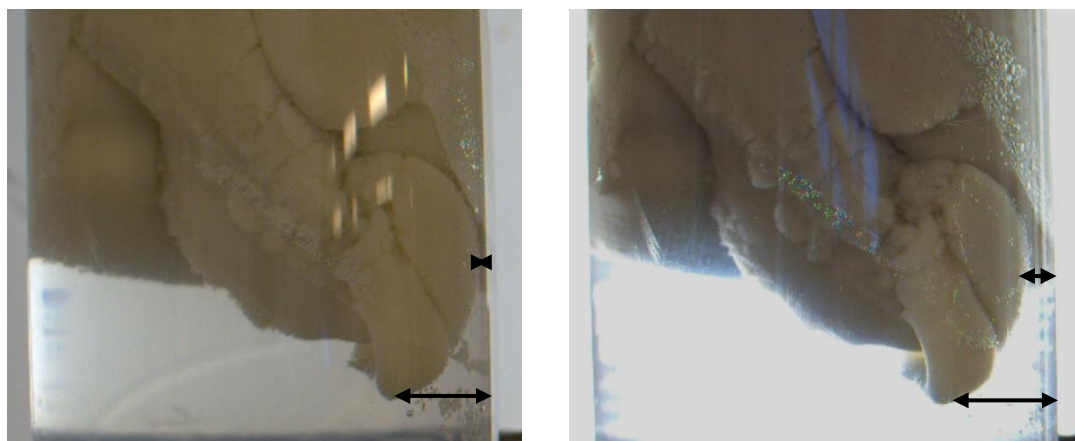


Fig. 4. 9 – Interface right after placement (left) and interface at end of test (right) on 40° inclined setup

The associated WBDF and bentonite pill interface is represented by Fig. 4. 11. On this particular test no pig operation was performed on the bentonite pill surface, leaving a thin layer of bentonite pill along the pipe wall as shown in Fig. 4.10. This thin layer supported the visualization of barite sag and bed accumulation behaviour. The effect of boycott driven barite sag led to the highest degree of vertical subsidence on the intersection level which is illustrated by arrows in Fig. 4. 11. The total hydrostatic fluid pressure above the bentonite pill was reduced significantly on the 40° setup compared to 20° and vertical. The bentonite pill hereby experiences less weight exerted by the overlying fluid column, despite subsidence of pill and WBDF interface is greatest. This might be originated by a more rapid and intense barite sag along the low side of the pipe wall pushing the entire bentonite pill surface downwards. The observation confirms that the pill column is compressed by the barite bed resting on top of the pill rather than the entire pill column being displaced.



Fig. 4. 10 - Bentonite pill surface after placement with thin pill layer across the pipe wall

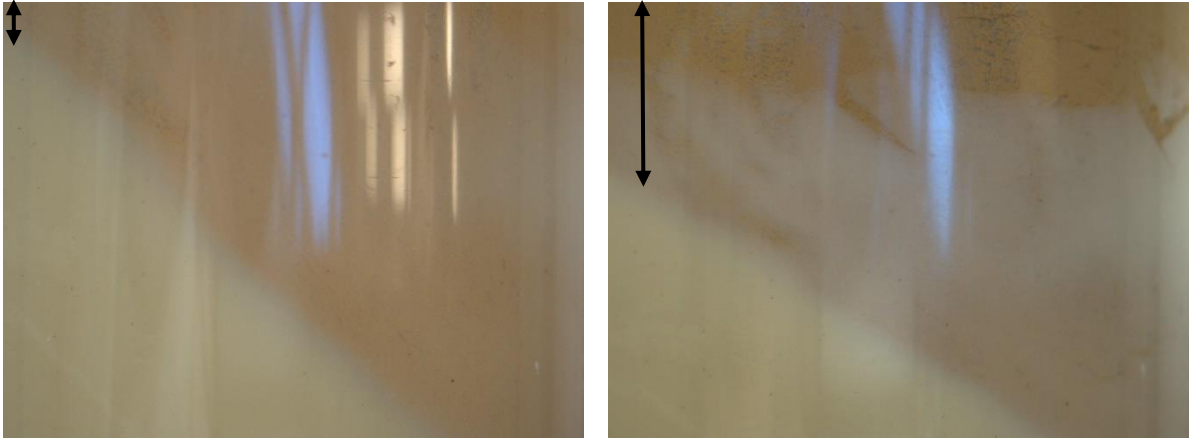


Fig. 4. 11 – Interface right after placement (left) and interface at end of test (right) on the 40° inclined setup

The theory regarding the pill column being compressed rather than displaced is approved as no sign of pill column displacement was observed, (see Fig. 4. 12). Results from the 40° inclined condition confirmed that the bentonite-based pill preserved full isolation by maintaining sufficient integrity, as shown in Fig. 4. 12 . No indication of channelling nor intermixing between the different fluid phases were observed throughout the 24 hours on all tests performed.

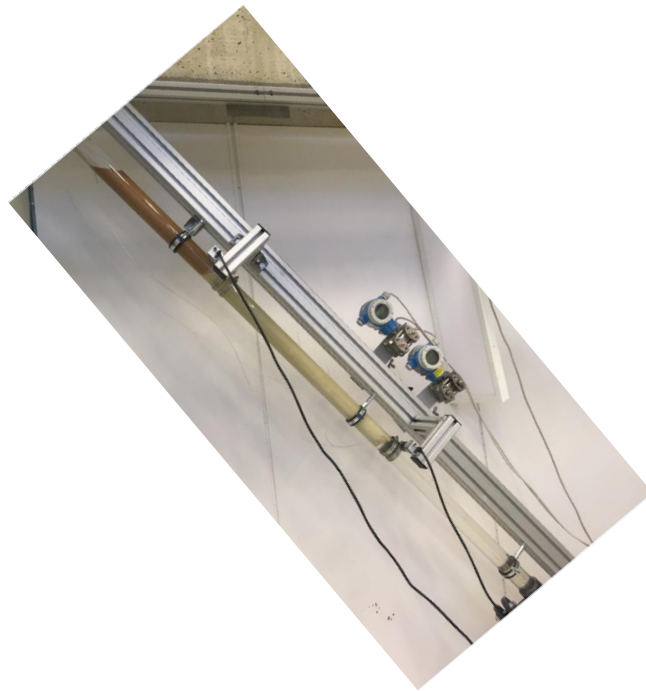


Fig. 4. 12 - Successful isolation by the bentonite-based pill on 40° test setup

4.1.3 Pressure Transmission during Placement and Test Period

This chapter presents results regarding the bentonite-based pill's ability to transmit pressure from the overlying fluid columns both during placement and the entire test period of 24 hours. In addition, pressure data associated with maintenance of constant bottom hole pressure will also be discussed. Pressure data will be presented in the same order as test series conducted on the test setup initiated with vertical followed by 20° and 40° inclination from vertical.

Pressure signals corresponding to the different fluids spotted will only be discussed in detail reviewing results obtained from the vertical test. Further, pressure signals displayed by the XP2i pressure sensor during fluid positioning showed a similar pattern on test results regarding the 20° and 40° inclined setup and will not be discussed as detailed as for the vertical setup. Only special operational situations, deviations or other effects affecting the pressure will be highlighted and discussed in more detail for the 20° and 40° setup, respectively. Duration of the fluid placement procedure was typically 2 to 3 hours individual for each test before the pipe was left undisturbed.

Vertical Test Setup

Fig. 4. 13 demonstrates the pressure signals received and monitored by the bottom hole pressure sensor (XP2i in blue) and both differential pressure sensors DP1 (grey) and DP2 (orange) for the fluid placement period.

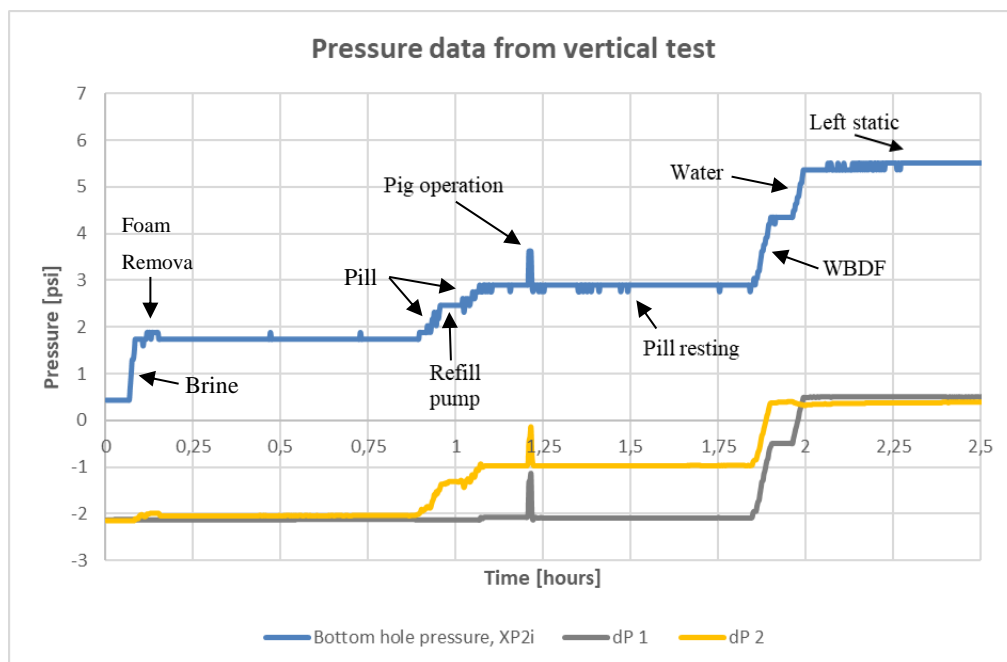


Fig. 4. 13 - Bottom hole, DP1 and DP2 pressure reading during placement period, vertical setup

The bottom hole pressure sensor (XP2i) measured all pressure increases caused by fluids added to the system marked by arrows. At the beginning of the test, the pipe was completely empty while outlet tubes installed along the pipe wall connected to the pressure sensors were filled with water. This explains why the bottom hole pressure sensor does not monitor zero hydrostatic pressure at the test begin. The same fact yields for differential pressure sensors DP1 and DP2. Pressure increases are detected by DP1 and DP2 once the lower outlets of the sensors were covered by fluids.

As shown, a rapid pressure increase is picked up by sensor XP2i when brine is placed in the system. A significantly smaller pressure increase in form of pressure instabilities are read when created foam on the surface of the brine was removed with a hose. Further, a period of constant pressure readings follows while preparation of the bentonite pill placement was conducted. Between the time interval of 0.75 and 1.0 hours, pressure increases further reflecting the placement of the pill. At around 1.0 hour, pressure was kept constant again while the pump used to hydraulically place the pill was refilled before pumping proceeded resulting in an additional pressure increase. After the bentonite-based pill was spotted, a pig operation was conducted at around 1.25 hours creating a sudden pressure increase indicated by the pressure spike read by XP2i, which stabilized when the pig was removed. The same pressure behaviour was detected by DP1 and DP2. Constant pressure was read for a longer time interval as the bentonite pill was left static to form a gel structure. During the interval of 1.75 and 2.0 hours, WBDF and water were placed in the system indicated by the arrows and represented by a stronger pressure increase, resulting in a total pressure of 5.36 psi at 2.0 hours.

The orange and grey plot corresponding to differential pressure sensor DP2 and DP1 associate the pressure profile of the bottom hole pressure sensor regarding the fluids placed in the system. As mentioned, DP1 monitors the differential pressure between the bentonite pill and water added on top of the WBDF, while DP2 monitors the difference in pressure between the brine and WBDF columns. As the lower outlet of DP2 is located in the brine phase, it detects all pressure signals corresponding to all fluids added and follows a similar trend as XP2i. DP1 starts to detect pressure signals after the bentonite-based pill was positioned following the same trend as DP2 and XP2i.

Focusing on the time period between 1.75 and 2.0 hours representing placement of WBDF and water on top of the pill, the obtained pressure data confirm that the bentonite-based pill transmits the hydrostatic pressure of the overlying fluid columns. The pressure increases transmitted by the pill when WBDF and water were added ranges from approximately 2.9 psi (at time 1.79 hours) to 5.36 psi (at time 2.0 hours). Based on these pressure data, the bentonite

pill is qualified as a fluid pressure transmission pill and does not act as a barrier blocking the pressure signals.

Another target to investigate and qualify, was the pill's ability to maintain hydrostatic pressure at the bottom of the pipe. The pressure data corresponding to sensor XP2i in Fig. 4. 14 presents a slight pressure increase throughout the test period.

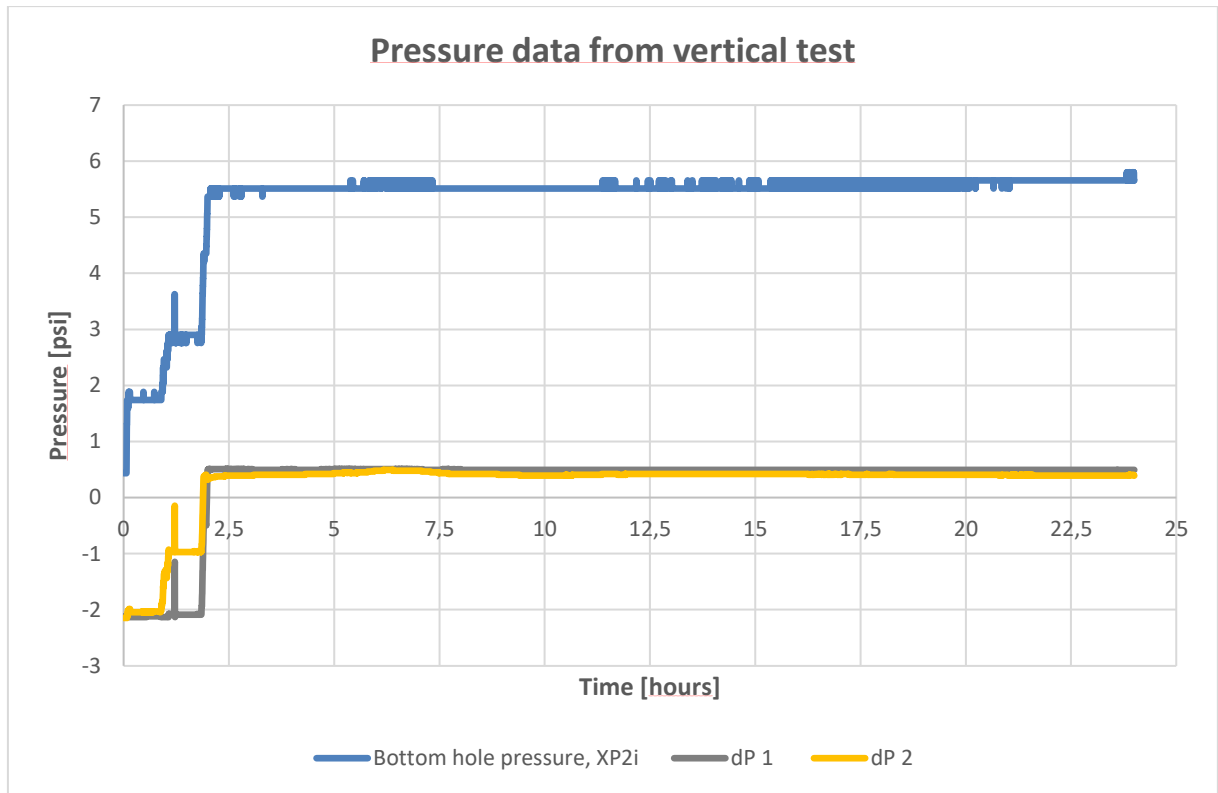


Fig. 4. 14 - Pressure monitoring during the test period of 24 hours, vertical setup

Studying the bottom hole pressure after fluid placement was completed with 5.36 psi at time 2.0 hours, the pressure profile indicates a rapid increase to 5.51 psi at time 2.09 hours. A bottom hole pressure of 5.51 psi is kept for a longer period before changes in pressure were detected during period of 11.4 to 21.3 hours with a bottom hole pressure kept at 5.65 psi. Eventually, pressure increases further to 5.8 psi at approximately 24.0 hours. With basis in time interval ranging from 2.0 to 24.0 hours, the total hydrostatic pressure changed from 5.36 to 5.8 psi resulting in an increase of 0.44 psi (0.03 bar) throughout this period.

Changes in bottom hole pressure can be a result of temperature variations affecting the pressure sensors. The temperature in the laboratory changes throughout day and night additionally influenced by the ventilation system being turned off from 23:00 to 09:00 o'clock in the laboratory. The assumption regarding pressure sensors being sensitive to temperature

changes is based on observations from pressure profiles when the setup was filled with water and monitored for 24 hours, (see Appendix B.7).

Another explanation for the pressure increase can be due to changes in the pill's gel strength properties influencing the pressure communication. It might be that the gel pill's ability to transmit pressure signals improved as the pill phase developed a more effective gel strength over time.

The fact that pressure changed during the test period was also detected by DP2. At time 2.0 hours, DP2 read 0.34 psi while the highest pressure read after 6.1 hours was 0.49 psi continuing with a pressure reduction to 0.39 psi at 24.0 hours. This pressure behaviour is reasonable considering barite sag. When barite sag occurs, the solid particles accumulate on the bentonite pill surface leaving a pure water phase covering the upper outlet of DP2 which originally was covered by a more uniform barite particle suspension in the WBDF column. Thus, resulting in a pressure reduction. DP1 monitoring the differential pressure between the pill and water column kept constant readings of 0.49 psi throughout the test.

20° Inclined Setup

Results from tests performed at 20° of inclination (see Fig. 4. 15) also confirmed the bentonite-based pill's ability to successfully transmit pressure signals from the WBDF and water spotted above the pill. This is proven by the pressure increase read by XP2i from 2.46 psi at 1.78 hours after the bentonite pill was placed to 4.78 psi at time 1.9 hours after WBDF and water were added.

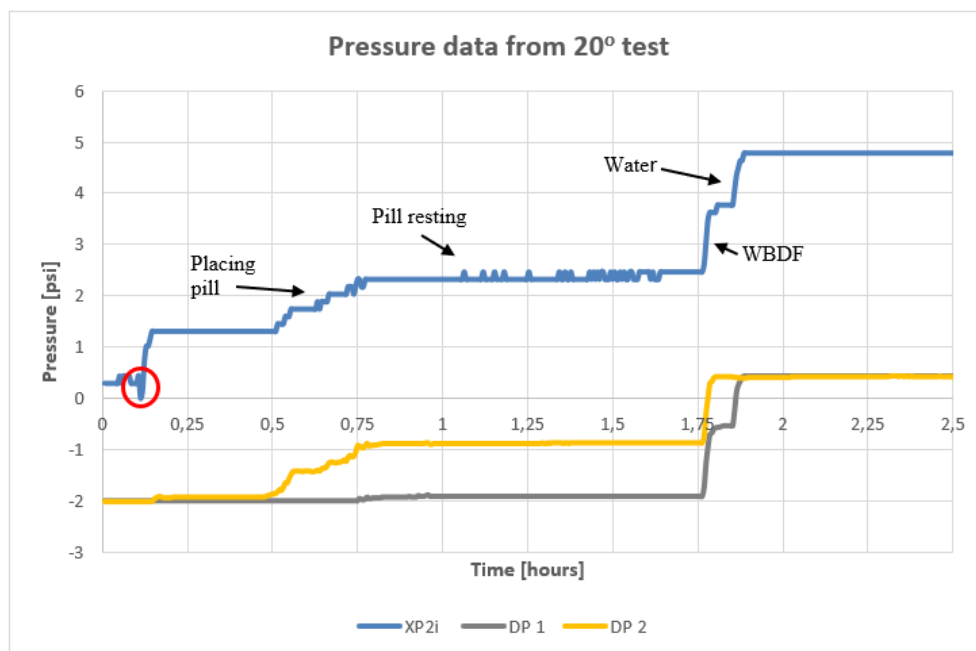


Fig. 4. 15 - Bottom hole, DP1 and DP2 pressure reading during placement period, 20° setup

Furthermore, the sudden pressure drop at around 0.12 hours indicated by the red circle in Fig. 4. 15 seems very unusual during fluid placement. In some cases, a pressure drop of this kind was detected by the XP2i pressure sensor when a small volume of brine was removed from the test pipe as the original brine volume exceeded the outlet of DP2 too much. This explained brine removal creating a pressure drop normally appeared on the XP2i plot after brine placement was completed. No logical reason can explain this sudden pressure drop other than instrumental errors in sensor XP2i considering no pressure instabilities observed by DP1 and pressure increase detected by DP2.

For the remaining test period (see Fig. 4. 16), starting with a total hydrostatic pressure of 4.78 psi at 1.9 hours roughly after fluid placement, the hydrostatic pressure increased to 4.93 psi at the test end at 24.0 hours. This is equivalent to a pressure increase of 0.15 psi (0.01 bar).

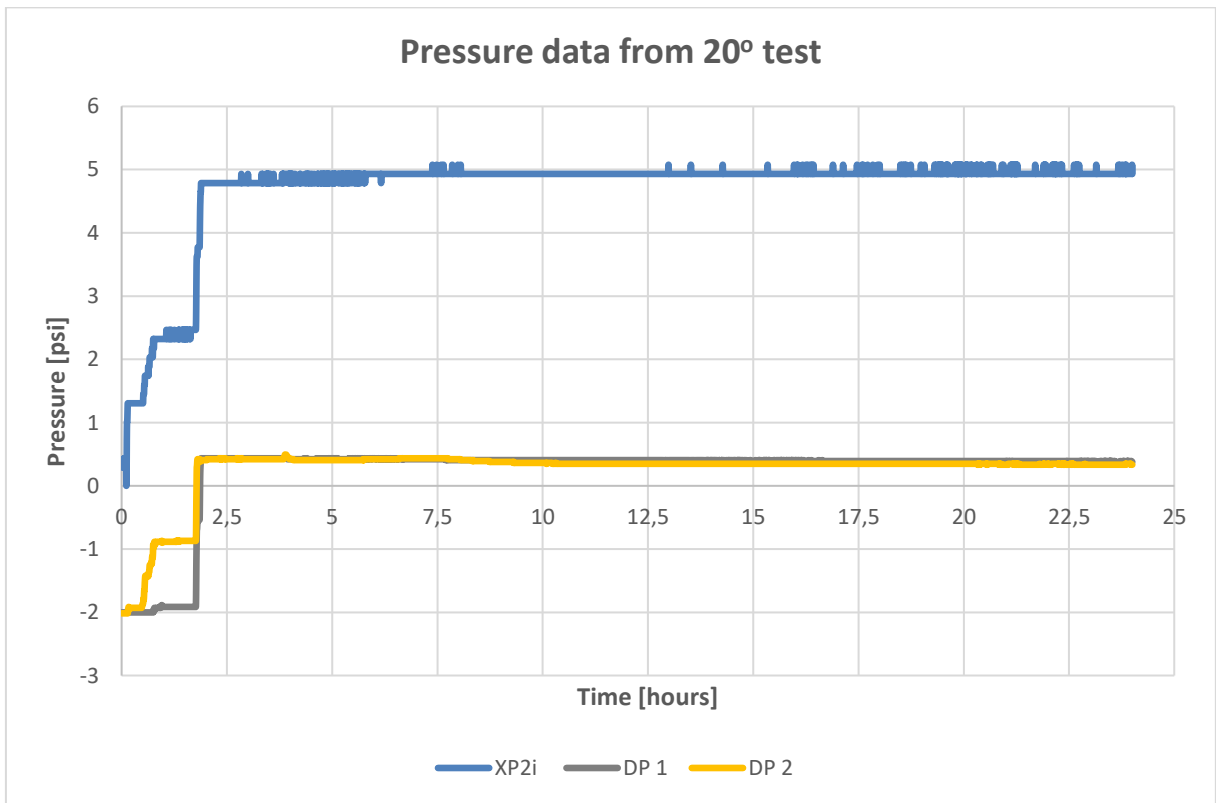


Fig. 4. 16 - Pressure monitoring during the test period of 24 hours, 20° setup

Outliers seen on the XP2i plot in Fig. 4. 16 after fluid placement might be caused by temperature changes in the laboratory.

Further, the plot corresponding to differential pressure DP2 in Fig. 4. 16 indicated a more stable change in pressure from 3.8 hours continuing with a pressure reduction after roughly 7.5 hours. This is caused by barite sag changing the hydrostatic fluid pressure in the

WBDF column. Thus, the observed pressure difference of 0.15 psi recorded by XP2i is most likely a combination of increased pressure communication by the pill and greater degree of sag on this setup.

40° Inclined Setup

Over to the last test setup of 40° inclination to investigate, pressure data during fluid placement are represented in Fig. 4. 17.

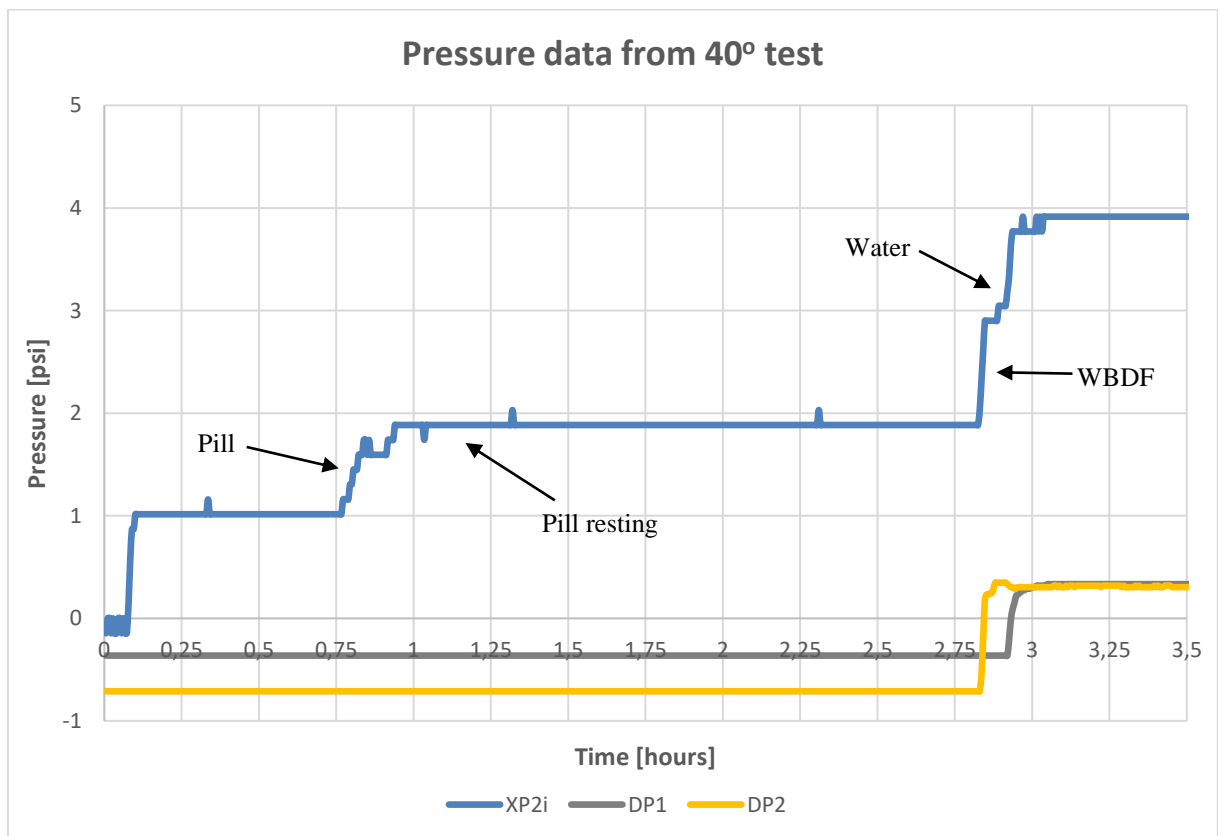


Fig. 4. 17 - Bottom hole, DP1 and DP2 pressure reading during placement period, 40° setup

Also, in the case of 40° inclination, the bentonite pill transmitted the pressure signals corresponding to an increase from 1.85 psi at 2.7 hours to 3.9 psi after 3.0 hours associated to the WBDF and water columns. As the total hydrostatic pressure decreases due to increased inclination, it was expected that the total bottom hole pressure measured was reduced compared to that of the 20° and vertical.

Fig. 4. 18 represents the pressure profiles for the entire test period. Constant bottom hole pressure was maintained by the bentonite pill after water was added at 3.0 hours reading 3.9 psi for a time period of roughly 2 hours according to sensor XP2i. After 5 hours sensor XP2i read

pressure instabilities resulting in a pressure drop. After pressure dropped, a hydrostatic pressure of 3.71 psi was kept throughout the remaining test period. The bottom hole pressure was in total reduced by 0.19 psi (0.013 bar) during the test. The pressure drop was also indicated by both differential pressure sensors, where DP2 measured a slightly larger pressure reduction. This pressure behaviour was expected based on barite particle sliding along and partial resting on the low side of the pipe. Hence, the more intense boycott driven settle regime on this setup reduced the barite particles contribution on the hydrostatic pressure. This presumption is further based on the total pressure reduction of 0.19 psi compared to observed pressure increases on the vertical and 20° setups.

A deviation in pressure detection of DP1 and DP2 compared to readings from the 20° and vertical setup was also observed. DP1 and DP2 did not detect any pressure increase until WBDF placement. Caution was always kept regarding proper covering of outlets with the corresponding fluids. Hence, no explanation other than the degree of inclination on this setup compared to the previous can be provided on this observation.

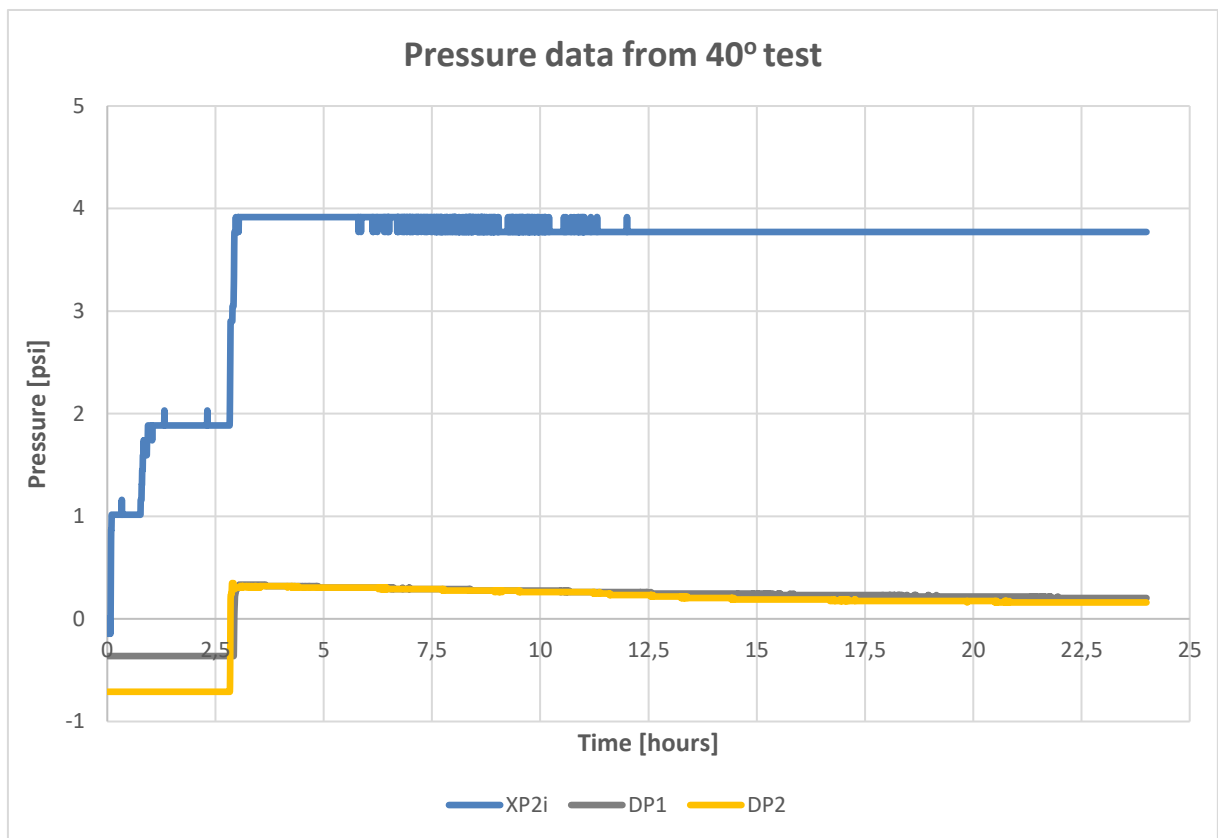


Fig. 4. 18 - Pressure monitoring during the test period of 24 hours, 40° setup

Combined Bottom Hole Pressure Profiles

Finally, all bottom hole pressures monitored by sensor XP2i corresponding to the different setups are summarized Fig. 4. 19. A clear trend of pressure decrease is seen going from vertical towards 40° inclination. The total hydrostatic pressure measured at bottom for the 40° inclination was 3.71 psi, compared to 4.93 psi for 20° and 5.66 psi on the vertical test setup at the test end.

Changes in pressure were observed during the test period on all inclinations. Neglecting the impact of temperature on the pressure sensors it seems more reasonable that other factors affected the pressure. The most significant factor associated with reduced hydrostatic pressure over the test period was the degree of inclination. Further, the hindered settling mechanism from the vertical changing to a boycott driven sag regime partly on the 20° inclination and considerably on the 40° setup also affected the pressures. Followed by the fact that particle settling distance is significantly lowered on the 40° setup. Particles do slide along and over time rest on the pipe wall and thereby having less impact on the hydrostatic fluid column above the pill. Hence, the degree of constant bottom hole pressure preservation by the bentonite-pill is difficult to confirm. It seems like the pressure communication improved over time based on increased pressure detected on vertical and 20° setups and decreased pressure on the 40° inclined tests. This pressure behaviour might be related to the effective gel strength of the pill being formed over time. Moreover, more studies should be conducted to determine the required time period for the gel pill to reach maximum gel strength and yield point. This would present a better relation between rheology properties and the degree of pressure transmission provided by pill. By considering the highest pressure change of 0.44 psi observed on the vertical setup, however, the preservation of bottom hole pressure is approximately constant.

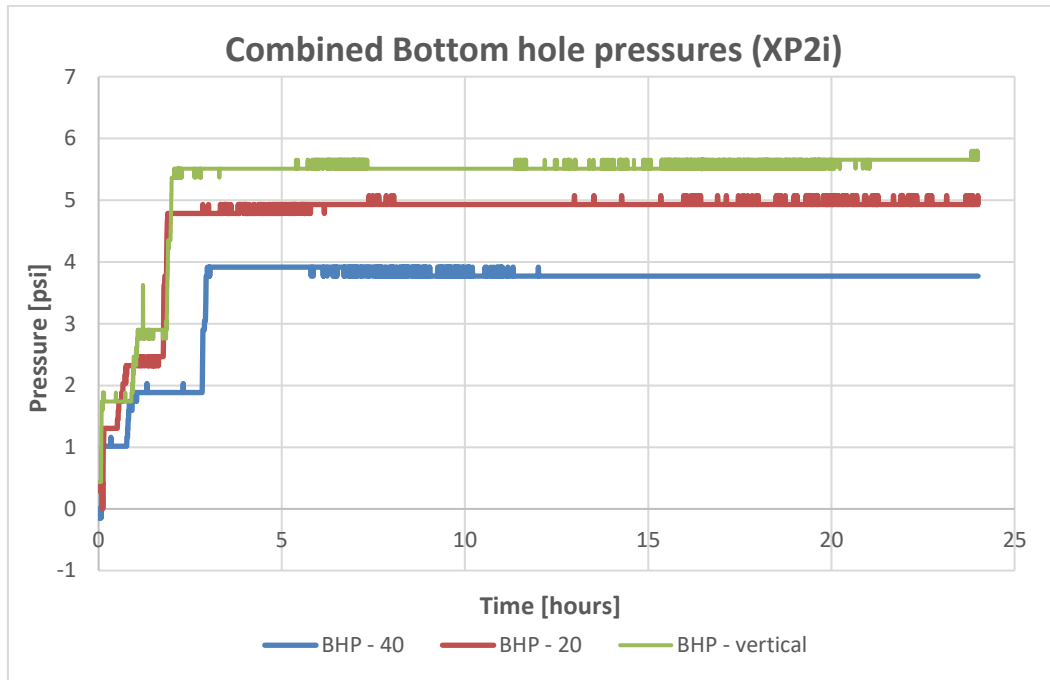


Fig. 4. 19 - Combined bottom hole pressure data from tests

4.2 Laponite RD-Based Sag Prevention Pill

As it was difficult to get an understanding of the fluid-fluid interfaces during the pill placement, it was chosen to work with the laponite-based gel pill to investigate causes of instabilities and failures. Laponite RD was chosen as it behaved in a similar manner as the bentonite pill. In addition to creating a transparent gel pill which provided a better insight of interface stability and pill integrity issues compared to the bentonite-based pill.

4.2.1 Fluid Design and Rheological Characterization

The development of the laponite-based sag prevention pill required more testing and analysis as laponite was a product of unknown rheological properties when experimental work started. Recipes 1, 3, and 4.L were created at a later stage during the third part of the experimental work to conduct a more thorough investigation on rheological properties before proceeding to the large-scale test setup. Fig. 4. 20 provides the rheological profiles of all recipes obtained on the original mixing day based on shear stress and shear rate values. Rheology measurements of recipe 5.L (20g laponite-based) were taken at an earlier stage than the remaining recipes. At this stage the procedure (see Table A. 2 step 10.0 to 10.3) used to obtain more accurate readings

at lower shear rate readings was not implemented. Explaining the more abrupt transition at lower shear rate readings compared to the other profiles. In general, all recipes except 5.L show a similar profile trend with shear stress values rising with increased laponite concentration.

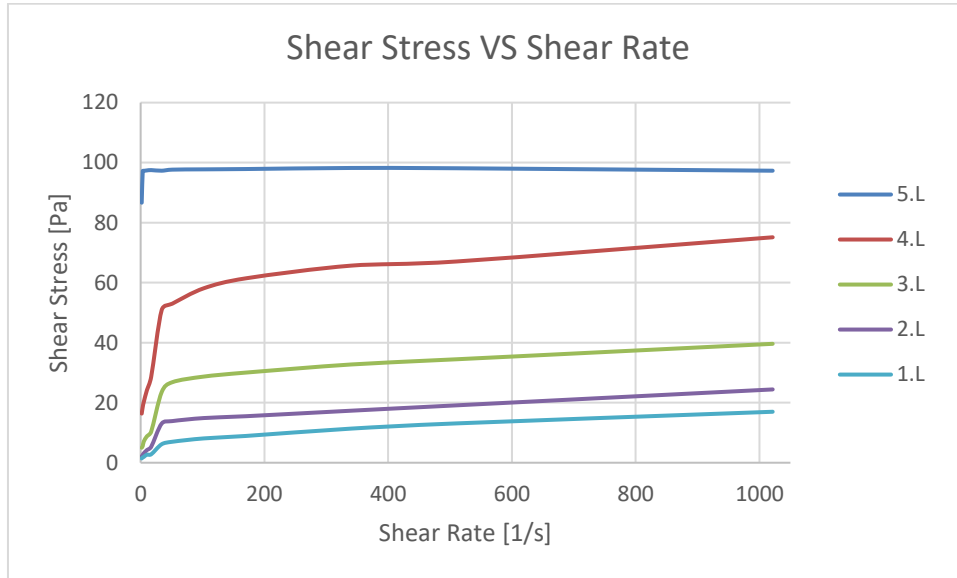


Fig. 4. 20 - Rheological profile of all laponite-based pill recipes

Based on criteria established (discussed in chapter 3.3.2), recipe 3. L was chosen and adjusted to recipe 3.LT (see Table 3. 3 and Table 3. 8) establishing the laponite-based gel pill for experiments on large-scale. The corresponding rheology profile of recipe 3.LT is represented in Fig. 4. 21 demonstrating a typical Herschel-Bulkley profile. The profiles of recipe 3.LT are based on shear stress and shear rate values provided in Table B. 10 (Appendix B.5). Common for the laponite-based pill was the increase in shear stress after 24 hours compared to the values obtained at initial condition.

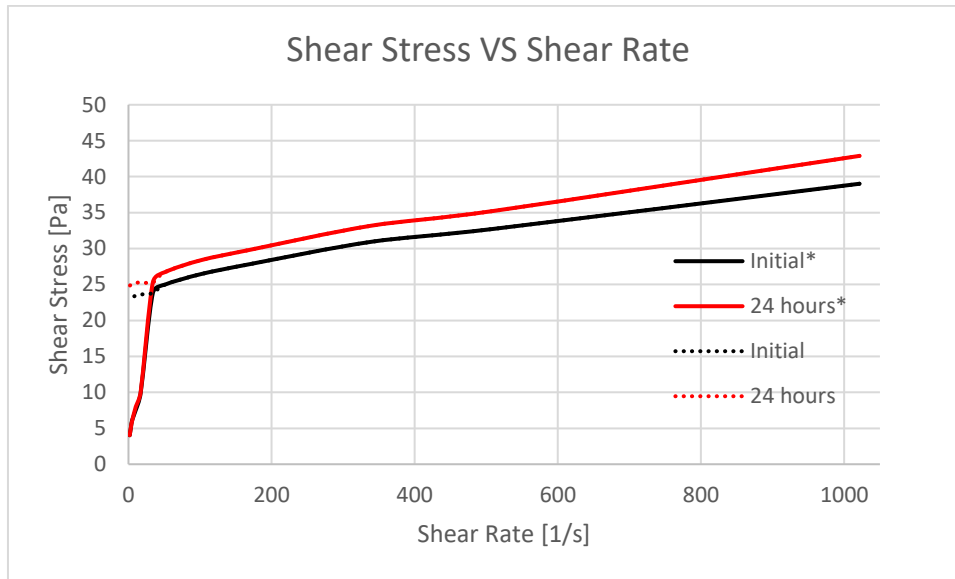


Fig. 4. 21 - Rheological profile of recipe 3. LT

Table 4. 2 contains important rheological parameters of recipe 3.LT. Parameters such as PV, YP and gel strength values were provided by the mud program on the viscometer. Parameters like τ_y , n and k were obtained by equations associated to the Herschel-Bulkley model described in chapter 3.3.1. An interesting observation was the slight reduction in 10-min gel strength and τ_y after 24 hours, as these two values are obtained on different grounds. It is therefore reasonable to address that the laponite-based pill had the greatest gel strength on the original mixing day, which also was observed on other rheological measurements.

Table 4. 2: Viscometer data and rheological parameter of recipe 3. LT.

	Initial Condition	After 24 hours
Temperature [°C]	20.7	21.6
pH	NA	12.14
Density	NA	1.01
Plastic Viscosity [cP]	14.7	16.4
Yield Point [lb/100ft ²]	45.7	49.8
Gel 10 sec	30.3	35.0
Gel 10 min	131.0	122.5
T _y [Pa]	4.69	4.03
n	0.12	0.11
k	12.50	14.56
ΔP [Pa]	3232.56	3022.82

4.2.2 Interface Stability and Isolation on the Large-Scale Test Setup

Also, the laponite-based pill's integrity and ability to isolate the upper and lower fluid sections were documented by camera recording during and after placement. Preserved isolation of the fluid intersections right after placement and at the end of the test will be discussed.

Vertical Setup

Fig. 4. 22 represents the interface between brine and laponite-pill right after placement and at the end of the test. No displacement of the interface to the vertical or lateral were observed. It seemed like the laponite pill was stiffer compared to the bentonite pill. This can be explained by significantly higher 10-min gel strength values regarding the laponite compared to the bentonite pill. This theory is further based on the greater subsidence of the brine and bentonite pill interface observed on the vertical setup.

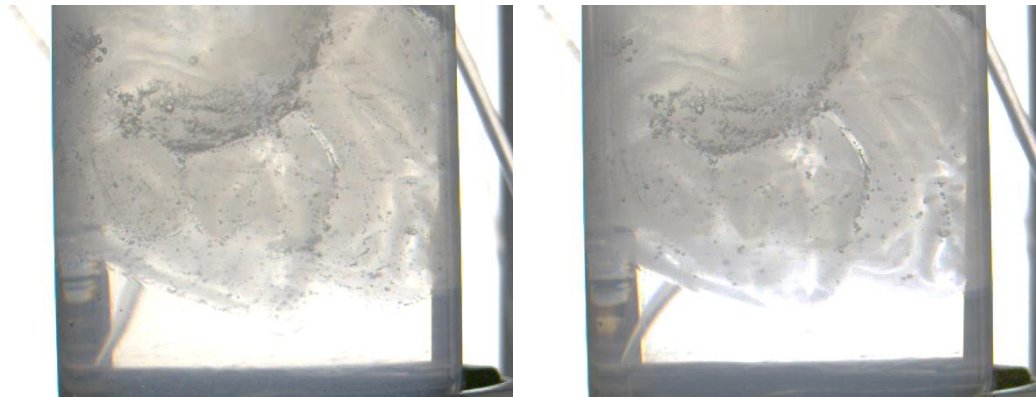


Fig. 4. 22 – Interface right after placement (left) and interface at end of test (right) on vertical setup

As it can be seen in Fig. 4. 23, a minimal vertical displacement of the WBDF and laponite pill interface was observed at the end of the test. This is pointed out by the black straight line and arrows pointing in the vertical direction. A more concentrated subsidence of the barite is indicated by the lateral pointing arrow. Subsidence of the interface was probably caused by the barite particle accumulation resting on the pills surface adding more weight and in return compressing the pill phase.

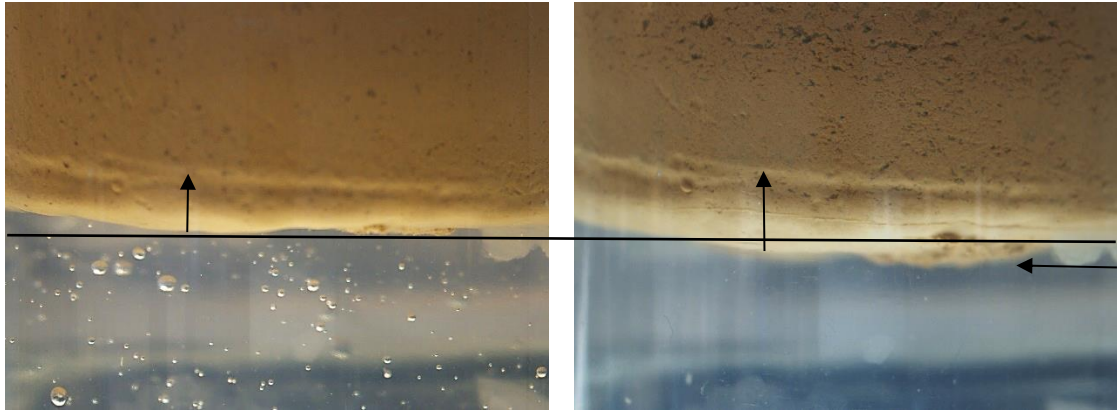


Fig. 4. 23 – Interface right after placement (left) and interface at end of test (right) on vertical setup

Regardless of the interface displacement caused by the barite sag, complete isolation and integrity was preserved for the entire test period as demonstrated in Fig. 4. 24.



Fig. 4. 24 - Successful isolation by the laponite-based pill on the vertical test setup

20° Inclined Setup

On the 20° inclined setup, vertical displacement was observed and is indicated by the arrows in Fig. 4. 25. It is seen that the lowest point of the laponite pill was displaced downwards, thus the entire interface has slightly moved downwards over time. This behaviour might rely on compression of trapped air bubbles in the brine phase over time. In return, the brine penetrated the front of the gel pill entering the gel structure at the interface similar to the behaviour of clay hydration.

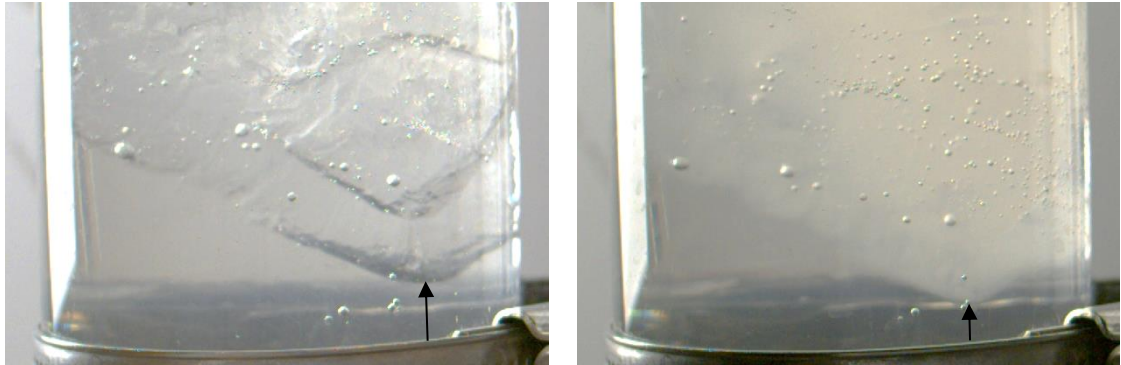


Fig. 4. 25 – Interface right after placement (left) and interface at test end (right) on the 20° inclined setup

Further, the entire interface of WBDF and laponite pill was lowered during the 24 hours as presented in Fig. 4.26. Despite the subsidence of both interfaces with respect to the laponite pill, no signs indicated that the entire pill phase was displaced. It is reasonable to assume that barite sag contributed to subsidence of the intersection and thereby compressing the pill.

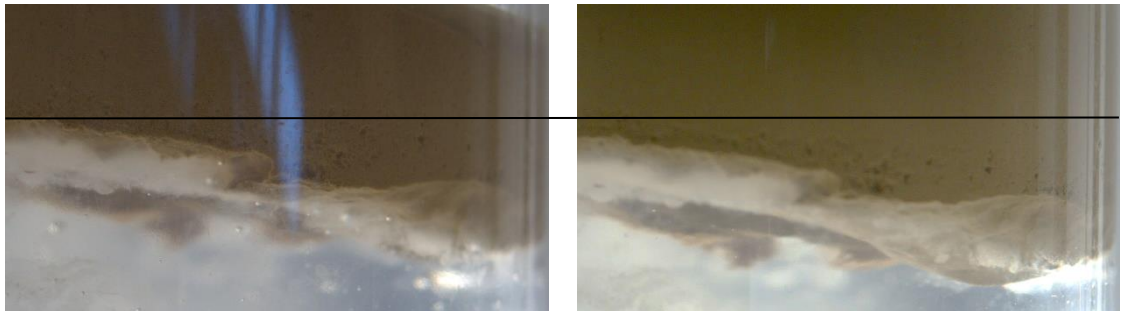


Fig. 4. 26 – Interface right after placement (left) and interface at test end (right) on the 20° inclined setup

Regardless the displacement of interface levels observed, the laponite-based pill successfully isolated the fluids in the system by providing sufficient integrity during the test as it can be seen in Fig. 4. 27.



Fig. 4. 27 - Successful isolation by the laponite-based pill on 20° test setup

40° Inclined Setup

In this particular test, the cameras had to be relocated as the interface levels were at different spots covering the outlets of the differential pressure sensors properly. Thus, the camera recording on this setup was compromised by metal rings installed on the pipe which are part of the supportive construction. Based on the documented interface no severe if no indication on displacement of the brine and laponite pill interface could be observed, (see Fig. 4. 28). This observation can be leaned on the fact that the pill is exposed to less overlying fluid weight. Also, a combination of a stiffer gel pill and less fluid weight might have reduced the impact on compressing the trapped air bubbles in the brine phase.



Fig. 4. 28 – Interface right after placement (left) and interface at test end (right) on the 40° inclined setup

As visibility was compromised considerably at the WBDF and laponite pill interface, no specific results regarding displacement can be discussed for sure. However, considering the fact that interface level subsidence caused by barite sag, and especially boycott driven barite sag present on the 40° inclination, it can be assumed that the interface level was lowered. This is demonstrated by the arrows seen in Fig. 4. 29.



Fig. 4. 29 – Interface right after placement (left) and interface at test end (right) on the 40° inclined setup

Despite the effect of inclination, the laponite-based pill preserved full isolation of the different fluids in addition to keeping sufficient integrity when left at static for the test period, (see Fig. 4. 30).



Fig. 4. 30 - Successful isolation by the laponite-based pill on 40° test setup

4.2.3 Pressure Transmission during Placement and Test Period

The laponite-based pill's ability to transmit pressure of the overlying fluid columns has also been investigated on the vertical, 20° and 40° inclined setups. In this section, pressure data obtained from the different tests will be presented and discussed. As for the bentonite-based pill, pressure data corresponding to the vertical setup will be viewed in more detail. For the remaining test data only deviant effects and procedure in the operation will be highlighted. Consequently, only placement of laponite pill and pressure transmission signals from the WBDF and water columns will be discussed for the 20° and 40° inclinations.

Vertical Setup

As is can be seen in Fig. 4. 31, the pressure profile of the bottom hole pressure, XP2i, corresponding to the blue graph reads all increases in pressure associated with fluids added to the system, also indicated by arrows.

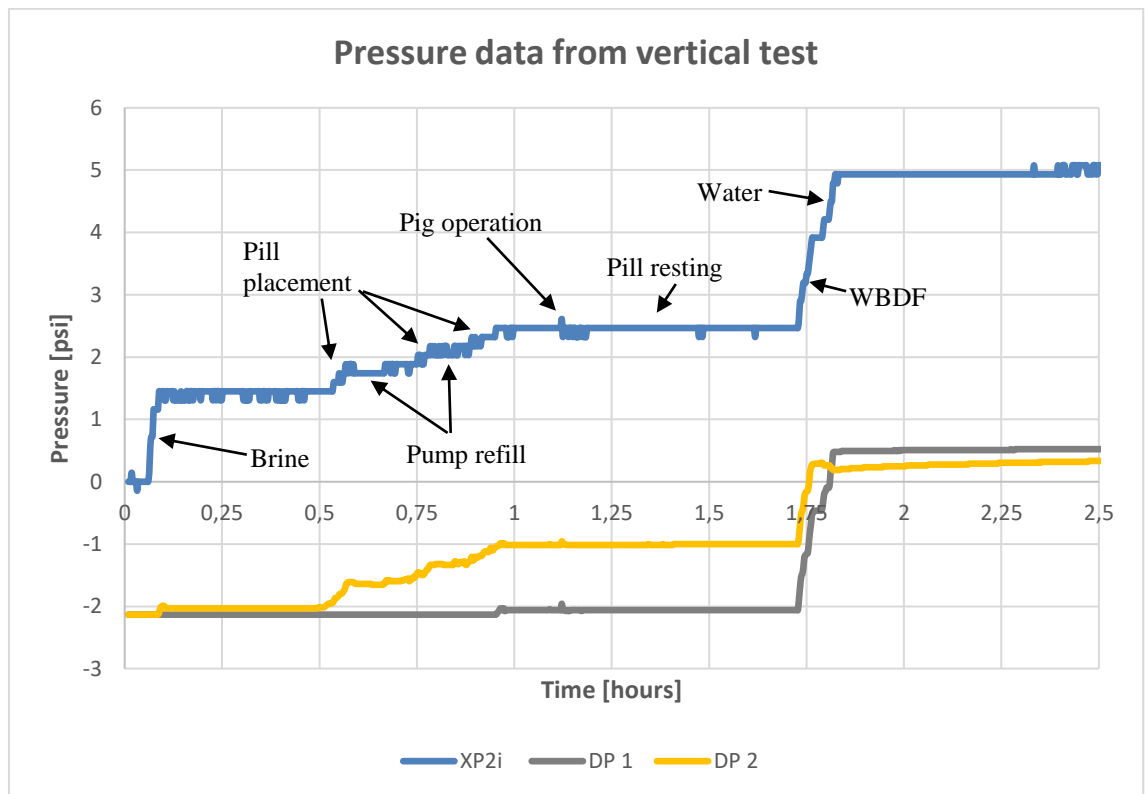


Fig. 4. 31 - Bottom hole, DP1 and DP2 pressure readings during placement period, vertical setup

In this particular test it was chosen to reset the bottom hole pressure sensor XP2i when the pipe was completely empty while the outlet tube connected to XP2i was filled with water.

This explains why the bottom hole pressure sensor reads zero pressure at the very test begin. An abrupt pressure increase is detected when brine was spotted in the test pipe. Followed by a longer period of constant bottom hole pressure as the placement operation for the laponite pill was prepared. This is also reflected by differential pressure sensor DP2, which measures the differential pressure between brine and WBDF column. After roughly 0.5 hours, further pressure increase was read by XP2i caused by the added laponite pill. Pressure continues to increase until the entire pill column was spotted. During placement of the pill, two constant pressure intervals were detected by the bottom hole sensor due to refilling of the hand-driven pump used to place the pill, also indicated by arrows. The graph corresponding to DP2 shows similar characteristics as the monitored pressure of XP2i. The laponite pill placement was completed at around 1.0 hour resulting in a constant pressure of 2.46 psi read by XP2i. Once the laponite pill was spotted, DP1 measured a pressure increase as the pill covered the lower outlet of DP1. A constant pressure of 2.61 psi measured by XP2i was kept until the pig operation was performed which is indicated by the sudden pressure increase at around 1.12 hours detected by all pressure sensors. Detection of the pig operation by the differential pressure sensors in addition to XP2i sensor creates reliability for the pressure profiles. After the pig operation, the pill was left at rest with constant pressure monitored by all sensors. Placement of WBDF and water columns were monitored by XP2i with a strong pressure increase from 2.61 psi after pill placement to 4.93 psi at 1.8 hours. While DP2 measured the increase caused by the WBDF and water with a similar profile as sensor XP2i, DP1 monitored a more uncharacteristic behaviour in pressure. Regardless, results confirm that the laponite-based pill transmits pressure signals from the fluid columns added on top of the pill.

When analysing pressure monitoring during the 24 hours test period, it is clearly observed in Fig. 4. 32 that the bottom hole pressure varies throughout the entire test. The same observation is confirmed by the pressure profile of differential pressure sensor DP2. In spite of the large pressure variations measured by XP2i after all fluids were placed, a total pressure of 5.08 psi was measured both shortly after fluid placement at 2.8 hours and at the test end at 24.0 hours. During this time interval, the lowest pressure measured by XP2i was 4.78 psi and the highest 5.22 psi. Considering the pressure trend profile of XP2i and DP2, temperature effects of technical errors on the bottom hole pressure sensor should in this case not be excluded.

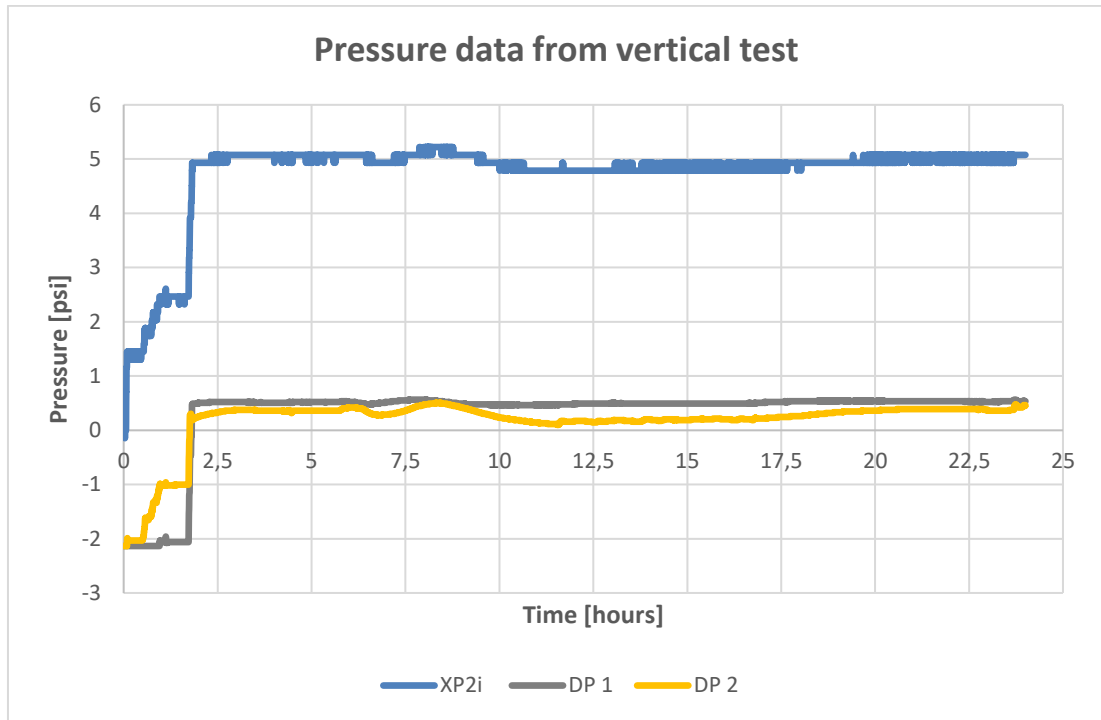


Fig. 4. 32 - Pressure monitoring during the test period of 24 hours, vertical setup

20° Inclined Setup

The pressure data presented in Fig. 4. 33 show that the laponite gel pill successfully transmits the pressure from the overlying fluid columns. This can be confirmed by sensor XP2i detecting a pressure increase from 2.61 psi with brine and laponite pill inside the pipe (at 1.8 hours) to 4.93 psi (at 1.99 hours) when all fluids were placed. In addition, the pressure profile of DP2 has the same characteristic behaviour as the one obtained from the vertical test setup and at the same time reflecting readings from XP2i. The sudden pressure drop from 0.25 psi (1.9 hours) to 1.13 psi (1.96 hours) monitored by DP2 when water was added has no reasonable explanation other than the removal of the hose being submerged inside the water column during placement.

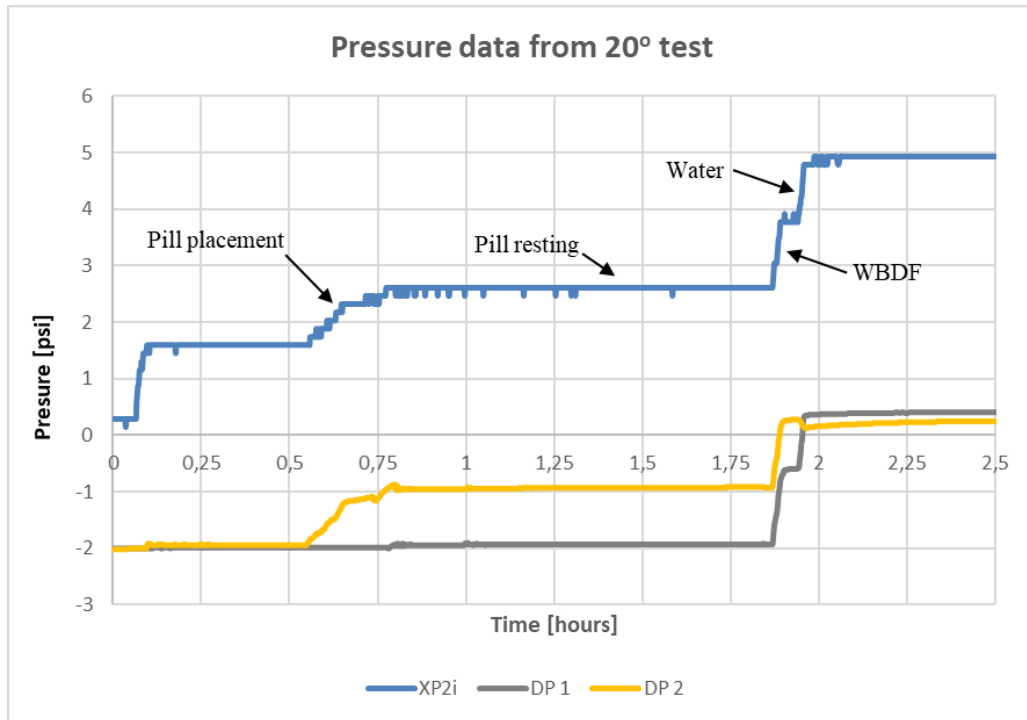


Fig. 4. 33 - Bottom hole, DP1 and DP2 pressure readings during placement period, 20° setup

When analysing the monitored pressure profiles for the entire test period in Fig. 4. 34, a clear pressure declination represented by sensor XP2i is observed. This can be explained by a quicker barite sag occurring on the 20° inclination compared to that of the vertical. A smoother declination of pressure is monitored by sensor DP1 reflecting the pressure development of XP2i. Differential pressure sensor DP2 also detected the pressure reduction during the test period but represents a less stable profile. Thus, pressure changed from 4.93 psi (1.99 hours) to 4.64 psi at 24 hours corresponding to a total reduction of 0.29 psi (0.02 bar).

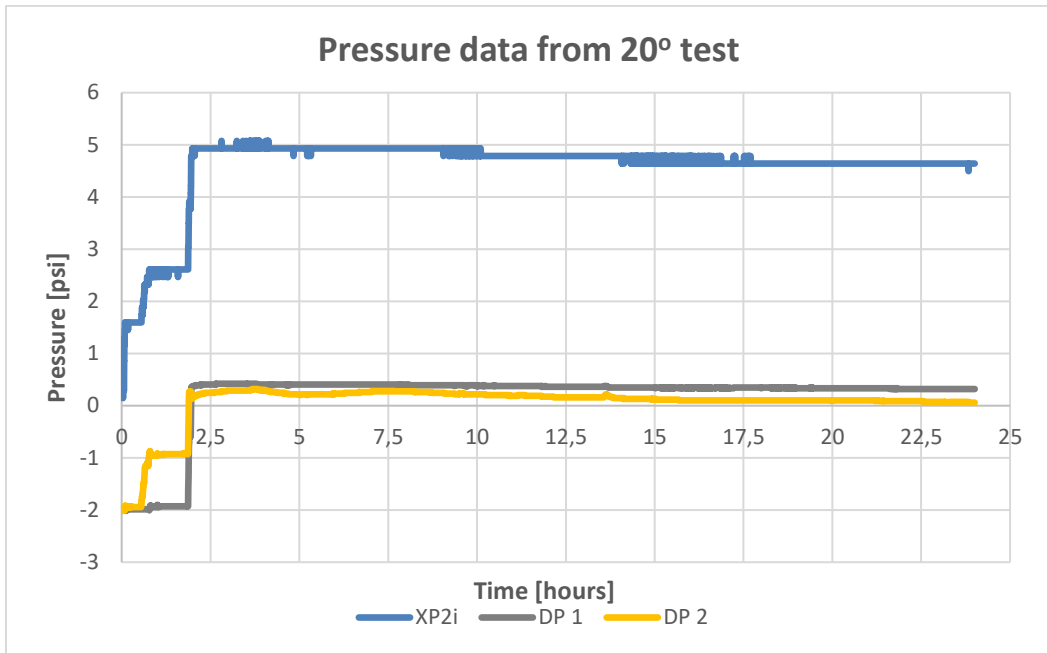


Fig. 4. 34 - Pressure monitoring during the test period of 24 hours, 20° setup

40° Inclined Setup

As seen in Fig. 4. 35, the pressure data from sensor XP2i references the laponite pill's ability to transmit pressure signals from the overlying fluid columns. In the time interval between laponite pill spotted and water added, the bottom hole pressure increased from 1.85 psi (at 2.5 hours) to 3.63 psi (at 2.6 hours).

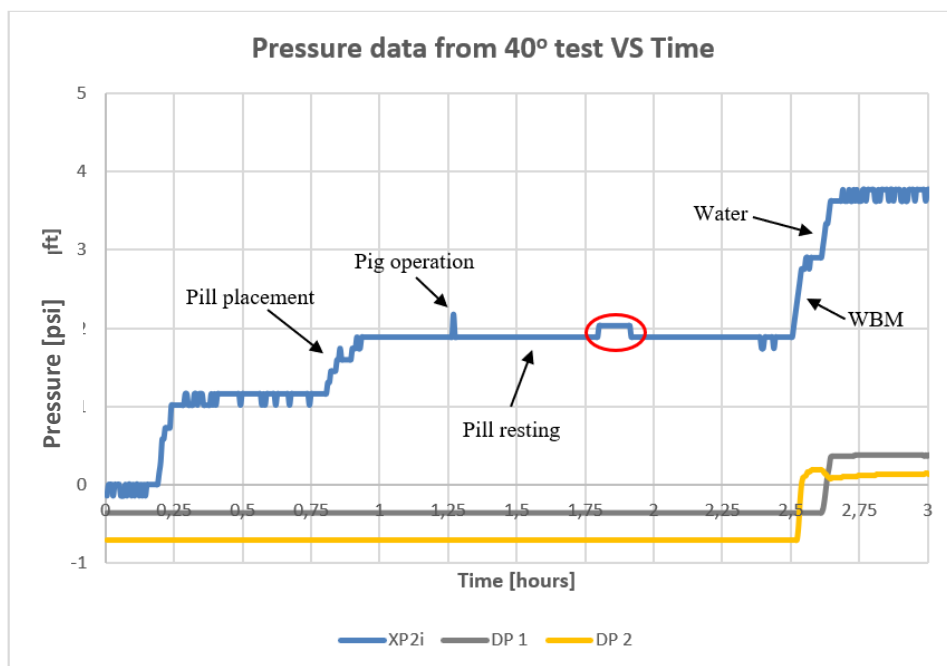


Fig. 4. 35 - Bottom hole, DP1 and DP2 pressure readings during placement period, 40° setup

Repeated in this test, DP2 monitors the same unusual pressure development in the period of WBDF and water positioning. The fact that this behaviour is repeated in all measurements, can exclude the suspicion of instrumental errors. No logical explanation other than a pressure reduction caused by the hose removal is reasonable, but at the same time unreliable.

The data obtained from DP1 shows an initial pressure of - 0.71 psi and following by not detecting pressure increase until water was spotted in this test is similar to the observation associated to the bentonite pill on the 40° setup. This examination provides a possible reason to exclude the measured data. The same is applicable for DP2 only measuring the positioning of WBDF and water. Caution was kept regarding covering the outlets of the differential pressure sensors with the desired fluids on all tests. Hence, no reasonable explanation can provide an answer on the lack of pressure detection by DP1 and DP2 until the point where WBDF was positioned.

Further, a sudden pressure increase from 1.89 psi to 2.03 psi was observed from XP2i between the time interval 1.75 to 2.0 hours, marked by the red circle in Fig. 4. 35. The test setup was left static at rest with no operational interference during this period, thus measuring error could have caused this discrepancy.

Taking into account a higher degree of inclination and the increased effect of barite sag, a more continuous pressure reduction monitored by sensor XP2i was expected as demonstrated in Fig. 4. 36. The bottom hole pressure measured when pressure stabilized at around 2.75 hours was 3.71 psi, while 3.63 psi was read at 24 hours. This results in a total pressure reduction of 0.08 psi (0.0055 bar).

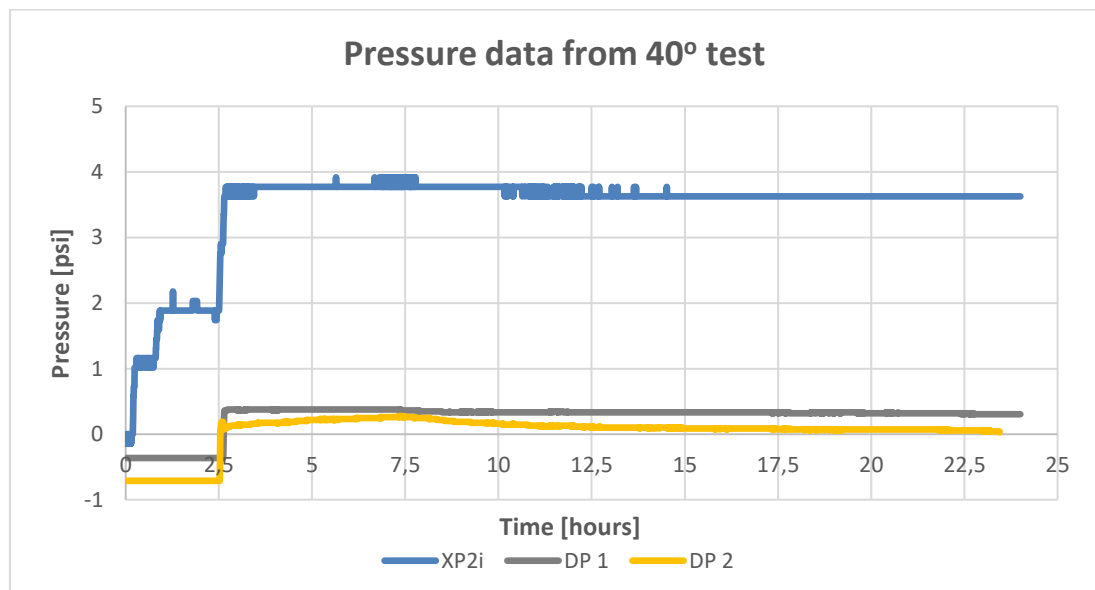


Fig. 4. 36 - Pressure monitoring during the test period of 24 hours, 40° setup

Combined Bottom Hole Pressure Profiles

Closing this subsection with bottom hole pressure profiles combined in Fig. 4. 37, demonstrate a trend of pressure reduction as test setup inclination increased from vertical. The total bottom hole pressures measured at 24 hours were 5.08 psi at vertical, 4.64 psi at 20° and 3.63 psi at 40° inclination. This trend was expected considering the effect of inclination on the total hydrostatic pressure column.

The pressure profile corresponding to the vertical setup represents a more unreasonable pressure pattern with larger pressure instabilities. Clearly seen from pressure profiles regarding 20° and 40° inclination showing a stepwise reduction in pressure over time. The same WBDF was employed on tests performed with the laponite pill. Hence, the same description for pressure reduction based on barite sag mechanisms explained for the bentonite pill also yield for the laponite pill. However, a more stable and continues pressure reduction over time was expected. This observation regarding a stepwise pressure reduction can rely on the higher gel strength structure formed creating a stiffer pill column. Thus, the laponite pill might have weaker pressure communication properties. The need for more thorough investigation on the gel strength development of the laponite pill is required to confirm the extent of pressure transmission by the laponite pill. However, by relying on the greatest pressure difference of 0.44 psi detected, the laponite gel pill preserved approximately constant bottom hole pressure.

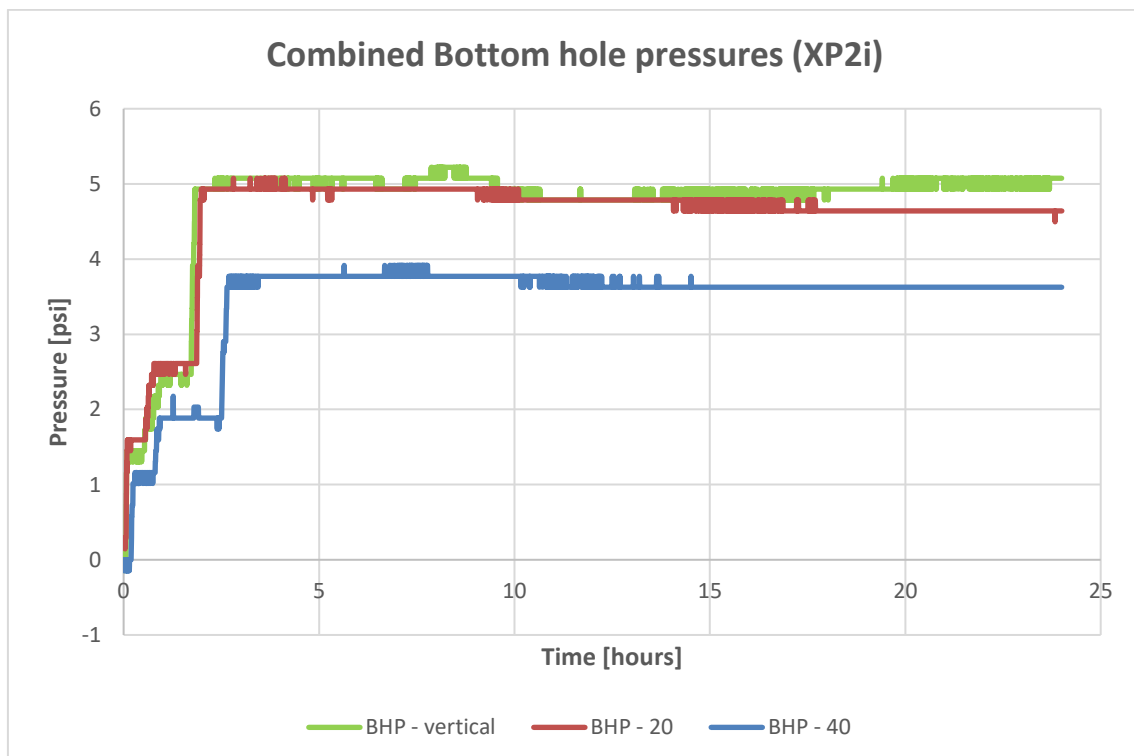


Fig. 4. 37 - Combined bottom hole pressure data from tests, laponite-based pill

4.3 Comparison of Test Results

One of the targets associated with testing two different clays was to analyse the differences and determine which gel pill type provide more adequate rheology properties for the tasks. Followed by analysing the pills ability to transmit pressure of overlying fluid columns and discuss the extent of constant bottom hole pressure preservation during the test period.

4.3.1 Comparison of Rheological Parameters

As it can be seen in Fig. 4. 38, the bentonite pill has generally higher shear stress values over the shear rate range compared to the laponite pill. However, the shear stress of the laponite pill increases after 24 hours compared to values obtained at initial condition. The opposite applies for the bentonite pill showing a slight decrease in shear stress as the values stabilize at higher shear rate readings. That may suggest hydration of laponite takes longer time.

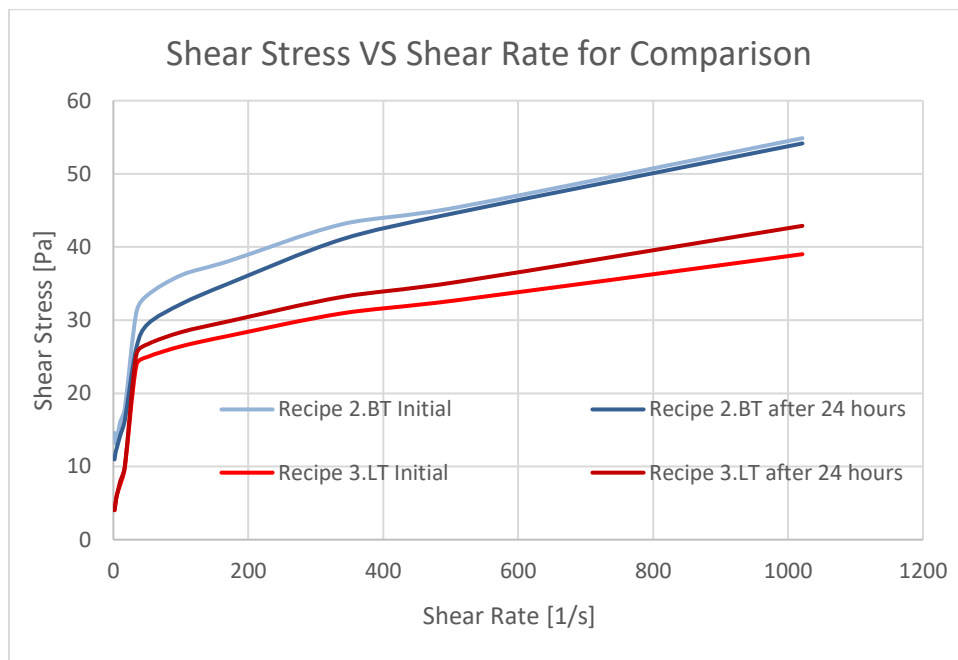


Fig. 4. 38 – Comparison of rheological profiles corresponding to recipe 2.BT and 3.LT

When analysing the rheological parameters provided in Table 4. 1 and Table 4.2 (see chapter 4.1.1 and 4.2.1), a similar trend is observed. Parameters regarding the bentonite pill are higher at initial condition and decrease after 24 hours, while the opposite yields for the laponite pill. An interesting observation was that the bentonite pill formed a 10-sec gel strength stronger than the laponite pill. The laponite pill, however, developed its gel structure at a slower pace,

but reached significantly higher 10-min gel strength values compared to the bentonite pill. This observation combined with lower viscosity values also explained why the laponite pill was more appropriate for hydraulic placement rather than the bentonite pill. The greater gel structure developed after 10 minutes is more practical for particle sag prevention provided by the laponite pill with sufficient barrier functionalities.

4.3.2 Comparison of Pressure Data

As already mentioned, both the bentonite and laponite pill confirmed pressure transmitting properties during all setup conditions. This can be seen by the XP2i profiles in Fig. 4. 39 corresponding to both pill types respectively showing similar trends during the entire fluid placement period.

As it can be seen below, the pressure profiles of XP2i regarding the bentonite pill show a generally higher bottom hole pressure trend for all setup conditions compared to the laponite pill. Results represented below do also confirm that the bentonite pill maintains a more stable bottom hole pressure trend. These observations confirm that the bentonite pill transmitted pressure to a greater extent than the laponite pill. With the difference in 10-min gel strengths, it can further be stated that a lower gel strength is more practical for fluid pressure transmissions tasks.

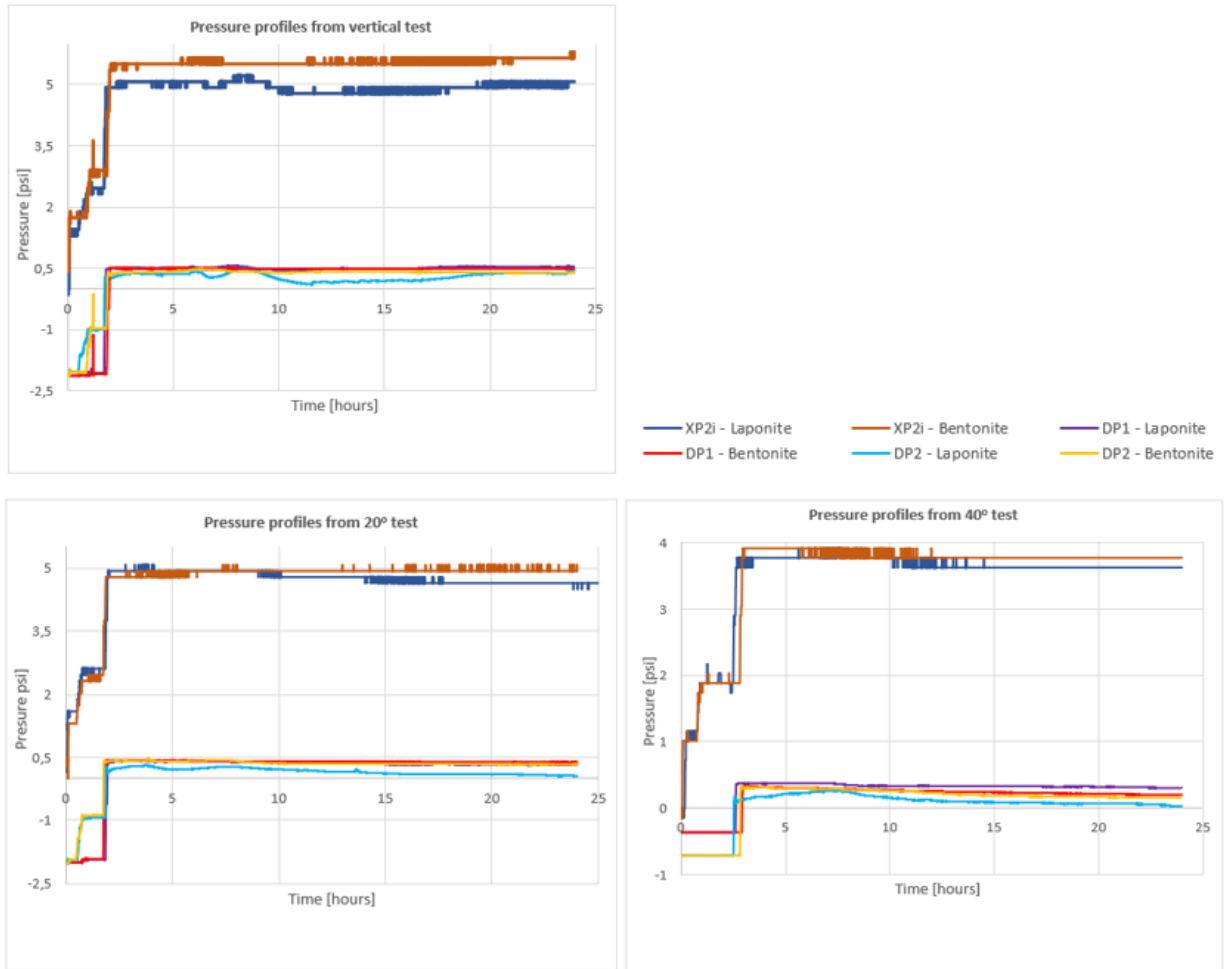


Fig. 4. 39 – Combined pressure data from tests performed using both pill types for comparison

It can also be seen that the laponite pill tends to more pressure instabilities with more abrupt and stepwise pressure reductions throughout the test period. This can indicate that the laponite pill transmits pressure in a smaller extent based on gel strength formation creating a stiffer pill.

4.5 Barite Sag Prevention

The bentonite and laponite-based gel pills successfully prevented barite sag on tests performed. However, during all series of tests performed, the bentonite gel pill experienced failures (discussed in the following chapter), while the laponite pill provided full success rates. Notwithstanding the failures occurred, sequences of tests performed on the bentonite pill and

the results obtained confirm that the bentonite-based pill can prevent barite sag and simultaneously maintain full integrity and isolation.

4.5.1 Effective Inclination Regarding Barite Settling and Sag Prevention

From results discussed in sections covering the interface stability and pressure transmission data of the gel pills, it can be confidently stated that the 40° setup caused the most intense barite sag and bed formation. Thus, exposing the gel pill surfaces to the greatest stress and strain. With background in series of tests conducted, it further can be stated that the 40° inclination was the most effective inclination regarding barite settling. This can also be seen in Fig. 4. 40 and Fig. 4. 41 comparing sag on the 40° inclined and vertical setup.

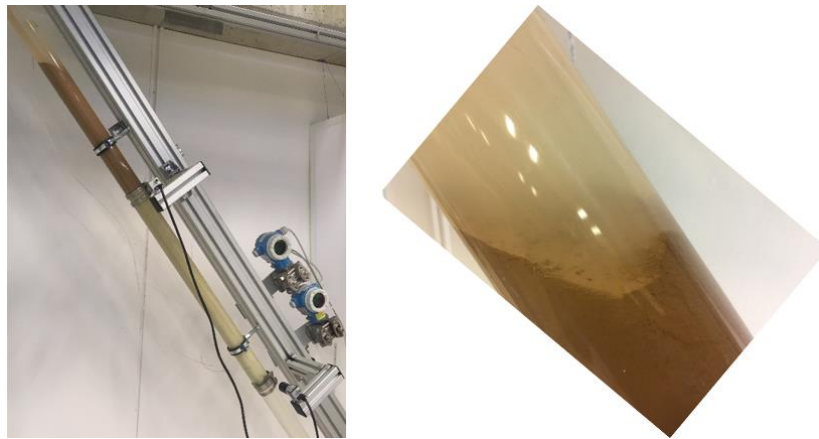


Fig. 4. 40 – Boycott driven barite sag on the 40° inclined test setup

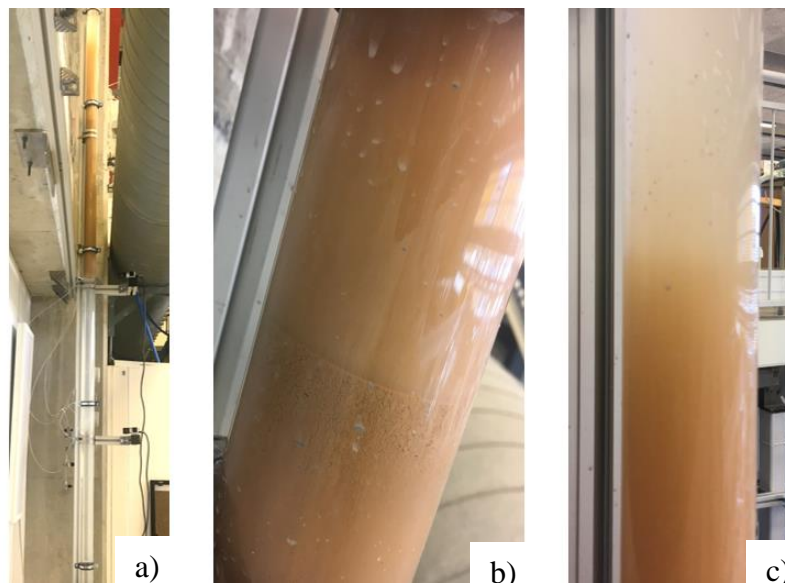


Fig. 4. 41 – Hindering effect on barite sag on the vertical test setup showing the sedimentation regimes in b) and c)

The contribution of boycott driven and hindering effect on barite sag is seen respectively in the figures above. Fig. 4. 40 demonstrates the boycott driven transition between the clear fluid and suspension zone. Associated to a vertical condition, Fig. 4. 41 shows the hindered effect on static barite settling. Also included in the figure are the sedimentation regimes described by Zamora (2009). Fig. 4. 41 b) shows the compaction below the hindered settling regime and Fig. 4. 41 c) the clarification regime above the settling regime.

Considering the exposure to more intense sag and bed formation on the 40° inclined pipe, the bentonite and laponite pill experienced less hydrostatic pressure from the overlying fluid columns. The reduced hydrostatic pressure is a result of barite particles accumulating along the pipe wall and thus affect the total hydrostatic bottom hole pressure. The total bottom hole pressure measured on the vertical setup was 5.08 psi compared to 3.63 psi on the 40° pipe at 24 hours. This hydrostatic pressure difference, which is a result of inclination alone, constitutes to a reduction of 1.45 psi (roughly 0.1 bar) when the pills were employed on the 40° inclined setup. Hence, the success of the sag prevention gel pill might be controversial considering the intense barite sag and significant reduction in hydrostatic pressure providing a milder stress on the pill column. This argument could be further confirmed by the fact that no failures caused by either pill type occurred on the 40° inclination setup. However, it seems like the effective inclination associated with the main function of the gel pill and sag incident is indeed the 40° inclined setup.

4.6 Challenges and Potential Reasons for Failure

As for all experimental work performed in the laboratory, challenges and failures are always met. Challenges were primarily to the fluid placement procedures contributing to failures which will be discussed in more detail.

The fact that the laponite-based gel pill did not fail during any test conditions, proof that the laponite pill is the more robust pill for this concept. Failures of the bentonite-based pill occurred on tests performed on the vertical setup and at inclination of 20°, while no failure occurred on the test setup with inclination of 40°.

The bentonite pill failed either during and or after placement of the WBDF. However, other factors appearing during the test and fluid placement procedure cannot be excluded. Herein, several potential factors might have led to instabilities of the bentonite-based gel pill.

These account for placement of the pill, pig operation on spotted gel pill, location of fluid break inside the pipe and placement of the WBDF.

A summary and description of factors are provided by an example of a deficient test on the vertical pipe setup. No deviations were observed on the rheological measurements of the fluids. The bentonite-based gel pill was prepared and spotted according to normal procedure and failed immediately when the WBDF was added. The WBDF started channelling through the pill along the pipe wall resulting in failure of the pill's stability and integrity as shown in Fig. 4. 42.



Fig. 4. 42 – Source of channel (left) and channelling of WBDF along the pipe wall (right)

However, the pill stayed intact preventing complete intermixing of the fluids. A description of potential factors leading to failure of the pill is disclosed.

- Placement of the pill:

The bentonite-based gel pill had a very high yield strength and formed its gel structure quickly and already at low shear rates. During the pump and pull operation, the pill was placed at very low and in situations uneven pump rate equalling low shear rates as the pill exits the hose. It is reasonable to expect that the pill was too stiff to fill the channel created by the submerged hose pulled upwards through the pill phase. Pulling of the inserted hose could have been performed at a too low pace, creating channels in the pill phase compromising the pill's integrity.

- Pig operation:

Before compressing the pill and cleaning the pipe wall right above the pill surface, the sponge was wetted with tap water. This was done to increase friction and improve contact between the sponge and the plastic wall. In this particular test, the sponge was too wet as it was not dried off properly and thereby contaminating the pill surface, see Fig. 4. 43.

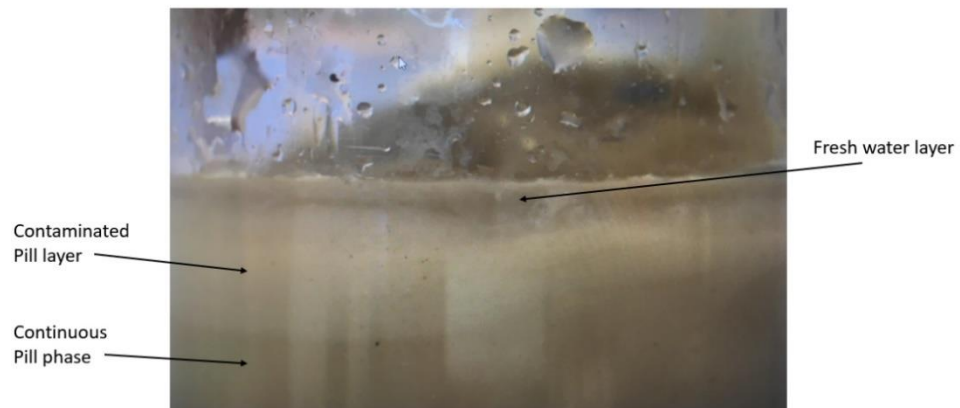


Fig. 4. 43 - Pill surface contaminated by fresh water from the sponge

- Fluid break location:

The fluid break is supposed to be located with the outlet closeup to the pipe wall for additional attenuation of the WBDF entering the hose, which was not executed in this test.

- Placement of WBDF:

The inserted hose gained extra height above the pipe opening on the vertical setup compared to the inclined. The additional hose length was hard to manage by the laboratory personnel responsible for pouring the WBDF into the hose at the same time as performing the pump and pull method. This challenge led to uncontrolled rate of pouring and uneven placement of the WBDF, which might have caused significant swirling of the fluid above the pill phase. This part was improved by using a stool to stand on during the WBDF placement.

5 Conclusion

The results obtained and discussed in this thesis work provides the foundation for the following conclusions:

- Both the bentonite and laponite-based gel pills preserved integrity while acting as a fluid barrier isolating the brine and WBDF inside the pipe on all large-scale setups.
- Both gel pills successfully transmitted pressure signals generated by the overlying WBDF and water columns added on top of the pill.
- Based on pressure profiles obtained, the bentonite-based gel pill showed better pressure communication properties compared to the laponite pill. The bentonite pill is herein the better practical option for pressure transmitting tasks.
- The bentonite-based gel pill proved to control the bottom hole pressure to a degree equivalent to a maximum pressure difference of 0.44 psi on the vertical setup. The same was observed for the laponite-based gel pill, and thus approximately constant bottom hole pressure was preserved throughout the test period.
- Both pill types acted as a resting bed for the barite particles and thereby prevented penetration of particles. However, based on 10-min gel strength values and success rate on large-scale tests, the laponite gel pill proved to prevent particle penetration to a greater extent.
- The laponite-based pill seemed to be the better qualified option based on the number of tests performed, all pressure related requirements met, no signs of instabilities nor failures documented.

6 References

- Almdal, K., Dyre, J., Hvidt, S., & Kramer, O. (1993). Towards a phenomenological definition of the term 'gel'. *Polymer Gels and Networks*, 1(1), 5-17. [doi:10.1016/0966-7822\(93\)90020-I](https://doi.org/10.1016/0966-7822(93)90020-I).
- American Society of Mechanical Engineers. Shale Shaker Committee. (2005). *Drilling fluids processing handbook* (Vol. V. 75, Advances in electronics and electron physics;). Burlington, MA;: Gulf Professional Publishing.
- Amoco Production Company. (1994). *Drilling Fluids Manual*. Revision 06.1994 accessed via <https://www.slideshare.net/VyanPersad/amoco-drilling-fluid-manual> (accessed 25 March 2020).
- Baroid Driling Fluids, Inc. (1998). Baroid Fluids Handbook. Revision 01.08.97 accessed via https://www.academia.edu/38385275/Baroid_Fluids_Handbook (accessed 04 February 2020).
- Bybee, K. (2004). Barite-Sag Management. *JPT, Journal of Petroleum Technology*, 56(11), 62-63. [doi:10.2118/1104-0062-JPT](https://doi.org/10.2118/1104-0062-JPT).
- BYK Additives & Instruments. (2014). *Laponite – Performance Additives*. Technical Information B-RI 21. Retrieved from https://www.byk.com/fileadmin/byk/additives/product_groups/rheology/former_rock_wood_additives/technical_brochures/BYK_B-RI21_LAPONITE_EN.pdf (accessed 29 April 2020).
- Caenn, R., & Chillingar, G. V. (1996). Drilling fluids: State of the art. *Journal of Petroleum Science and Engineering*, 14(3-4), 221-230. [doi:10.1016/0920-4105\(95\)00051-8](https://doi.org/10.1016/0920-4105(95)00051-8).
- Caenn, R., Darley, H., & Gray, G. R. (2017). *Composition and Properties of Drilling and Completion Fluids, 7th Edition*. Gulf Professional Publishing.
- Dankers, P. J. T., & Winterwerp, J. C. (2007). Hindered settling of mud flocs: Theory and validation. *Continental Shelf Research*, 27(14), 1893-1907. <https://doi.org/10.1016/j.csr.2007.03.005>.
- Dobson JR, J. W., Tresco, K. O., & Geerdes, B. K. (2011). Ultra High Viscosity Pill and Methods for Use With and Oil-Based Drilling System. US Patent No. US 2011/0009298 A1. U.S. Patent Application Publication.
- Equinor. (2018). Drilling Fluids, Completion Fluids and Drilling Waste Management. Internal Guideline, GL3518, Version 5.0.

- Fosso, S. W., Tina, M., Frigaard, I. A., & Crawshaw, J. P. (2000). *Viscous-Pill Design Methodology Leads to Increased Cement Plug Success Rates; Application and Case Studies from Southern Algeria*. Paper presented at the IADC/SPE Asia Pacific Drilling Technology, Kuala Lumpur, Malaysia. <https://doi.org/10.2118/62752-MS>.
- Gabolde, G. (2014). *DDH : Drilling data handbook* (9th ed.). Paris: Editions Technip.
- Halliburton. (2012, 19. December). "The Halliburton Baroid Ecosystem – Barite Sag". [Video clip]. Retrieved from <https://www.youtube.com/watch?v=mNs8xoZFOW4&t=7s> (accessed 05 May 2020).
- Kageler, P. L. (2014). Drilling and Completion Applications of Magnetorheological Fluid Barrier Pills. U.S. Patent No. 2014/0262268 A1. U.S. Patent Application Publication.
- Liu, D., Ren, L., Wen, C., & Dong, J. (2018). Investigation of the compatibility of xanthan gum (XG) and calcium polysulfide and the rheological properties of XG solutions. *Environmental Technology*, 39(5), 607-615. [doi:10.1080/09593330.2017.1309073](https://doi.org/10.1080/09593330.2017.1309073).
- Loomis, A. G., Ford, T. F., & Fidiem, J. F. (1941). Colloid Chemistry of Clay Drilling Fluids. *Transactions of the AIME*, 142(01), 86-99. [doi:10.2118/941086-G](https://doi.org/10.2118/941086-G).
- M-I SWACO. (1998). *Drilling Fluids Engineering Manual*. Revision No: A-0 / Revision Date: 03.31.98 accessed via https://www.slideshare.net/minhnguyen_humg/m-i-swaco-engineering-drilling-fluid-manual (accessed 18 February 2020).
- Ofite. (2015). *Model 900 Viscometer – Instruction Manual*. US Patent No. 6,766,028. Retrieved from http://www.ofite.com/doc/130-76-C_instructions.pdf (accessed 12 February 2020).
- Omland, T. H., Saasen, A., & Amundsen, P. A. (2007). Detection Techniques Determining Weighting Material Sag in Drilling Fluid and Relationship to Rheology. *Nordic Rheology Society*, 15, 1-9. Accessed via <https://nordicrheologysociety.org/AnnualTransactions/ShowAllTransactions?selectedYear=2007> (accessed 07 April 2020).
- Quemada, D. (1998). Rheological modelling of complex fluids. I. The concept of effective volume fraction revisited. *The European Physical Journal - Applied Physics*, 1(1), 119-127. <https://doi.org/10.1051/epjap:1998125>.
- Riker, R., Turner, J. K., Lovorn, R., & Kale, T. (2012). *A Thixotropic Barrier Fluid Used To Prevent the Commingling of Fluids While Tripping on Managed Pressure Drilling Wells*. Paper presented at the SPE/IADC Managed Pressure Drilling and Underbalanced Operations Conference and Exhibition, Milan, Italy. <https://doi.org/10.2118/156904-MS>.

- Ronaes, E., Prebensen, O. I., Mikalsen, R., Taugbol, K., Syltoy, S., & Torvund, S. (2008). *An Innovative Fluid Pressure Transmission Pill Successfully Used During Managed-Pressure Drilling Operations in an HTHP Environment*. Paper presented at the IADC/SPE Drilling Conference, Orlando, Florida, USA. <https://doi.org/10.2118/112528-MS>.
- Ruzicka, B., & Zaccarelli, E. (2011). A fresh look at the Laponite phase diagram. *Soft matter*, 7, 1268-1286. <https://doi.org/10.1039/C0SM00590H>.
- Saasen, A., Liu, D., & Marken, C. D. (1995). *Prediction of Barite Sag Potential of Drilling Fluids From Rheological Measurements*. Paper presented at the SPE/IADC Drilling Conference, Amsterdam, Netherlands. <https://doi.org/10.2118/29410-MS>.
- Skalle, P., Backe, K. R., Lyomov, S., & Sveen, J. (1997). *Barite Segregation In Inclined Boreholes*. Paper presented at the Annual Technical Meeting, Calgary, Alberta. <https://doi.org/10.2118/97-76>.
- Skjeggstad, O. (1989). *Boreslamteknologi : Teori og praksis*. Bergen: Alma Mater.
- Taylor, G. I. (1950). The Instability of Liquid Surfaces when Accelerated in a Direction Perpendicular to their Planes. *Proc. London Math. Soc. (A)*, 201, 192-196. <https://doi.org/10.1098/rspa.1950.0052>.
- Temple, C., Paterson, A. F., & Leith, C. D. (2006). Method for Reducing Sag in Drilling, Completion and Workover Fluids. US Patent No. US 6,989,353 B2. U.S. Patent Application Publication.
- Webber, C., & Turner, J. (2019). *A New Fluid-Based Isolation Spacer Increases Success When Spotting Off-Bottom Cement Plugs*. Paper presented at the SPE Annual Technical Conference and Exhibition, Calgary, Alberta, Canada. <https://doi.org/10.2118/195879-MS>.
- Zamora, M. (2009). *Mechanisms, Measurement And Mitigation Of Barite Sag*. Paper presented at the Offshore Mediterranean Conference and Exhibition, Ravenna, Italy. Retrieved from https://www-onepetro-org.ezproxy.uis.no/conference-paper/OMC-2009-105?sort=&start=0&q=Mechanism%2C+Measurement+and+mitigation+of+barite+sag&from_year=&peer_reviewed=&published_between=&fromSearchResults=true&to_year=&rows=25# (accessed 12 April 2020).
- Zamora, M., & Power D. (2002). Making a Case for AADE Hydraulics and the Unified Rheological Model. Paper AADE-02-DFWM-HO-13, the AADE 2002 Technology Conference, Houston. Retrieved from

<https://www.aade.org/application/files/9615/7295/5856/AADE-02-DFWM-HO-13.pdf>
(accessed 03 April 2020).

Zamora, M., & Stephens, M. (n.d). 5 Drilling Fluids. M-I L.L.C. Accessed via
<https://www.scribd.com/document/434299510/PWC05> (accessed 12 May 2020).

Appendix A – Complimentary Information for Methodology

A.1 Modifications on the Water-Based Drilling Fluid

Modifications on the WBDF were necessary as rapid barite sag was required for the large-scale tests. Table A. 1 presents recipe B1 and B2 which created the foundation of the modified recipe BT used on large-scale tests. The intention of designing recipe B1 and B2 was to study the barite sag and degree of particle sedimentation during a short period when left static.

Table A. 1: Original base recipes used to develop and modify the WBDF recipe.

Chemicals	Recipe B1	Recipe B2
Water	248.87 [g]	248.87 [g]
Xanthan Gum	0.375 [g]	0.25 [g]
Barite	37.15 [g]	37.15 [g]

The corresponding Fig. A. 1 represents recipe B1 (left) and recipe B2 (right) demonstrating the degree of barite sedimentation after approximately 15 to 20 minutes. The sedimentation rate obtained by recipe B2 was to intense, while recipe B1 showed minimal barite sedimentation.

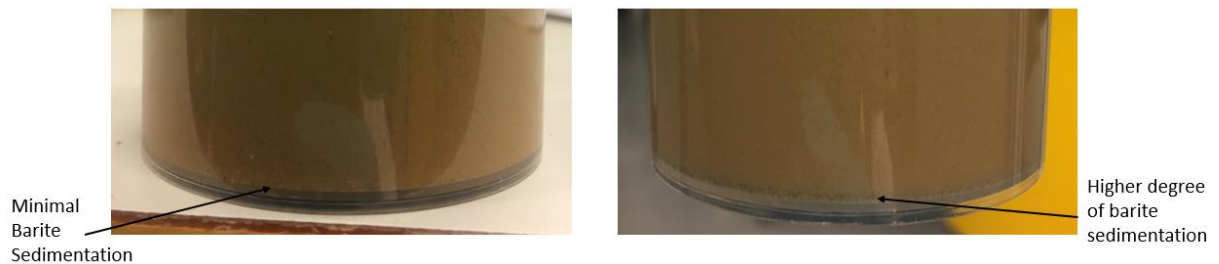


Fig. A. 1 - Degree of barite sedimentation for recipe B1 (left) and recipe B2 (right)

To guarantee a higher density, the barite concentration was increased significantly from the original 148.6 g/L (37.15 g) to 739.68 g/L (184.92 g) resulting in a density of 1.48 SG corresponding to recipe BT. To maintain rapid barite sag in addition to the increased amount of barite, a XG concentration of 1.2 g/L (0.3 g) was chosen instead of the original amount used in recipe B1 and B2. These modifications in barite and XG concentration were further used to create recipe BT which was adjusted for larger volumes shown in Table 3.10.

A.2 Rheology Measurement Procedure for the Gel Pills

Table A. 2 and Table A. 3 provide the procedure for rheological measurements on the pill recipes on both the original mixing day (initial condition) and after 24 hours.

Table A. 2: Procedure for rheological measurements on original mixing day for the gel pill recipes.

Procedure for rheological measurements on original mixing day:

1. Viscometer was cleaned and checked for contamination before use.
2. Rotor sleeve was attached to the rotor.
3. Viscometer was turned on and calibrated automatically.
4. Test fluid in sample cup was positioned by the platform until rotor was immersed exactly to the scribed line shown on the rotor.
5. Thermometer was inserted in the test fluid.
6. Mud program was started and automatically measured, calculated and displayed plastic viscosity in centipoise, yield point in lb/100ft², 10-second and 10-minutes Gel.
7. Fluid sample was premixed for approximately seven minutes at 700 rpm by the Heidolph stirrer to break the formed gel structure.
8. After premixing, the fluid sample was placed for further measurements as described in step 4 and 5.
9. Instrument readings such as shear stress, viscosity and temperature were taken in the order of 600 rpm stepwise towards 1 rpm with a measuring period of one minute between each rpm stage.
- 10.0 Due to quick gel structure development occurring beneath 20 rpm influencing the rheological property readings, additional readings were taken from 10 towards 1 rpm.
- 10.1 600 rpm was selected and run for 30 seconds with the intention to break or minimize the gel structure.
- 10.2 Instrument readings were taken within the first 5 seconds after transition from 600 rpm to the desired value of rpm.
- 10.3 Step 10.1 and 10.2 were repeated for all rpm intervals ranging from 10 to 1 rpm.
11. Fluid sample was removed from viscometer, covered with parafilm and stored undisturbed for 24 hours.
12. Viscometer was properly cleaned and dried off.

Table A. 3: Procedure for rheological measurements after 24 hours for the gel pill recipes.

Procedure for rheological measurements after 24 hours:

1. After resting, the fluid sample was premixed by the Heidolph stirrer for approximately 10 minutes at rpm ranging from 1000 to 2000 rpm depending on the viscosity and gel structure of the pill.
2. After premixing, the sample fluid in the cup was pounded in the table forcing captured air bubbles submerged inside the fluid during premixing to be released.
3. Rheological measurements and instrument readings were re-taken in the same order as on the original day, explained by step 1 to 12 in Table A. 2.

A.3 Stability Tests Performed on Gel Pills

Stability tests were the main element of the second part of the work done in this project. Series of tests were performed on both bentonite and laponite-based recipes. At the first stage, a simple stability test was executed by tilting the sample cup containing the pill to horizontal. These tests were performed after the pill being undisturbed and resting for 24 hours forming a gel structure. Approval was based on visual observation with criteria such as the gel structure not breaking entirely or starting to flow. Fig. A. 2 demonstrates a successful stability test performed on bentonite pill recipe 2.B.



Fig. A. 2 - Bentonite pill of recipe 2.B in sample cup tilted to horizontal

The next step involved a 9.8 cm long transparent plastic cup with a 4.8 cm ID. A small volume of brine was filled into the cup covering the lower part, followed by the 10g bentonite-based pill (recipe 1.B). The pill was placed using a spoon which explains the bulky phase of the pill (see Fig. A. 3). Eventually, WBDF was poured on top of the pill.



Fig. A. 3 - Recipe 1.B stability test

No tests on this scale were conducted on recipe 2.B, as it was assumed that the 20g bentonite-based pill was more likely to pass this test.

Also, stability tests such as float tests were executed on the laponite recipe at a later stage reasoned by the greater gel strength values and viscosity compared to the bentonite recipes. Moreover, behaviour of the laponite fluid mixture when in contact with brine and its ability to stay on top of it during and after placement was tested using the same type of transparent plastic cup. Fig. A. 4 illustrates the float test with laponite pill recipe 5.L.



Fig. A. 4 – Recipe 5.L.float test

The final stage of the stability testing was based on the criterion of isolating two fluid sections. This was investigated on a 46.0 cm long transparent plastic tube with 3.8 cm ID. The pill's capability to isolate two fluid sections while preserve its stability for 24 hours was a

crucial qualification to scale up to the large-scale setup. The following recipes 1.B, 2.B and 2.L were used in this test. In a typical test, brine was filled into the plastic tube covering the lower part, followed by a pill column placed using a syringe and WBDF eventually poured slowly on top of the pill immediately after positioning of the pill.

A.4 Improvement of Fluid Placement Procedure on Large-Scale

Fluid placement was a crucial part of the test and was improved throughout test performances at the early stage to increase the success rate. Improvements were further implemented and adjusted to establish a standard procedure for fluid placement on the large-scale test setup. Furthermore, the procedure for fluid placement was also found to be the reason causing failures of the bentonite-based gel pill experienced on some tests.

For instance, the placement of WBDF was improved using a fluid break (see Fig. A. 5) attached at the outlet of the hose. Thus, forcing the WBDF to enter the house in a horizontal direction instead of vertically. In addition, a pump and pull method was used for WBDF placement with the intention to not whirl up the already placed WBDF.



Fig. A. 5 - Fluid break from the side (left) and from above (right)

In that way, the fluid's kinetic energy was forced towards the wall conducting in a lower velocity flow of the WBDF exposing the pill surface. In addition, the hose was twisted in such a way that the fluid break opening was placed as close as possible to the pipe wall for additional deceleration of the WBDF. For demonstration, Fig. A. 6 a) and b) show the positioning of the fluid break and how the WBDF entered the fluid break along the pipe wall.

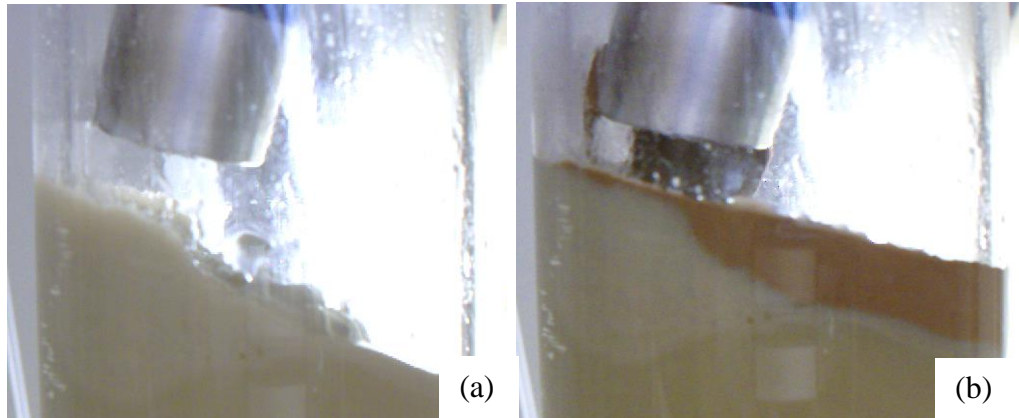


Fig. A. 6 a) Fluid break placed up close to the pipe wall. b) WBDF flowing along the pipe wall

Other improvements involved a transparent elastic plastic hose instead of the originally non transparent hose used. As the gel pill was placed hydraulically it was essential to control the continuously of the pill inside the hose to prevent placement of large air volume compromising the integrity.

Further, formed foam on the surface of the brine after placement was removed by rotating and twisting the house at the surface of the brine as demonstrated in figure Fig. A. 7.



Fig. A. 7 – Foam removal using a hose

When the pill was placed successfully a pig was run down along the pipe wall to ensure visibility for camera recording. In addition, the pig was used to compress the pill from above with the intention to compact potential channels or air pockets created inside the pill phase. The employed pig was made of a sponge and fastened at the end of a hose, (see Fig. A. 8).



Fig. A. 8 - Pig used to clean the pipe wall and compress the pill from above

Appendix B - Additional Information

B.1 Viscosified Brine Design and Rheological Properties

The rheology profile of the brine of recipe AT is shown in Fig. B. 1 with the corresponding shear stress and shear rate values provided in Table B. 1. Fluids such as brine normally are characterized as Newtonian fluids due to the lack of solid material content. However, the contribution of xanthan gum provided a minor yield strength to the brine which in return in not typical for Newtonian fluids. Moreover, the profiles obtained showed typical shear thinning properties and matches a Bingham plastic behaviour.

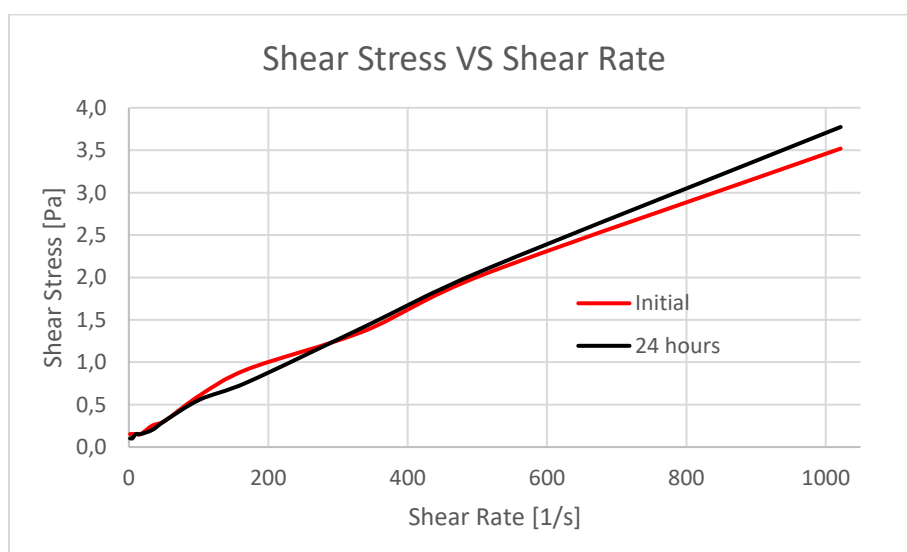


Fig. B. 1 - Rheological profile of brine, recipe AT

All viscometer values obtained from the brine showed common behaviour with increasing shear stress values at shear rates ranging from 34.05 to 1021.38 1/s after 24 hours compared to values measured on the original mixing day (see Table B. 1). Also, all rheological measurements showed more stable shear stress values at lower shear rates ranging from 17.02 towards 1,7 1/s, which was common during all measurements performed. Viscosity values on the other hand tend to decay after 24 hours which is explained by the reduced temperature of the brine affecting the viscosity when measurements were taken. It is besides more reasonable to observe an increase in viscosity after 24 hours due to completed XG polymer structures in the fluid. More characteristic rheology parameters are provided in Table B. 2.

Table B. 1: Viscometer data and rheology parameters of the brine, recipe AT.

Parameters		Recipe AT on original day			Recipe AT after 24 hours		
RPM	Shear Rate [1/s]	Shear Stress [Pa]	Viscosity [cP]	Viscosity [Pa.s]	Shear Stress [Pa]	Viscosity [cP]	Viscosity [Pa.s]
600	1021.38	3.5	3.3	3.4	3.8	3.5	3.7
300	510.69	2.0	3.7	4.0	2.1	3.9	4.1
200	340.46	1.4	3.8	4.0	1.4	3.9	4.2
100	170.23	0.9	5.1	5.4	0.8	4.2	4.5
60	102.14	0.6	5.6	6.0	0.6	5.2	5.5
30	51.07	0.3	5.7	6.0	0.3	5.9	6.0
20	34.05	0.3	6.3	7.5	0.2	6.2	6.0
10	17.02	0.2	9.6	9.0	0.2	9.3	9.0
6	10.21	0.2	14.2	15.0	0.2	13.2	15.0
3	5.11	0.2	27.1	29.9	0.1	21.6	20.0
2	3.4	0.2	37.2	45.0	0.1	30.9	30.0
1	1.7	0.2	71.2	90.0	0.1	55.3	60.0

Table B. 2: Rheological parameters of the brine, recipe AT.

	Initial condition	After 24 hours
Temperature [°C]	27.1	20.2
Density [s.g]	NA	1.21
pH	NA	5.5
Plastic viscosity [cP]	3.0	3.0
Yield Point [lb/100ft ²]	0.7	0.9
Gel 10 sec	0.2	0.1
Gel 10 min	0.2	0.1
τ_y	0.15	0.05
n	1.99	1.85
k	0.0	0.0

B.2 Water-Based Drilling Fluid Design and Rheological Properties

The rheology profile of the WBDF (recipe BT) is shown in Fig. B. 2, with the corresponding shear stress and shear rate values given in Table B. 3. As for all profiles established, measurements were taken at room temperature both at initial condition and after 24 hours.

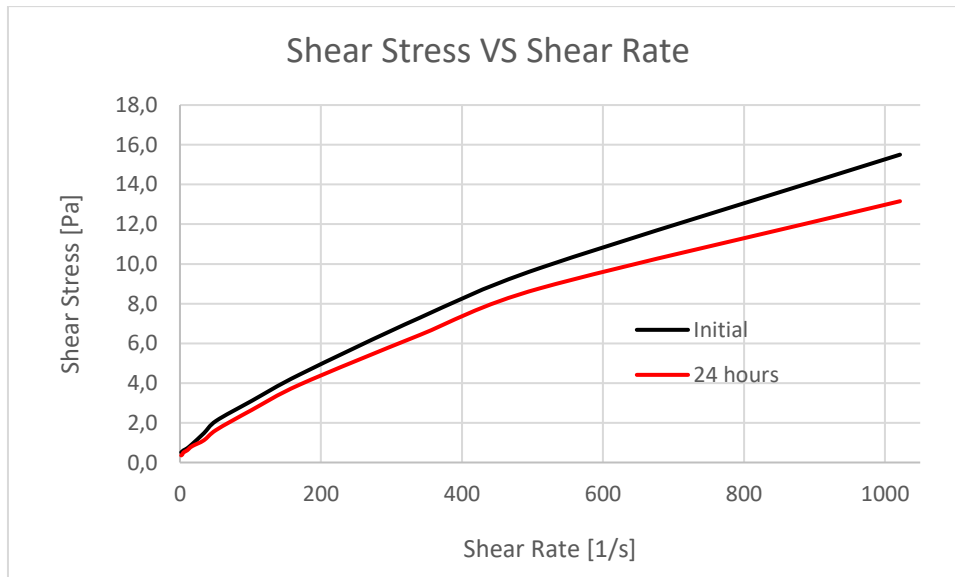


Fig. B. 2 - Rheological profile of WBDF, recipe BT

The rheological profile of recipe BT matches the Herschel-Buckley model describing a pseudoplastic fluid profile with associated shear thinning properties. This is based on the present yield point value provided by the content of XG. The associated H-B parameters are

provided in Table B. 4 among other characteristic data. All rheological measurements performed on the WBDF showed the same rheological profile and a similar pattern in obtained rheological parameters, creating a reliability. Also identical for all data and parameters obtained were the reduction in rheological values after 24 hours. This can be explained by decomposition of xanthan gum resulting in lower thickening properties and reduced stabilization of barite particle suspension.

Table B. 3: Viscometer data of the WBDF, recipe BT.

Parameters		Recipe BT on original day			Recipe BT after 24 hours		
RPM	Shear Rate [1/s]	Shear Stress [Pa]	Viscosity [cP]	Viscosity [Pa.s]	Shear Stress [Pa]	Viscosity [cP]	Viscosity [Pa.s]
600	1021.38	15.5	14.4	15.2	13.2	12.3	12.9
300	510.69	9.8	18.0	19.2	8.8	16.2	17.2
200	340.46	7.3	20.2	21.4	6.4	17.7	18.9
100	170.23	4.4	24.6	26.1	3.9	21.7	23.1
60	102.14	3.1	28.7	30.5	2.7	24.3	26.0
30	51.07	2.1	38.3	40.9	1.6	30.5	32.0
20	34.05	1.5	41.5	43.4	1.1	31.2	33.0
10	17.02	0.9	50.1	53.9	0.8	43.8	47.9
6	10.21	0.7	67.3	69.9	0.6	58.1	59.9
3	5.11	0.6	109.4	119.8	0.5	91.3	99.8
2	3.4	0.6	153.2	165.0	0.4	115.3	120.0
1	1.7	0.5	279.1	300.0	0.4	194.0	210.0

Table B. 4: Rheological parameters of WBDF, recipe BT.

	Initial condition	After 24 hours
Temperature [°C]	20.6	19.6
Density [s.g]	NA	1.48
pH	NA	8.57
Plastic viscosity [cP]	10.9	9.7
Yield Point [lb/100ft ²]	8.4	7.0
Gel 10 sec	1.5	0.9
Gel 10 min	7.4	5.1
τ_y	0.51	0.41
n	0.81	0.88
k	0.06	0.04

B.3 Bentonite-Based Pill Design and Rheological Properties

As mentioned, development of the final recipe 2.BT was based on recipe 1.B and 2.B. These recipes were tested for stability and their rheological properties analysed based on established criteria (see chapter 3.3.2). This was done to simplify the determination of which recipe to adjust and implement on large-scale.

Fig. B. 3 presents the rheology profiles of recipe 1.B and 2.B based on shear stress and shear rate values provided in Table B. 5 and Table B. 6. Common for both recipes was the increase in shear stress after 24 hours due to complete clay hydration. As expected, were general higher shear stress values observed regarding recipe 2.B compared to recipe 1.B. This can be explained by higher bentonite concentrations increasing the friction and particle interactions in the suspension.

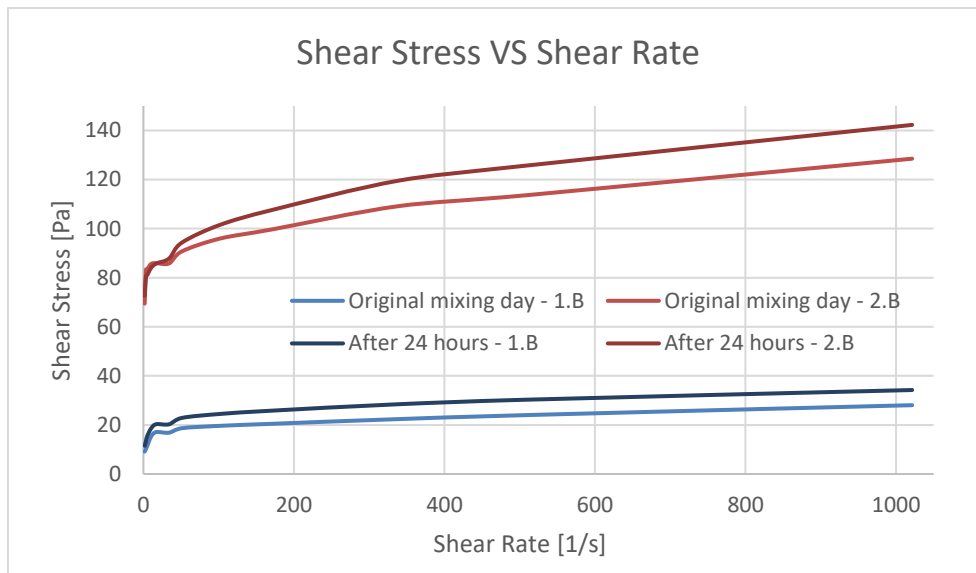


Fig. B. 3 - Rheological profile of recipe 1.B and 2.B combined

Table B. 5: Viscometer data of recipe 1.B.

Parameters		Recipe 1. B on original day		Recipe 1. B after 24 hours	
RPM	Shear Rate [1/s]	Shear Stress [lb/100ft ²]	Viscosity [cP]	Shear Stress [lb/100ft ²]	Viscosity [cP]
600	1021.38	55.0	25.9	67.1	31.6
300	510.69	47.1	44.3	59.4	55.9
200	340.46	43.9	62.0	55.8	78.6
100	170.23	40.1	113.1	50.6	142.5
60	102.14	38.5	180.9	48.0	225.7
30	51.07	36.6	344.6	44.8	420.6
20	34.05	33.0	469.7	39.7	563.7
10	17.02	33.5	947.8	39.8	1122.6
6	10.21	29.9	1402.7	36.4	1708.3
3	5.11	22.5	2115.9	30.3	2844.2
2	3.4	20.0	2825.0	26.4	13726.9
1	1.7	17.9	5031.7	22.5	6549.3

Table B. 6: Viscometer data of recipe 2.B.

Parameters		Recipe 2. B on original day		Recipe 2. B after 24 hours	
RPM	Shear Rate [1/s]	Shear Stress [lb/100ft ²]	Viscosity [cP]	Shear Stress [lb/100ft ²]	Viscosity [cP]
600	1021.38	252.0	118.3	279.0	131.1
300	510.69	222.9	209.4	246.6	232.0
200	340.46	214.2	302.1	234.6	330.8
100	170.23	195.4	550.9	210.9	594.8
60	102.14	188.2	844.5	199.2	936.4
30	51.07	117.9	1671.9	184.9	1737.8
20	34.05	168.3	2374.4	172.2	2427.6
10	17.02	168.5	4748.3	168.2	4742.0
6	10.21	167.9	7888.2	164.7	7736.7
3	5.11	163.7	15378.4	159.0	14942.5
2	3.4	163.3	23013.3	158.3	22308.2
1	1.7	136.2	38086.5	142.5	40162.7

The large difference in rheological properties of these recipes was expected based on the difference in bentonite concentration. This is further confirmed by significant higher rheological parameters of recipe 2.B compared to 1.B, shown in Table B. 7 and Table B. 8.

Table B. 7: Rheological parameters of recipe 1.B.

Recipe 1.B	Initial condition	After 24 hours
Temperature [°C]	20.6	21.9
Plastic viscosity [cP]	9.1	9.0
Yield Point [lb/100ft ²]	42.3	50.6
Gel 10 sec	19.8	22.1
Gel 10 min	24.6	23.4

Table B. 8: Rheological parameters of recipe 2.B.

Recipe 2.B	Initial condition	After 24 hours
Temperature [°C]	25.1	24.7
Plastic viscosity [cP]	45.6	48.6
Yield Point [lb/100ft ²]	193.1	204.8
Gel 10 sec	109.7	115.0
Gel 10 min	117.5	131.7

Thus, recipe 2.B was adjusted to recipe 2.BT which was implemented on all large-scale tests. Results regarding recipe 2.BT are discussed in chapter 4.1.1. In this section, only corresponding shear stress and shear rate values of the rheological profile of recipe 2.BT (shown in Fig. 4. 1) are provided in Table B. 9.

The viscometer data in Table B. 9 show an overall decrease in values obtained after 24 hours, which is interesting based on the significant increase of other parameters associated to recipe 2.B. Despite that bentonite concentration was kept constant while adjusted to the larger aqueous base fluid volume. It is reasonable to assume that the bentonite particles experience greater distance to each other in the suspension and therefore are not able to effectively form gel structures. Further, recipe 2.B and 2.BT were mixed using two different mixing devices. The Heidolph mixer provided significant higher torque compared to the Hobart bench mixer used on recipe 2.BT. Higher mixing rates transfer more energy to the fluid resulting in a better dispersed system. This might be an additionally reason on the difference in rheological parameters of recipe 2.B and 2.BT. However, recipe 2.BT formed gel structures already at shear rates of 17.02 1/s and hence additional measurements were performed using the procedure described in Table A. 2 and Table A. 3. These measurements are marked in red in Table B. 9.

Table B. 9: Viscometer data of recipe 2. BT.

Parameters		Recipe 2. BT on original day			Recipe 2. BT after 24 hours		
RPM	Shear Rate [1/s]	Shear Stress [Pa]	Viscosity [cP]	Viscosity [Pa.s]	Shear Stress [Pa]	Viscosity [cP]	Viscosity [Pa.s]
600	1021.38	54.9	50.4	53.7	54.2	49.9	53.0
300	510.69	45.4	83.9	89.0	44.7	82.4	87.6
200	340.46	43.1	199.3	126.7	41.1	113.7	120.7
100	170.23	38.0	210.4	223.5	35.0	193.5	205.5
60	102.14	36.2	333.5	354.5	32.3	297.2	316.1
30	51.07	33.5	616.6	655.1	29.5	543.8	577.2
20	34.05	31.1	861.8	912.2	26.2	728.7	769.9
10	17.02	31.2	1754.9	1833.8	26.7	1474.5	1567.2
6	10.21	31.8	2933.6	3116.9	26.6	2451.8	2607.4
3	5.11	31.9	5887.2	6247.7	26.5	4874.2	5179.8
2	3.4	32.3	8923.7	9495.0	26.6	7350.6	7830.0
1	1.7	32.2	17806.4	18960.0	26.5	14635.4	15570.0
10	17.02	18.0	1005.2	1054.8	16.4	963.9	961.9
6	10.21	16.1	1484.5	1578.5	14.3	1316.9	1398.6
3	5.11	13.7	2513.5	2674.8	12.5	2308.6	2455.2
2	3.4	13.1	3627.6	3855.0	12.0	3312.3	3535.0
1	1.7	14.6	8065.2	8580.0	11.0	6056.0	6450.0

B.4 Bentonite-Based Pill Stability Tests

Stability tests were performed throughout up scaled versions of the previous test and can be divided into three targets. Even though recipe 1.B did not meet all established criteria it was chosen to work on the 10g bentonite-based pill at the early stage in this project.

The first target involved a simple stability test performed by tilting the sample cup containing the bentonite pill towards horizontal. Recipe 2.B experienced minimal integrity issues and stayed intact for several minutes at static due to sufficient yield point and gel strength, (see Fig. A. 2). This type of test was not conducted on recipe 1.B as it flowed easily when tilted or stirred by hand initiated circular motions.

The second target involved maintenance of stability while isolating two fluid sections. This scaled up stability test was performed on a 9.8 cm long transparent plastic cup with 4.8 cm ID. Brine, Recipe 1.B and WBDF were placed as demonstrated in Fig. B. 4.



Fig. B. 4 - Isolation and stability test performed on recipe 1.B

As shown in the figure above, recipe 1.B was not capable of fully isolating the brine and WBDF as clear contact between brine and WBDF is visual. The WBDF channelled through and accumulated in the upper section of the pill phase. It was further assumed that recipe 2.B would hold the criterion for stability and isolation.

Full isolation and adequate integrity were achieved using recipe 2.B during the third target, see Fig. B. 5. This test involved a 46 cm long transparent plastic tube with a 3.8 cm ID. The pill did maintain sufficient stability and isolated all fluids during the test period of 24 hours. All the same isolation was preserved, the surface of the pill allowed small amounts of WBDF to channel through and accumulate right below the pill and WBDF interface. The channel was created when the WBDF was accidentally poured too intensively during placement.

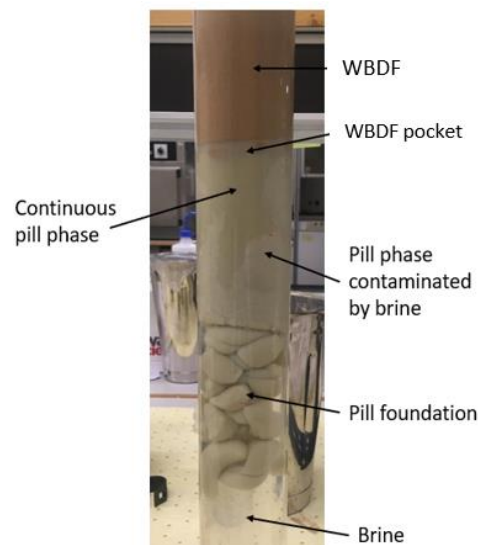


Fig. B. 5 - Successful stability test using recipe 2.B

Despite the defined test period of 24 hours, this specific test was continued to study the behaviour of the fluids left static over time. No changes were observed after 48 hours, but after five days the bentonite-based pill split up. The lower part settled to the bottom and the upper part floated upwards with the WBDF trapped in the upper pill phase as shown in Fig. B. 6. The fluids distribution remained in the same order for a couple more days. When passing the twelfth day, the upper part of the pill containing the accumulated WBDF did eventually sink and settled on top of the initially lower part (see Fig. B. 6). Larger volumes of brine compared to the test results after five days were forced upwards covering the upper section at the tube. This motion was caused by density differences of the fluids with the heavy WBDF pushing the pill column downwards. At this point, the source of WBDF channel created was visible and is presented in Fig. B. 7. The studied behaviour of the fluid system could potentially explain how the fluid phases behave in the large-scale test pipe when left static and undisturbed for a longer period.

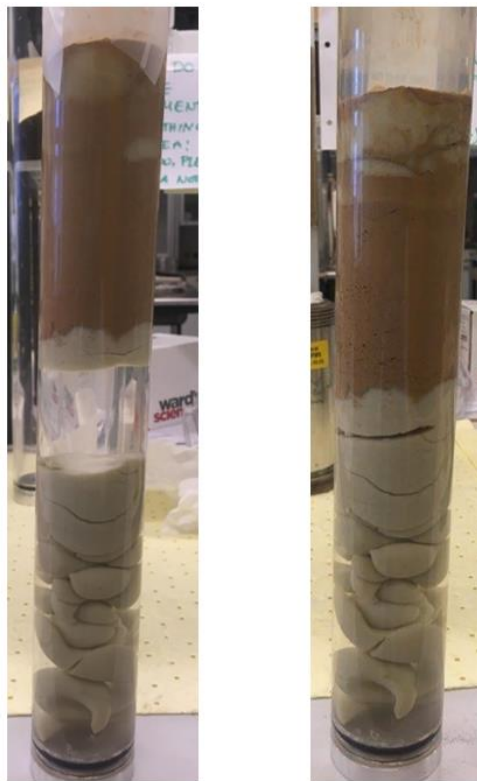


Fig. B. 6 – Test result after five days (left) and after twelve days (right)



Fig. B. 7 - Source of WBDF channel created by pouring

Further tests were conducted using recipe 1.B, with no successful stability and isolation achieved. The first test, see Fig. B. 8 a) and b), resulted in a channel established immediately after WBDF placement and eventual breakthrough of the WBDF. The second test resulted in a complete failure with WBDF breakthrough and intermixing of all fluid phases, see Fig. B. 8 c).

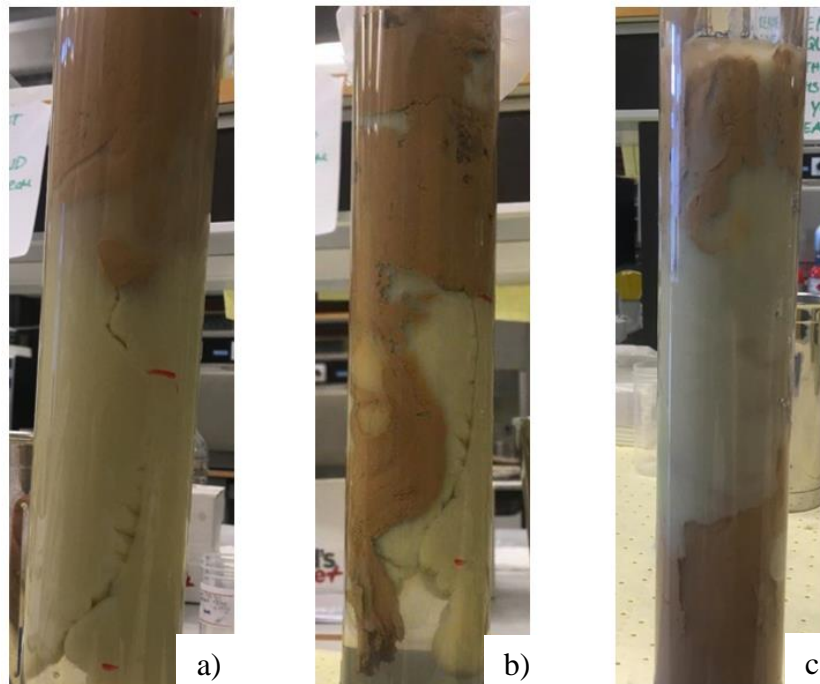


Fig. B. 8 a) First test – channel, b) First test – breakthrough and c) Second test – complete failure

B.5 Viscometer Data of the Laponite-Based Pill

Table B. 10 provides the corresponding shear stress and shear rate values of the rheology profile shown in Fig. 4. 21 (see chapter 4.2.1). Typical for all recipes of type 3.LT were the increase in shear stress and viscosity values after 24 hours. This increase is caused by clay hydration developing larger networks of particles and flocs dispersed in the system. Also common for this recipe was the development of gel structure at low shear rates. This is observed by the small decrease in shear stress values below shear rates of 17.02 1/s towards 1.7 1/s. Further compared to the larger span between shear stress values corresponding to shear rates above 34.05 1/s. Due to the formation of gel strength starting at low shear rates, additional viscometer measurements (marked in red) were obtained using step 10.0 to 10.3 described in Table A. 2.

Table B. 10: Viscometer data of Recipe 3.LT.

Parameters		Recipe 3. LT on original day		Recipe 3. LT after 24 hours	
RPM	Shear Rate [1/s]	Shear Stress [lb/100 ft ²]	Viscosity [cP]	Shear Stress [lb/100 ft ²]	Viscosity [cP]
600	1021.38	76.5	35.9	84.1	39.5
300	510.69	64.2	60.4	69.1	65.1
200	340.46	60.7	85.5	65.1	91.8
100	170.23	54.6	153.9	58.5	165.1
60	102.14	51.9	243.8	55.7	261.8
30	51.07	49.0	460.8	52.4	492.1
20	34.05	46.7	655.0	49.6	701.0
10	17.02	46.3	1306.3	49.6	1399.2
6	10.21	46.0	2160.4	49.4	2320.4
3	5.11	45.5	4276.5	48.9	4598.7
2	3.4	45.4	6397.1	48.9	6897.2
1	1.7	45.2	12728.3	48.7	13750.2
10	17.02	19.4	548.0	19.7	556.3
6	10.21	14.8	694.4	15.7	736.8
3	5.11	12.0	1138.8	11.8	1110.0
2	3.4	10.0	1404.5	10.1	1424.6
1	1.7	7.9	2230.1	7.9	2226.8

B.6 Laponite-Based Pill Stability Tests

Only one stability test was performed on the laponite-based pill due to limited time. The stability test conducted on recipe 2.L (10g laponite-based) is shown in Fig. B. 9. As it can be seen, channelling occurred with the WBDF accumulating in the upper pill phase. However, this test would most likely been successful if the entire WBDF volume were poured carefully along the tube wall. At one-point during placement, the tube slipped and WBDF was accidentally poured too intense breaking the surface and gel structure of the pill. Based on rheological data and significantly higher gel strength values it was further assumed that recipes of higher laponite concentration would pass this stability test successfully.



Fig. B. 9 – Channelling of WBDF through recipe 2.L

B.7 Water Used for Analysis of Pressure Instabilities

It was early discovered that the pressure sensors, especially sensor XP2i, were sensitive to temperature variations. Appearance of pressure instabilities and in some cases unreasonable pressure patterns were observed when analysing pressure profiles provided in chapter 4. It was therefore chosen to run pressure monitoring on the vertical test setup filled with water. This was done to investigate whether pressure instabilities and deviations were caused by the gel

pills or temperature effects. Fig. B. 10 shows the pressure profiles of XP2i, DP1 and DP2 for a period of 24 hours on the vertical setup filled with water.

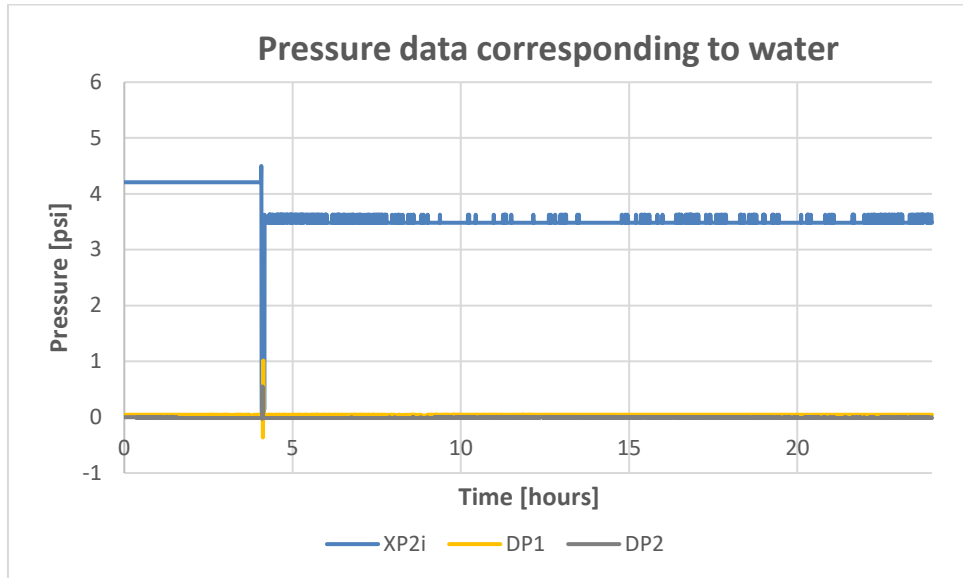


Fig. B. 10 – Pressure profiles corresponding to test pipe filled with water on the vertical setup

As it can be seen, sensor XP2i monitored unreasonable pressure behaviour at roughly 4.0 hours followed by pressure instabilities for the remaining period. The same pressure peak was detected by sensor DP1 and DP2. These observations are evidence in temperature changes having an impact on the pressure sensors. Hence, pressure instabilities observed on pressure data associated to the bentonite and laponite pills might indeed be caused by temperature to an uncertain degree.

Appendix C - Suggestions on Improvement and Future Work

C.1 Potential Improvements

Most of the suggested improvements are associated with equipment and further disclosed:

- Implementing a hydraulic or automatic pump to improve the fluid placement by a smoother and more controlled pumping operation, which was difficult to accomplish by the hand-driven piston pump.

- Installation of pressure gauge sensors with lower pressure span for more accurate pressure readings as the sensors used were fabricated for higher pressure regions as 3 psi for the differential pressure sensors and 200 bar for the XP2i sensor.
- Improvement of a mixing device used for larger volumes. The Hobart machine was during this project used by several students and hard to clean properly which raised the probability of contamination.

C.2 Way Forward

The work behind this project has developed a basis in the development of a sag prevention gel pill with promising results confirming the potential of such a fluid pill system. Suggestions for future work involve further investigation of the fluid pill's properties and study the conditions and environments present in the laboratory versus a well bore. Based on the foundation created, suggestions on the way forwards are herein listed as:

- Studies could be performed on temperature dependent rheological measurements to obtain an understanding of the pills behaviour and properties when exposed to more like temperature conditions present in the field.
- Investigations on the pills properties by using oscillating and frequency sweeps to analyse gel strength development, ideal setting time, maximum effective gel strength formation and other important properties.
- Study of the gel strength development, swelling mechanism and electrical forces of the pill phase to define or understand the type of gel strength formation.
- Experiments performed on the large-scale test setup could involve studies on minimum required pill length to both isolate fluid sections and transmit pressure.
- Further experiments on the large-scale could include a water-based drilling fluid of significant higher fluid weight.